The Institute of Paper Chemistry

Appleton, Wisconsin

Doctor's Dissertation

An Investigation of the Vibrational Spectra of the Pentitols and Erythritol

Gary Michael Watson

June, 1974

AN INVESTIGATION OF THE VIBRATIONAL SPECTRA OF THE PENTITOLS AND ERYTHRITOL

A thesis submitted by

Gary Michael Watson

B.A.(Chem) 1969, Western Washington State College — Bellingham

M.S. 1971, Lawrence University

in partial fulfillment of the requirements
of The Institute of Paper Chemistry
for the degree of Doctor of Philosophy
from Lawrence University
Appleton, Wisconsin

Publication Rights Reserved by
The Institute of Paper Chemistry

June, 1974

TABLE OF CONTENTS

SUMMARY

The vibrational spectra of the pentitols and erythritol were investigated. The Raman and infrared spectra of these crystalline compounds were measured from 4000 to approximately 150 wave numbers (cm^{-1}). Their spectra are complex and interpretive efforts are complicated by extensive vibrational coupling of the internal modes below 1500 cm^{-1}. Consequently, detailed normal coordinate calculations were used in this investigation.

A series of computer programs were used to construct and solve the vibrational secular equation of ribitol, xylitol and erythritol. To solve each secular equation required the use of explicit structural data and an approximate set of intramolecular force constant parameters. The calculated frequency parameters derived from solving the vibrational secular equations were correlated with the experimentally measured frequencies. The difference between the calculated and experimental frequencies was used to formulate a basis for a refinement of the initial set of force constants. An iterative nonlinear least squares technique, based on the Fletcher-Powell method, was used to simultaneously adjust the force constants until the difference between the calculated and experimental frequencies were minimized. After refinement there was an overall average difference of 9.1 cm^{-1} between the calculated and assigned experimental frequencies.

The force field derived from the refinement process was shown to be capable of predicting the vibrational spectrum of D-arabinitol. The ability to predict the distribution of bands in the D-arabinitol spectra has clearly opened up the possibility of extending this approach to other alditols. As a matter of interest, the observed spectra of both D and D,L-arabinitol were compared. Differences in their spectra were noted and have been attributed to suspected

differences in the geometry of their unit cells and/or differences in the intermolecular hydrogen bonding.

The results of the analyses demonstrate that the vibrational spectra of the pentitols and erythritol can be understood in terms of a relatively simple force field. The major differences among the pentitol spectra result primarily from changes in the vibrational coupling caused by the structural differences among the isomers. This suggests that most of the molecular vibrations arise, to a first approximation, from the isolated molecule, apart from its environmental surroundings. Although interactions among the molecules in the unit cell were detected, the effects on the spectra were localized in particular bands. The effects of hydrogen bonding appear to be of secondary importance in understanding the vibrational spectra of these compounds. The overall band distribution is most sensitive to the coupling of the atomic vibrations within the molecule.

INTRODUCTION

Attempts to analyze comprehensively the vibrational spectra of carbohydrates[1] have been renewed recently in an effort to broaden the application of vibrational spectroscopy as a tool for studying the physical chemistry of these complex molecules. Interest has been particularly aroused because of the importance of the saccharides in the technology of natural products and in medicine.

For example, in nature the saccharides often occur in polymeric form such as the anhydroglucose polymer cellulose. Cellulose, which is one of the few abundant and renewable natural resources, is a basic raw material for the textile and paper industries. Also the saccharides are biologically important structural components in living tissues, and are involved in metabolic pathways: (1) glycolysis and alcoholic fermentation, and (2) pentose phosphate metabolism. Furthermore, they enter into a number of important biochemical mechanisms such as blood coagulation and antigen antibody interactions, and they are constituents of some of the clinically important antibiotics.

Even though some progress has been made in the interpretation of carbohydrate spectra, much remains to be done before the potential of vibrational spectroscopy is fully realized. The infrared (IR) spectra of the saccharides have been investigated quite extensively. However, the complexity of the spectra and the difficulties in resolving the lower frequency regions have limited the progress of interpretive efforts. Most interpretive efforts have necessarily relied on the group frequency approach. The group frequency approach is an empirical

---

[1] The term carbohydrates, in this context is used to identify the class of compounds which, in addition to the saccharides, includes their derivatives and other related compounds such as the cyclitols.

method based on the assumption that vibrations for a certain atomic group (e.g., C = C bonds) are independent of the rest of the atoms in the molecule. Thus, by comparing the spectra of a large number of compounds having a common group, it is possible, in some instances, to find absorption bands which remain relatively constant. The frequency of these bands can then be considered to be characteristic of the vibrational motion of the common atomic group.

However, due to the similarity of the atomic groupings in many carbohydrate molecules, the majority of the bands are thought to result from complex mixtures of vibrational motion (i.e., most of the frequencies are combinations of many kinds of motion coupled together). Thus, it is difficult to make comprehensive interpretations from systematic comparisons of the carbohydrate spectra with the spectra of simple compounds which have been interpreted more completely. Some regions, like the fingerprint region, simply cannot be interpreted using this approach.

Although interest in developing vibrational spectroscopy as a tool in physical chemical investigations of the carbohydrates has existed for some time, the interest and the methodology necessary to expand the application have not always coincided. Consequently, vibrational spectroscopy (mostly IR) has functioned primarily as an analytical tool in investigations relating to the chemistry of the saccharides. However, now the methodology does exist. Developments in both experimental and computational techniques in the field of spectroscopy have made possible more rigorous analyses of the spectra of complex molecules possessing more than 20 atoms.

More specifically, the availability of laser Raman spectrometers and the gradual development of more effective computer methods for normal coordinate calculations have been responsible for the most recent advances. Improved

Raman spectrometers provide complementary spectral information to IR absorption measurements, and the normal coordinate calculations allow for the detailed investigation of the vibrational dynamics of large molecules. Thus, these advances suggest that comprehensive analyses of the spectra of certain carbohydrate-related molecules are now possible. The results obtained from further analyses would considerably advance our basic understanding of the vibrational dynamics of these molecular systems.

The thesis research reported here is actually one part of a broader effort to analyze systematically and eventually interpret the vibrational spectra of various anhydroglucose polymers, including cellulose. It is felt that, in order to accomplish this broader goal, two inseparable problems must be solved: (1) interpreting the spectra of the pyranoses, and (2) interpreting the spectra of the anhydroglucose polymers. Similarly, understanding the spectra of the pyranoses requires an understanding of the spectra of simpler though structurally related carbohydrate compounds, such as the 1,5-anhydropentitols (1,5-AHP's) and the pentitols.

A comprehensive study of the solid-state vibrational spectra of the 1,5-AHP's has recently been completed (1). The major portion of this thesis examines the solid-state vibrational spectra of (I) ribitol, (II) xylitol, (III) D-arabinitol (the pentitols) and (IV) erythritol.

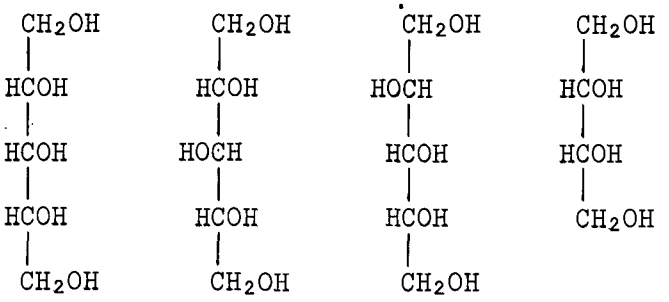

I II III IV

The purpose of the investigation is to analyze the spectra of these compounds and to provide information to assist in the spectral interpretation of other related carbohydrate molecules.

BACKGROUND

There are numerous difficulties involved in interpreting the spectra of the carbohydrates. First, the spectral bands are often crowded and the problem of assigning and interpreting the individual modes is extremely difficult. Secondly, below 1350 cm^{-1} the origins of the vibrations are likely to involve more than a localized vibration of a specific group within the molecule. Deuteration work has long suggested this possibility (2,3). In the IR spectra of cellulose and xylan, for instance, there are about 17 bands between 1500-980 cm^{-1} (2). Of these, the bands between 1500-1200 cm^{-1} have been accounted for as either OH in-plane (ip) or CH and CH_2 bending modes (2). As a result, much of the work has been confined to the region between 1100-700 cm^{-1}. For example, bands between 1075-980 cm^{-1} in the spectra of cellulose, laminarin, amylose, and xylan have been interpreted as CO and CC stretching modes (4). However, further clarification of some of the spectral features in this region is required (2,4).

The status of the work prior to 1964 has been described in a comprehensive review by Spedding (2). Most of his discussion related to work on the IR spectra of the carbohydrates. Essentially two methods were used for interpretive purposes in the region between 960-730 cm^{-1} in the spectra of carbohydrates. One method was based on the correlation of features in the IR spectrum of tetrahydropyran (THP) with similar features in the spectra of the pyranoses and related carbohydrates. Bands associated with particular ring vibrations in the THP molecule were correlated on the basis of their frequencies and intensities to similar bands appearing in pyranose compounds. This is an example of the use of structurally simpler compounds to help understand the spectra of more complex molecules.

The other method focused on spectral features associated with the anomeric carbon atom. In this method a wide range of compounds having similar atomic groupings at the anomeric carbon atom were compared. Frequencies in the spectra of these compounds which remain constant were assigned to modes involving the atoms associated with the anomeric carbon atom.

Important contributions have been made by a number of workers which have, for the most part, utilized both of these methods. Tipson's (5) review in 1968 provides a comprehensive discussion of the characteristic infrared bands shown by various atomic groups in carbohydrate molecules.

Polarized IR spectra have also been used for interpretive purposes in the CH stretching region, 3000-2800 cm^{-1}, of cellulose. Marchessault assigned the 2853 cm^{-1} band in cellulose to the symmetric CH_2 stretching mode based on IR polarization data (6).

Deuterium substitution has been used effectively in some cases to identify OH bending modes. Also, by comparing the spectra of cellulose with the spectra of deuterated cellulose and related polymers, the bands between 1075-980 cm^{-1}, mentioned earlier, were interpreted as CO and CC stretching modes (4).

In the early 1960's progress in the methodology of vibrational spectroscopy led to another approach to analyzing the spectra of complex molecules. The work of Schachtschneider and Snyder (7,8) on the hydrocarbons and of Snyder and Zerbi (9) on the ethers, including THP, established that systematic normal coordinate (NC) analyses of the spectra of groups of related compounds was possible.

An NC analysis is a mathematical treatment designed to calculate the fundamental vibrations (i.e., normal modes) of a molecule and to analyze the motions associated with these vibrations. In a nonlinear polyatomic molecule of n atoms there are $3n-6$ vibrational degrees of freedom. Thus, the vibrational spectra of a nonlinear molecule will reveal $3n-6$ fundamental frequencies[2]. Each observed fundamental frequency represents a normal mode, which can be described by an associated normal coordinate. The normal coordinate may be a mixture of various internal displacement coordinates such as bond stretching or angle deformations. One objective of the analysis is to resolve this mixture into its major components. When a particular mode is excited, all the atoms involved oscillate in phase with the same angular frequency. Depending on the masses of the atoms and the nature of the bonds the amplitudes may be different. By correlating the $3n-6$ calculated normal modes with the experimentally observed frequencies it is possible to interpret the vibrational spectrum.

Prior to the analyses of Snyder and Zerbi on the ethers, some interpretive work had been done on THP as reviewed by Spedding (2). In particular, Burket and Badger (10) examined the infrared spectrum of THP and assigned various bands between 1060 and 800 cm^{-1} to ring stretching vibrations [including the symmetric (sym.) and asymmetric (asym.) C-O-C stretch]. Their interpretation of THP was based on the NC analysis of cyclohexane by Becket, et al. (11). However, the actual NC analysis of THP (and related ethers) by Snyder and Zerbi was not completed until 1967. More recently, Pickett and Strauss (12) adapted the computational methods of Schachtschneider and Snyder in a study

[2]Assuming that all transitions are allowed in either the Raman (R) or IR, which is not necessarily the case, and that there are no overtone or combination bands, and no accidental degeneracies.

of the ring bending vibrations of cyclohexane and related oxanes including THP. They determined the ring bending potential of the various oxanes using the NC analysis and used this information to calculate rate constants for chair to boat conversion.

Three other investigations have been completed in the early 1970's in an effort to develop the basis for an interpretation of the vibrational spectra of some of the more important saccharides. First, Vasko (13) examined the Raman scattering of a large number of carbohydrates. He also computed the vibrational frequencies of α-D-glucose using force constants selected from the published literature on more simple molecules and structural data based on the neutron diffraction work of Brown and Levy cited in (14). Even though no structural approximations were necessary, there were serious gaps between the computed and experimental band distributions suggesting the need for an improved set of force constants.

Secondly, Pray (4) made an *a priori* calculation of the skeletal planar vibrations and internal vibrations of certain atomic groups in cellulose using the "multiple origin method" of Deeds (15) and initially selected constants from Wilson, *et al.* (16) and Takahashi, *et al.* (17). An approximate structural model of glucose was used by Pray as a simplified cellulose model. To simplify the calculations the coupling between in-plane (ip) and out-of-plane (op) vibrational motions [i.e., the plane formed by the C(1), C(3), and C(5) atoms] was neglected. However, the spectral interpretations resulting from Pray's analysis are not consistent with prior knowledge relating to the vibrational spectra of the carbohydrates.

Although both of these latter investigations represent attempts to analyze mathematically the molecular vibrations of glucose, the results

suggest that the complexity of the problem requires (1) a more systematic approach (such as that taken by Snyder and Zerbi) and (2) a more representative intramolecular force field. Pitzner's (1) investigation of the 1,5-AHP compounds, mentioned earlier, supports this view. He was able to successfully analyze the vibrational spectra of the 1,5-AHP molecules using a procedure for the analysis similar to the one developed by Schachtschneider (18,19). In each case, the computed spectra approximated the observed spectra reasonably well. Furthermore, the interpretations, based on an analysis of the calculated normal coordinates, were determined to be consistent with prior experience about carbohydrate spectra using group frequency correlations. Intramolecular force constants representative of the 1,5-AHP's were calculated by making simultaneous adjustments to an initial set of force constant values until the difference between the calculated and experimental frequencies were minimized. The values of the initial constants were taken from Snyder and Zerbi's NC analysis of THP and related ether compounds.

More importantly, Pitzner found that the numerous differences in the location of the observed spectral bands among the 1,5-AHP's were primarily due to $\underset{\sim}{G}$ matrix effects or kinetic energy effects as they are sometimes called[3]. Kinetic energy effects result from structural differences among related molecules (these can be either configurational or conformational differences). In the case of the 1,5-AHP molecules the primary structural difference is configurational and related to the orientation (either axial or equatorial) of the vicinal hydroxyl groups. These structural changes alter the vibrational

[3]Actually the $\underset{\sim}{G}$ matrix is the inverse of the kinetic energy matrix, and should not be confused with the kinetic energy of the system, which is a scalar quantity.

coupling among the oscillations associated with the fundamental vibrations. Because the coupling patterns are altered the frequencies and intensities of the vibrations change.

The success of Pitzner's NC analyses of the 1,5-AHP compounds has clearly opened up the possibility of extending this approach to more complex carbohydrate molecules.

THESIS OBJECTIVES

The major objective of this thesis was to provide a basis for the interpretation of the vibrational spectra of the alditols. To achieve this objective, erythritol, ribitol, xylitol, and D-arabinitol were selected as representative alditols. Normal coordinate analyses of the molecular vibrations of these molecules were carried out in an effort to formulate an interpretive basis for this class of compounds.

Pitzner's work on the 1,5-AHP's (1) clearly established the possibility of developing a force field for the alditols. A force field with some predictive capability would provide a basis for an interpretation of the alditol spectra. Thus, the problems confronted in this investigation were twofold:

(1) Develop the best possible force field for these selected models.

(2) Determine the transferability of this force field to related alditol molecules.

Three of the four alditols, ribitol, xylitol, and erythritol were used to develop a common force field. These compounds were selected for several reasons. First, their crystal structures have all been determined. Thus, with direct structural data available no approximations were necessary with regard to the conformations adopted by the molecules in the solid state. The fourth molecule, D-arabinitol, was excluded from the development because its structure is unknown. Hunter and Rosenstein (20) have determined the crystal structure of D,L-arabinitol. However, there is no basis for assuming that the structure of the D isomer in D,L-arabinitol is the same as its structure in the crystalline D isomer. This uncertainty may be resolved by comparing both the D and D,L spectra with the calculated spectrum of the D isomer as it exists in the D,L crystal. Secondly, ribitol and xylitol are structurally related to both the 1,5-AHP's and the

pentoses. They possess the same relative configuration at C(2), C(3), and C(4) as the corresponding members in the other two groups. The atomic groups at these three locations are identical. Thus, the constants in the force field developed by Pitzner could be used as an initial approximation to the force field of the alditols.

Finally, xylitol and ribitol have similar "flexed" chain conformations while erythritol has an "extended" chain or planar zigzag conformation. The flexed chain conformation is characterized by rotation about a CC bond which alters the otherwise planar zigzag conformation of the carbon backbone. A parallel interaction between C_2O and C_4O (i.e., a syn-axial interaction) in both ribitol and xylitol is relieved by a 120° rotation about C(2) - C(3) or about C(3) - C(4) as shown in the following equations.

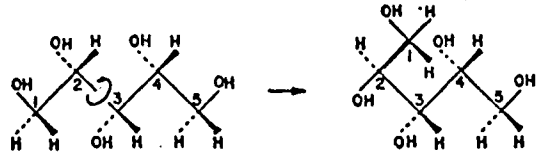

XYLITOL

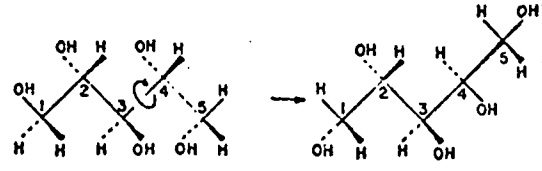

RIBITOL

These two kinds of conformations (i.e., the flexed and the extended chain) are characteristic of the tetritols, pentitols, and hexitols (21). Thus, these three compounds are structurally representative of the alditols. A field capable of describing the intramolecular forces in each of these molecules would be expected to transfer reasonably well to other alditols possessing either type of conformation.

To develop a force field for the alditols, the vibrational spectra of ribitol, xylitol, and erythritol were computed by solving their vibrational secular equations. Based on these calculations the computed frequencies were

correlated with experimentally measured frequencies. An effort was then made to reduce the least squares deviation between the two sets of data by a succession of adjustments to the common force constants in the $\underset{\sim}{F}$ matrices of these model compounds. Thus, the approach to the solution of the first problem had four essential steps:

(1) Measure the observed vibrational frequencies of ribitol, xylitol, and erythritol.

(2) Compute the vibrational frequencies of each molecule, given the necessary structural data and an initial set of common force constants.

(3) Assign the calculated modes to the measured frequencies of vibration.

(4) Refine the initial force constants by minimizing the least-squares deviation between the observed and calculated frequencies.

Several important constraints were imposed on the fourth step. The first constraint related to the actual refining process. The total number of refined force constants was not allowed to exceed the number of known experimental frequencies. Pitzner established that it was possible to develop a force field for the 1,5-AHP's by perturbation of existing parameters. However, to maximize the interpretive value of the constants obtained from such treatments it is important that these parameters be capable of reproducing a number of independent experimental frequencies which is greater than the number of variables used in the refinement.

Secondly, it was required that the spectral interpretations based on the NC analyses be consistent with prior experience in group frequency correlations. Finally, the final values of the constants were expected to be consistent with the values of similar constants in related molecular systems. In this regard, however, some differences between the initial and final constants were

anticipated in view of the differences between the pentitols and the 1,5-AHP's. The absence of both the ether linkage and the ring structure were expected to affect some of the constants. Also, the chainlike structure of the alditols may affect the degree of intermolecular hydrogen bonding between the vicinal hydroxyl groups. Such an effect would be expected to result in differences among similarly defined force constants.

The second objective was to test the transferability of the constants developed by minimizing the least squares deviation between the observed and calculated data for ribitol, xylitol, and erythritol. Although force fields have been developed for the n-paraffins (7), aliphatic ethers (9), and 1,5-AHP's using perturbation treatments, transferability of the force constants to related molecules has not been demonstrated. A third pentitol, D-arabinitol, was used to determine whether the constants could be applied to related molecules. Using the available data on the structure of D-arabinitol as it exists in the D,L crystal and the final set of refined force constants, the spectrum of the molecule was calculated. A reasonable correlation between the calculated and observed bands in the D-arabinitol spectra (Raman and IR) would provide a measure of the predictive capabilities of the field.

EXPERIMENTAL

SAMPLE PREPARATION

With the exception of D,L-arabinitol, all other compounds were available from commercial sources. The D,L-arabinitol crystals (m.p. = 105°C) were obtained by slow evaporation from a (95/5, v/v) ethanol-water solution of an equal molar mixture of the D and L isomers. Deuteration of the hydroxyl groups of ribitol, xylitol, and erythritol was accomplished by repeated crystallization from monodeuterated ethanol-D_2O mixtures (75:20, v/v). The deuterated crystals were separated by filtration, washed with small amounts of monodeuterated ethanol, and dried in a vacuum desiccator. The degree of deuteration was not rigorously established.

SPECTRA

The Raman spectra were measured with a Spex Raman system with a Coherent Radiation Model 52A Argon ion laser source. A laser frequency of 5145 A (19435 cm^{-1}) was used. The slit widths were set for a minimum resolution of 5 cm^{-1}.

The Raman spectra of the solid samples were obtained using pressed powder pellets mounted in a 180° back-scattering arrangement. The beam was focused directly upon the face of the pellet. Before scanning the crystalline pellets were exposed to the laser beam for a time interval of approximately 50 minutes to allow the fluorescence to diminish. The solution spectra were obtained from concentrated aqueous samples sealed in capillary tubes mounted in the standard sampling mode.

The standard procedure for preparing pellets was modified somewhat for the deuterated samples to minimize hydrogen-deuterium exchange with water vapor.

The powder and die for pressing the pellets were prepared in an anhydrous air bag. Also, the time interval before scanning was reduced as much as possible.

Infrared spectra of the powdered solids were recorded with a Perkin-Elmer 621 IR spectrometer using KBr pellets prepared in the standard manner.

COMPUTER PROGRAMS

The computational work was performed on an IBM 360 Model 44 digital computer. The vibrational problem was set up in terms of internal displacement coordinates using the Wilson GF method (16). The programs for solving the secular equations were developed by Schachtschneider (18,19) and adapted for the IBM 360 OS operating system by Pitzner (1). The function minimization algorithm of Fletcher and Powell (22) was used for the nonlinear least-squares refinement of the force constants. These programs are on permanent file in the computer center library at The Institute of Paper Chemistry (Library Source Tape: IPC.TH.001).

RESULTS

INFRARED AND RAMAN SPECTRA

RIBITOL

The Raman spectra of ribitol and deuterated ribitol are shown in Fig. 1. Solution spectra in both H_2O and D_2O are shown in Fig. 2. An IR spectrum of a KBr mounted ribitol sample appears in Fig. 3. The frequencies of the observed bands in each spectrum are listed in Table I.

XYLITOL

The Raman spectra from pellets of xylitol and deuterated xylitol are shown in Fig. 4 along with an H_2O solution spectrum. An IR spectrum of xylitol is shown in Fig. 3. The frequencies of the observed bands in each spectrum are listed in Table II.

ERYTHRITOL

Aside from the conformational differences and differences in the location and degree of intermolecular bonding, erythritol possesses another property not characteristic of the other alditols. The basic structural backbone of the erythritol molecule is reported to have a center of symmetry (23). The unit cell is also centro-symmetric. In centro-symmetric molecules, transitions that are allowed in the IR are forbidden in the Raman spectrum. The converse is also true. The Raman and IR spectra of erythritol are shown in Fig. 5. An H_2O solution spectrum (Raman) is shown in Fig. 5 also. The IR spectra of erythritol and deuterated erythritol are compared in Fig. 6. The measured frequencies in each spectrum are tabulated in Table III. From Table III it is apparent that the rule of mutual exclusion is not rigorously obeyed.

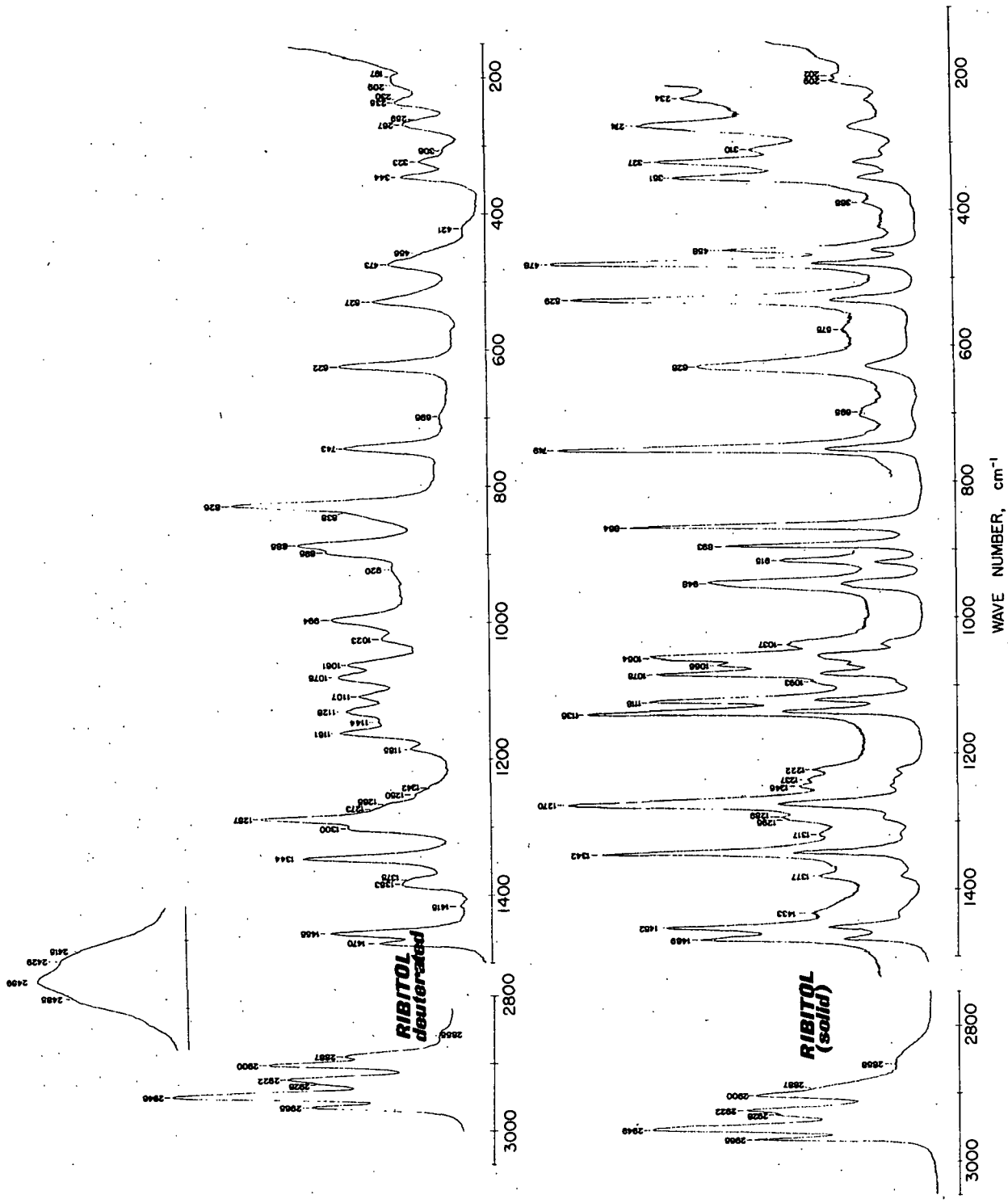

Figure 1. Raman Spectra of Ribitol

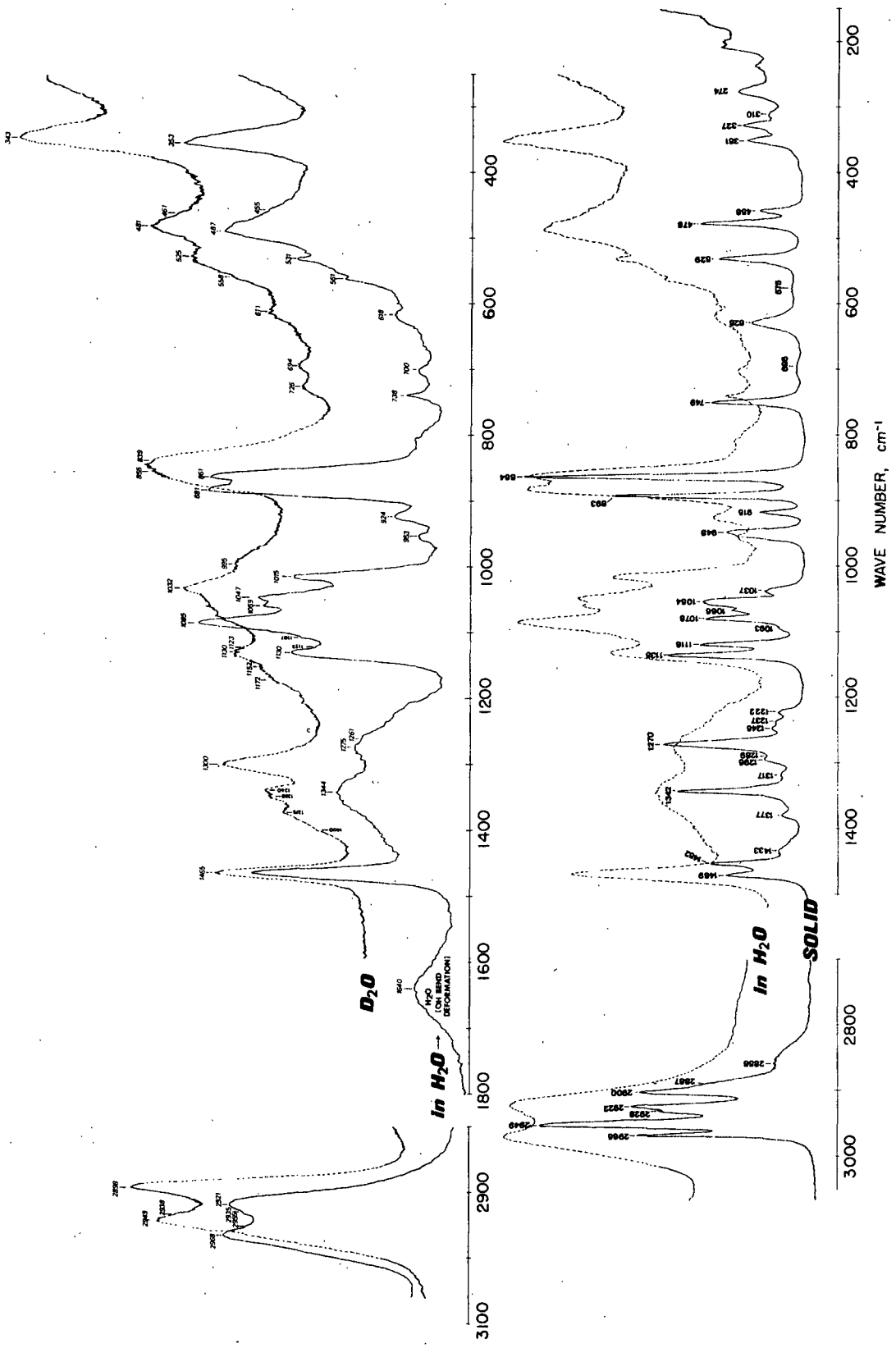

Figure 2. Raman Spectra of Ribitol

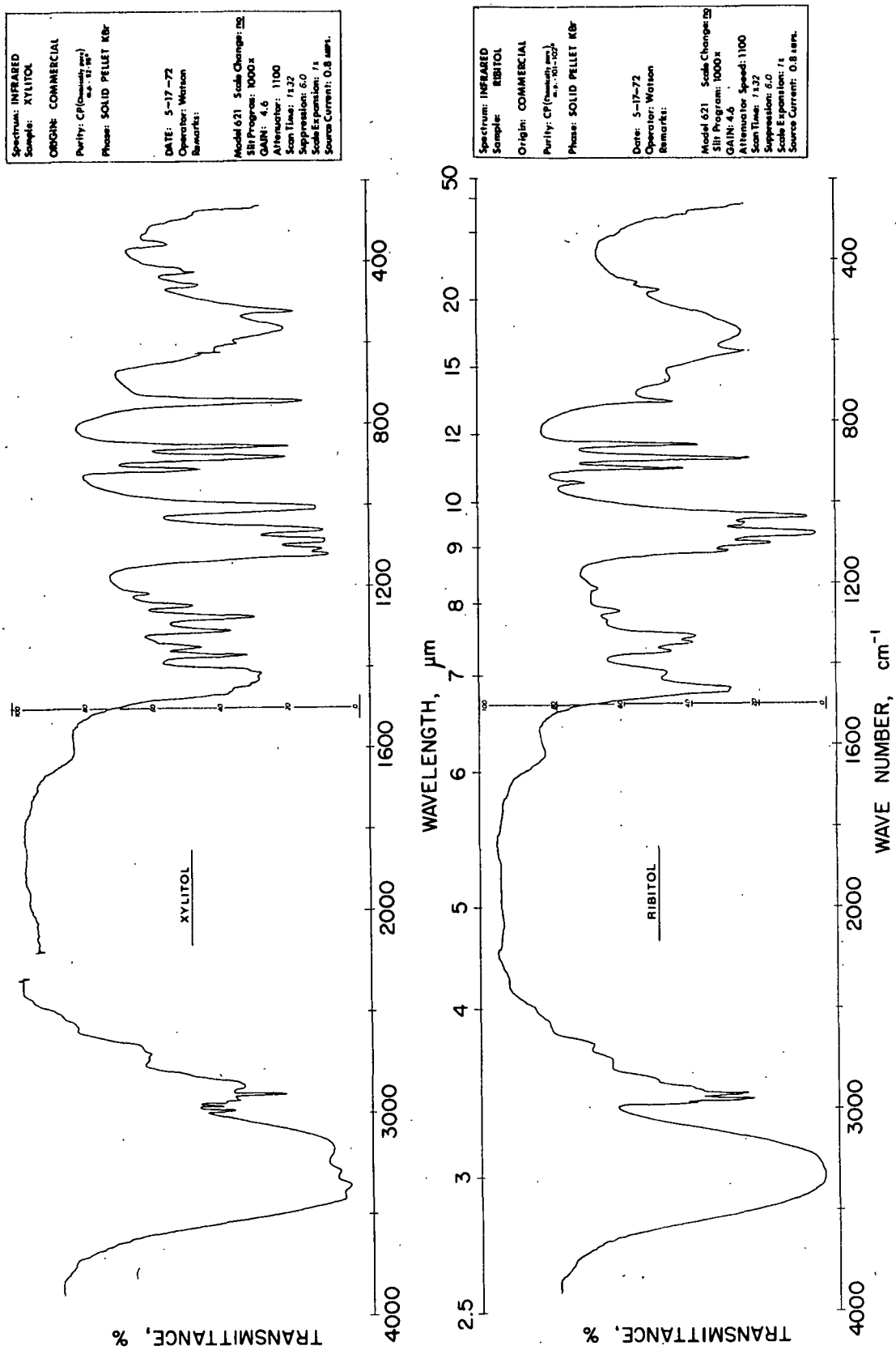

Figure 3. Infrared Spectra of Xylitol and Ribitol

TABLE I

VIBRATIONAL SPECTRA OF RIBITOL

Solid		Deuterated	Solution[a]	
$\Delta\nu$, Raman, cm^{-1}	ν, IR, cm^{-1}	$\Delta\nu$, Raman, cm^{-1}	$\Delta\nu$, (H_2O) Raman, cm^{-1}	$\Delta\nu$, (D_2O) Raman, cm^{-1}
	∿3340(vs,b)[b]			
	∿3250(vs,b)			
	2972(s)			
2965(s)	2960(vs)	2965(s)	2968(vs,b)	
2949(vs)		2949(vs)	2955(sh)	2949(vs,b)
∿2928(s,sh)	2928(vs)	2928(s,sh)	2935(sh)	2938(sh)
2922(s)		2922(s)	2921(vs,b)	
	2913(sh)			
2900(s)		2900(vs)		2898(vs,b)
2887(s,sh)	2893(s,sh)	2887(s)		
2858(vw)	2853(w,b)	2855(vw)		
		2485(sh)		
		2459(s)		
		2429(s,vb)		
		2415(sh)		
1469(s)	1467(s)	1470(m)	1466(s)	1465(s)
1452(s)	1458(s)	1455(s)		
∿1433(w,b)	∿1422(m,b)	∿1415(vvw)	∿1400(w,b)[pr]	∿1400(w,sh)[pr]
1378(w,b)		∿1383(m,b)		∿1375(m,b)[pr]
	1364(m)			∿1350(m)[pr]
1342(s)	1344(m)	1344(s)	∿1344(m,b)[pr]	∿1340(m,b)[pr]
	1328(m)			
1317(vw,b)				
1295(m,sh)		1300(s,sh)		1300(s,b)
∿1289(m)	1289(w)	1287(vs)		
1270(s)		∿1273(m,sh)	∿1275(m,b)[pr]	
1265(sh)		∿1265(sh)	∿1260(sh)[pr]	
1246(m)		∿1250(w)	∿1245(w,sh)[pr]	
1237(w,b)		∿1242(w,sh)		
1222(w,b)			∿1215(vw,b)[pr]	∿1215(w,b)[pr]

TABLE I (Continued)

VIBRATIONAL SPECTRA OF RIBITOL

Solid		Deuterated	Solution[a]	
Δν, Raman, cm^{-1}	ν, IR, cm^{-1}	Δν, Raman, cm^{-1}	Δν, (H_2O) Raman, cm^{-1}	Δν, (D_2O) Raman, cm^{-1}
	∿1209(w)			
		1185(m)		
		1161(s)		∿1172(m,b)
		∿1144(m)		∿1152(m,b)
1135(s)	1133(m)		1130(s,sh)	∿1130(s,b)
1118(s)	1117(s)	1128(s)	∿1122(s,sh)[pr]	
∿1092(w,sh)	1098(vs)	1107(m,b)	∿1102(sh)[pr]	
			1085(vs)	
1078(s)	1074(s)	1078(s)		1075(s,b)[pr]
1066(s)	∿1068(sh)	1061(m)	1059(s)	1060(s,b)[pr]
1054(s)	1049(m)			
1050(s)	1045(m)		1047(s)	
1037(m)	1032(vs)			1032(s,b)
		1023(m)		
			1015(s)	
		994(s)		∿995(s,sh)[pr]
953(s)			∿953(w,b)[pr]	
948(s)	948(w)			
		∿920(m,b)[pr]	924(m,b)	
915(w)	912(s)			
893(vs)	888(vs)	∿895(sh)[pr]		
		885(s)	881(vs)	
860(vs)	859(s)		861(vs)	
				∿855(vs,sh)[pr]
		∿838(sh)		∿840(vs)[pr]
		828(vs)		
			∿802(w,sh)[pr]	
749(s)	748(s)	743(s)		
			738(m)	
				726(w,b)

TABLE I (Continued)

VIBRATIONAL SPECTRA OF RIBITOL

Solid		Deuterated	Solution[a]	
Δν, Raman, cm^{-1}	ν, IR, cm^{-1}	Δν, Raman, cm^{-1}	Δν, (H_2O) Raman, cm^{-1}	Δν, (D_2O) Raman, cm^{-1}
∿695(vvw,b)	∿695(sh,b)	∿695(vw,b)	∿700(w,b)	∿694(w,b)
628(m,b)	624(s,b)	622(s)		
			∿618(m,b)	∿611(m,b)[pr]
∿575(vvw,b)	574(s,vb)	∿578(vw,b)	561(m,sh)	∿558(m,sh)[pr]
529(s)	∿529(m,sh)	527(s,b)	531(s)	∿525(s,sh)[pr]
			487(s,b)	481(s,b)
478(m)	470(m,sh)	473(m)		
458(w)	453(m,sh)	∿458(sh)	∿455(sh)	∿461(sh)
∿388(vw)				
351(w)			353(vs)	343(vs)
		344(m)		
327(w)				
		323(w)		
∿310(vw,b)		∿308(w,b)		
274(w,b)				
		267(m,b)		
234(w,b)		∿235(m,b)		
209(m)		∿209(m)		
202(m)		∿197(m)		

[a] Saturated.

[b] Conventional symbolism indicating relative intensity: vs = very strong; s = strong; m = medium; w = weak; v = very; b = broad; sh = shoulder.

[pr] Poor resolution.

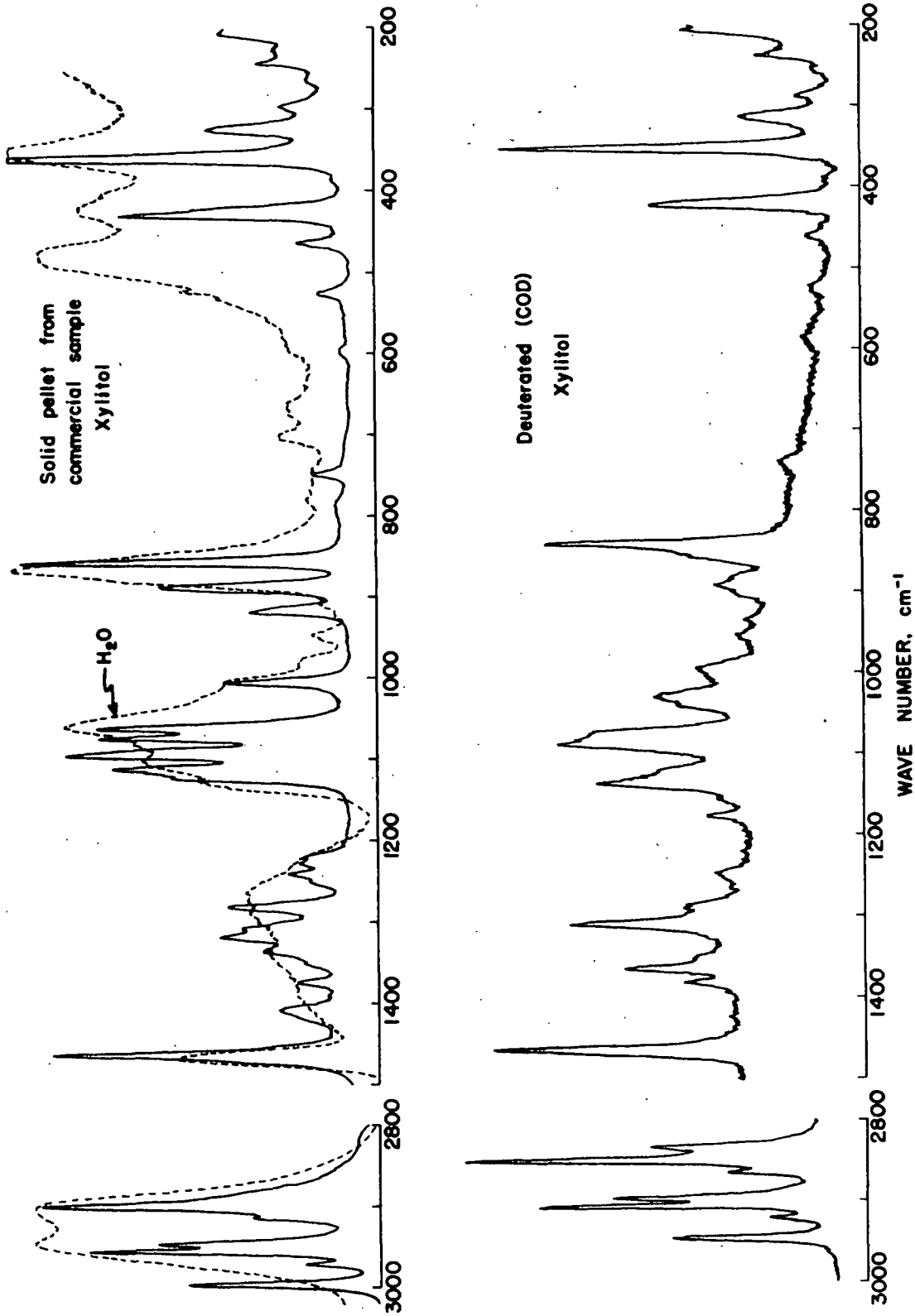

Figure 4. Raman Spectra of Xylitol

TABLE II

VIBRATIONAL SPECTRA OF XYLITOL

Solid		Deuterated	Solution (H_2O)[a]
$\Delta\nu$, Raman, cm^{-1}	ν, IR, cm^{-1}	$\Delta\nu$, Raman, cm^{-1}	$\Delta\nu$, Raman, cm^{-1}
3435[pr]	3420(vs,b)[b]		
3362[pr]	3360(vs,b)		
3302[pr]	3290(vs,b)		
2998(s)	2997(s)	2997(s)	
2972(w)	2972(m)	2972(w)	
2957(vs)	2955(m)	2956(vs)	
2948(s)	2945(s)	2946(s)	2948(vs,b)
2915(m)	2916(vs)	2914(m)	
2900(vs)		2899(vs)	2905(vs,b)
2889(sh)		2883(s)	
		2545(w)	
		2500(m)	
		2428(w)	
		∿2405(w)	
		∿2360(w,b)	
1464(vs)		1465(vs)	2468(s)
1452(sh)[pr]		1454(m,sh)	
1440(vw)			
1424(sh)			
			∿1415(vw,b)
1407(w)	1409(s)		
			∿1390(w,b)
		1380(m)	
1374(w,sh)	1374(s)	1364(s)	
1352(vw,b)	1351(s)	1353(m,sh)	∿1352(m,b)
1346(w,sh)			
1335(w)	1331(vw)		∿1337(m,b)
1319(m)	1312(s)		∿1315(m,b)
1308(m)	1305(sh)	1309(s)	∿1300(m,b)
?1298(w)			

TABLE II (Continued)

VIBRATIONAL SPECTRA OF XYLITOL

Solid		Deuterated	Solution (H_2O)[a]
$\Delta\nu$, Raman, cm^{-1}	ν, IR, cm^{-1}	$\Delta\nu$, Raman, cm^{-1}	$\Delta\nu$, Raman, cm^{-1}
1281(s)	1280(s)	1288(m)	∿1287(m,b)
			∿1267(m,b)
1243(m)	1248(m)	1247(w)[pr]	∿1254(sh,b)
1231(w)[pr]			
1225(w)[pr]			∿1225(w,b)
1219(w)	1218(vw)		∿1210(vw,b)
		1176(w)	
		1157(w,sh)[pr]	
		1137(s)	
1122(sh)	1124(vs)	1126(sh)[pr]	1128(s,sh)[pr]
		1120(m)[pr]	
1110(s)	1111(vs)		1110(sh)[pr]
			1103(s)
1094(vs)	1094(vs)		
1089(vs,sh)	1087(vs,sh)	1087(s)	1080(b)[pr]
1073(vs)	1076(sh)	1075(s,sh)[pr]	
1061(vs)	1067(vs)		1060(vs,b)
		1040(sh)	
1032(vw)		1030(m)	1030(sh)?[pr]
1007(m)	1010(vs)		1007(s)
		998(m)	
			983(w,b)[pr]
		∿942(vvw)[pr]	948(w,b)
		∿930(vvw)[pr]	
921(m)			920(vvw)[pr]
914(m)			910(vw)[pr]
		∿905(sh)	
889(s)	887(s)	893(w)	
		880(vw)	878(sh)
			865(vs,b)

TABLE II (Continued)

VIBRATIONAL SPECTRA OF XYLITOL

Solid		Deuterated	Solution (H_2O)[a]
$\Delta\nu$, Raman, cm^{-1}	ν, IR, cm^{-1}	$\Delta\nu$, Raman, cm^{-1}	$\Delta\nu$, Raman, cm^{-1}
858(vs)	860(vs)	853(m,sh)	
		840(vs)	∿780(vvw,b)[pr]
750(v,vw)	742(vs)	∿738(vvw)	∿750(vvw,b)[pr]
	∿698(vvw,sh)		704(w)
			665(w,b)[pr]
∿600(vvw)	∿598(s)		592(w,b)[pr]
		∿575(vvw,b)	578(w,b)[pr]
	563(s)		560(sh)[pr]
			530(sh)
520(w)	520(vs)	∿525(vvw,b)	522(sh)
			480(vs,b)
464(w)		∿460(vvw)	
428(vs)	433(w)	420(s)	421(vs,b)
			402(sh)[pr]
385(w)			
360(vs)			
		351(vvs)	350(vvs)
324(m)			
		313(m)[pr]	
297(w)			
		288(w,b)	
∿277(w)			
		254(vvw)[pr]	
243(vw)		236(m)	
226(w)			
207(m)		205(s)	
		196(s)	

[a] Saturated.

[b] Conventional symbolism indicating relative intensity: vs = very strong; s = strong; m = medium; w = weak; v = very; b = broad; sh = shoulder.

[pr] Poor resolution.

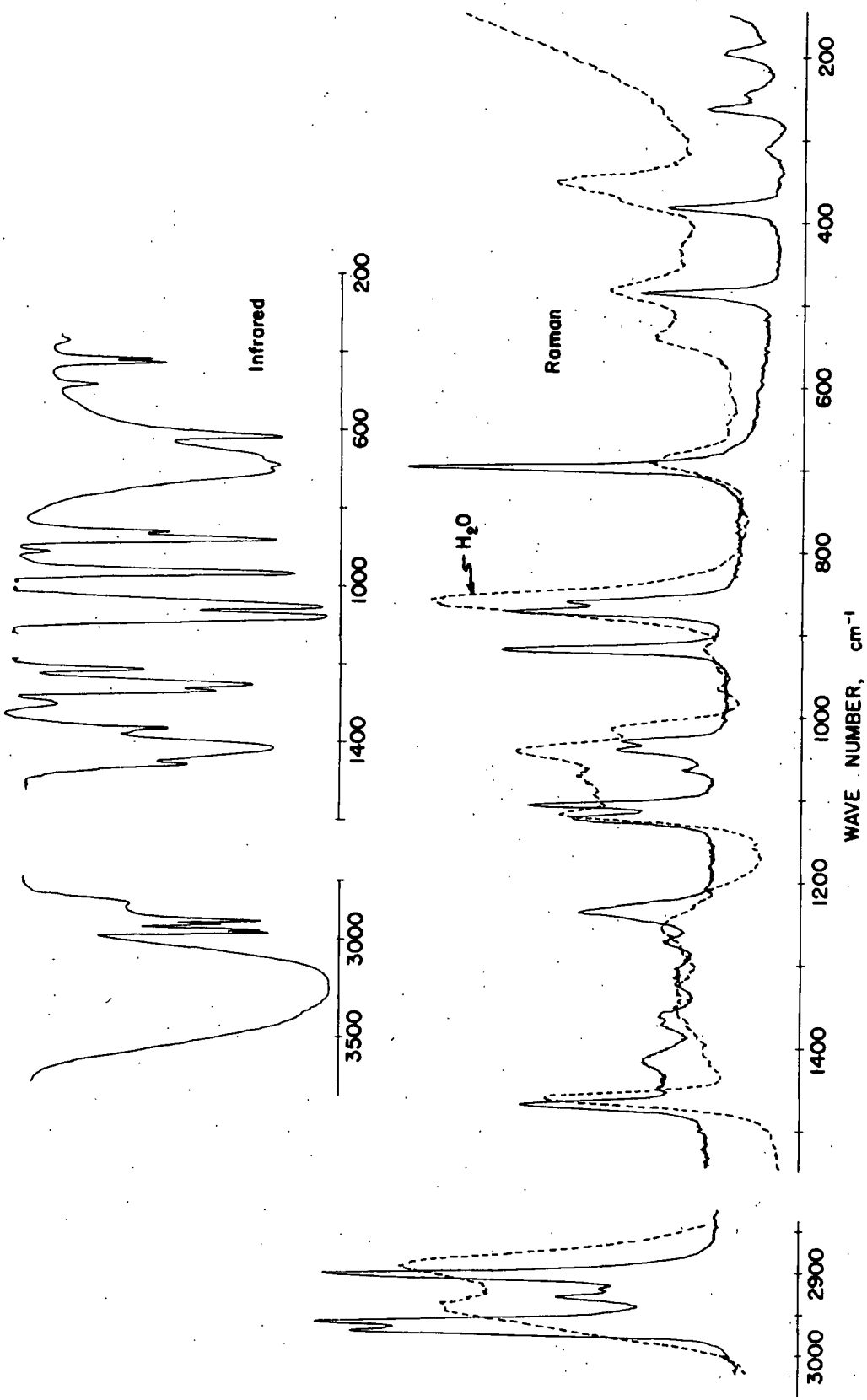

Figure 5. Vibrational Spectra of Erythritol

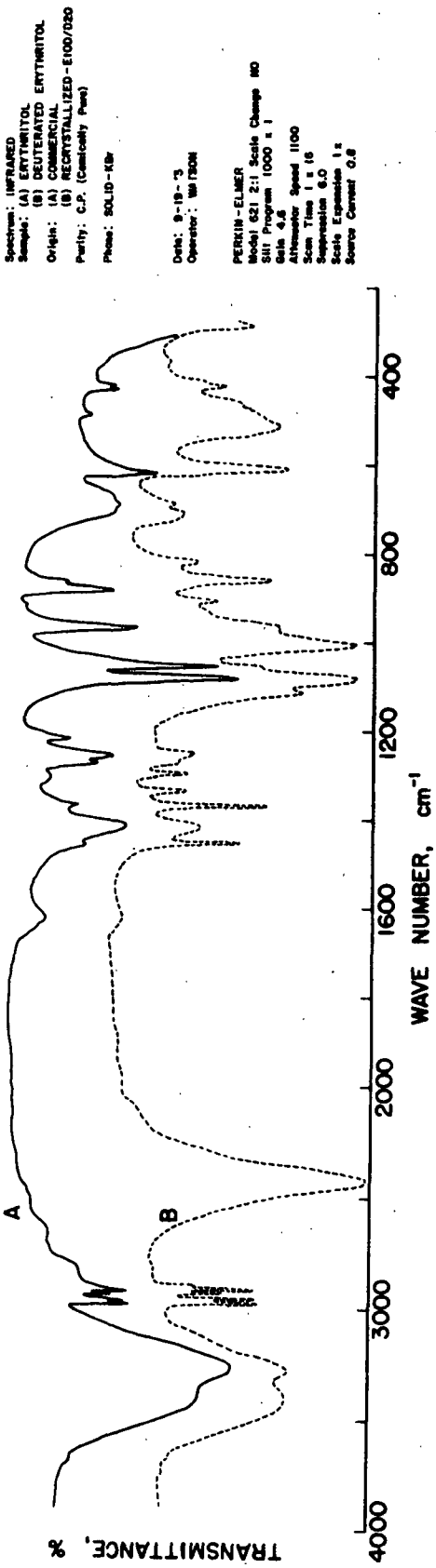

Figure 6. Infrared Spectra of Erythritol and Deuterated Erythritol

TABLE III

VIBRATIONAL SPECTRA OF ERYTHRITOL

Solid		Deuterated	Solution (H_2O)[a]
$\Delta\nu$, Raman, cm^{-1}	ν, IR, cm^{-1}	ν, IR, cm^{-1}	$\Delta\nu$, Raman, cm^{-1}
	3285(b)[b]		
	3250(b)		
2972(vs)	2975(vs)		
2963(vs)	2965(vs)		
			2943(vs,b)
2930(s)	2935(s)		
2919(m)	2918(vs)		
2903(vs)	2902(m)		
	2890?		2894(vs,b)
		2425(vs,b)	
		2380(sh)	
1469(s)	1469(m)		1461(s)
1450(w)	1456(s)	1455(s)	
1415(w)	1414(vs)	∿1418(m,b)	∿1420(w,b)[pr]
			∿1404(w,b)[pr]
1373(w)	1375(w,sh)	1370(s)	∿1373(m,b)[pr]
1366(w)	1366(m)		
		1335(m)	∿1340(m,b)[pr]
1324(vw)			
1306(vw)	1307(w)		
		1295(m)	
			∿1282(m,b)[pr]
1273(m)	1271(s)	1270(w,sh)	
	1254(s)	1252(m,b)	∿1257(m,b)[pr]
1245(sh)			
1236(m)			
			∿1228(w,sh)[pr]
	1216(m)		
			∿1210(w,sh)
			∿1155(vvw)

TABLE III (Continued)

VIBRATIONAL SPECTRA OF ERYTHRITOL

Solid		Deuterated	Solution (H_2O)[a]
$\Delta\nu$, Raman, cm^{-1}	ν, IR, cm^{-1}	ν, IR, cm^{-1}	$\Delta\nu$, Raman, cm^{-1}
1121(m)	1121(vw)		1118(s)
		1115(vs,sh)	∿1110(sh)[pr]
1107(s)			
		1083(vs)	∿1095(s)[pr]
∿1068(w)	1078(vs)		∿1070(s)[pr]
	1053(vs)	1055(s,sh)	1053(sh)
1040(m)	1038(sh)		1043(vs,b)
1030(m)			
			1015(s)
		1008(vs)	
		990(s,sh)[pr]	
	968(vs)	965(s,sh)	∿965(w)
		935(m,sh)[pr]	∿935(w,b)[pr]
918(vs)	918(vw)		∿915(w,b)[pr]
		908(m)	
874(vs)	880(vs)		
862(s)	865(s)	860(s)	862(vs)
		820(m)	
		∿800(sh)[pr]	
			∿742(vvw)
	709(sh)	711(m,b)	
698(vs)	692(vs,b)	690(m,sh)	692(s,b)
	?672(sh)		
			∿645(vvw)
	620(vs)		
		611(s)	
		540(sh)[pr]	540(m,b)
			∿525(sh)[pr]
		515(s,b)	
486(m)	488(m)	490(sh)	483(s,b)

TABLE III (Continued)

VIBRATIONAL SPECTRA OF ERYTHRITOL

Solid		Deuterated	Solution (H_2O)[a]
$\Delta\nu$, Raman, cm^{-1}	ν, IR, cm^{-1}	ν, IR, cm^{-1}	$\Delta\nu$ Raman, cm^{-1}
		465(sh)[pr]	
	431(m)		
	422(m)		
		425(m)	
		415(sh)[pr]	
383(m)	378(vw)	370(w,b)[pr]	∿374(sh)
350(vw)			354(s,b)
312(w)			
263(m)			
245(w)			

[a] Saturated.

[b] Conventional symbolism indicating relative intensity: vs = very strong; s = strong; m = medium; w = weak; v = very; b = broad; sh = shoulder.

[pr] Poor resolution.

ARABINITOLS

The spectra of D,L-arabinitol were measured in an effort to determine whether there were any significant differences between the spectra of the racemic form and the spectra of the D and L isomers. The Raman and IR spectra of D and D,L-arabinitol are compared in Fig. 7 and 8, respectively. The frequencies of the observed bands are listed in Table IV. Since the L spectra are identical to the D spectra, they have not been reported. From Fig. 7 and 8 it is apparent that the spectra of these two crystalline forms are different. The nature of the observed differences will be discussed in detail later.

By comparing the frequencies of the observed bands in the solid-state spectra of the pentitols, differences are seen to occur in all regions. Also, the Raman spectra recorded for concentrated H_2O solutions of ribitol, xylitol, and erythritol are distinctly different in many regions when compared to the spectra of the powdered solids. Broadening due to solute-solvent interactions limited the resolution of many bands. This was especially true of the CH stretching region. However, a major departure from the solid-state spectra was the appearance of new bands in the spectra of the solutions. The new bands usually appeared in the regions below 1100 cm^{-1}.

VIBRATIONAL ANALYSES

The central part of the analysis is the solution of the vibrational secular equation. The equation arises as the condition for the existence of simultaneous solutions to the differential equations describing the motion of a molecule in each of the different degrees of freedom.

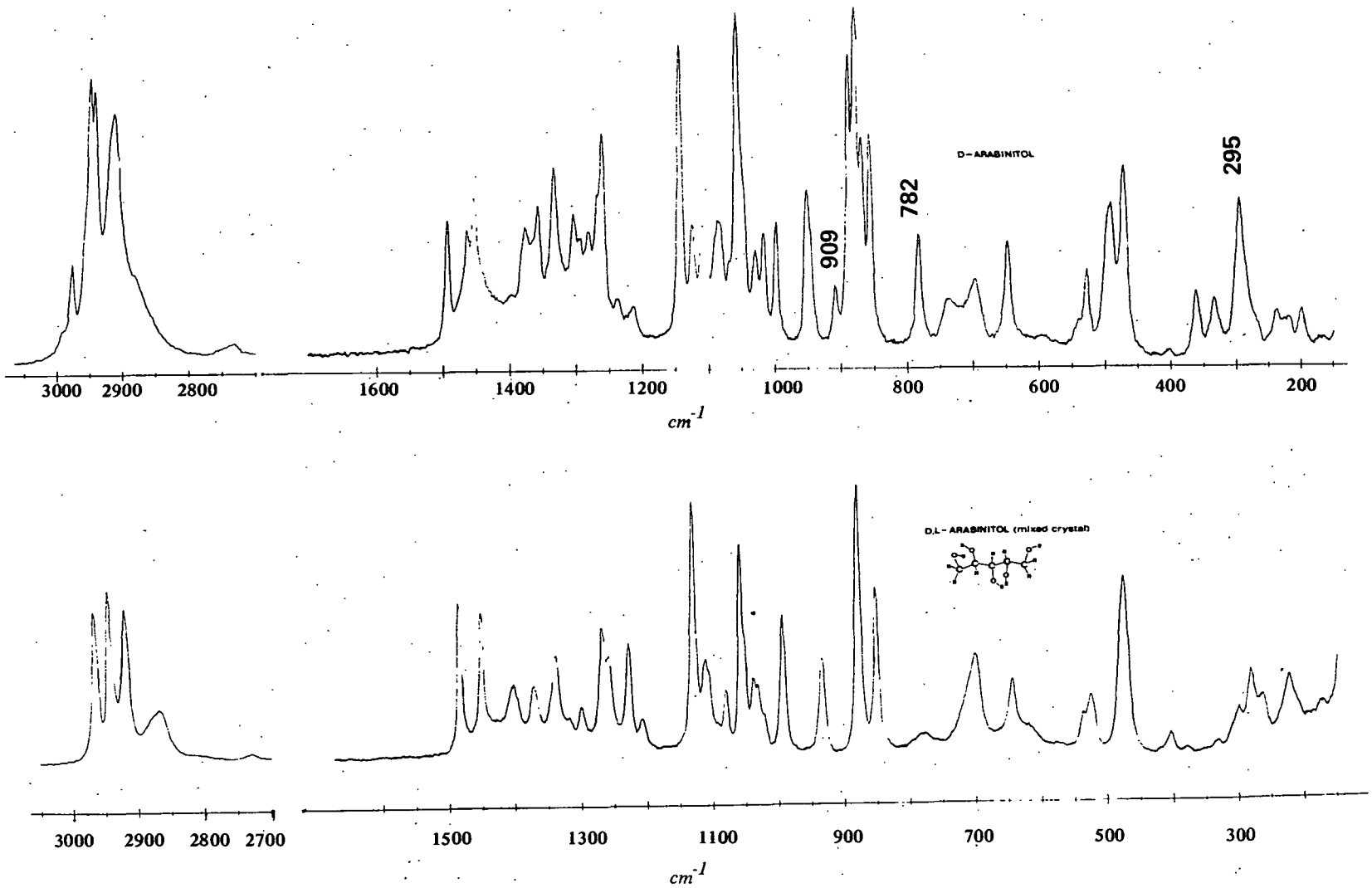

Figure 7. Raman Spectra of D,L-Arabinitol and D-Arabinitol

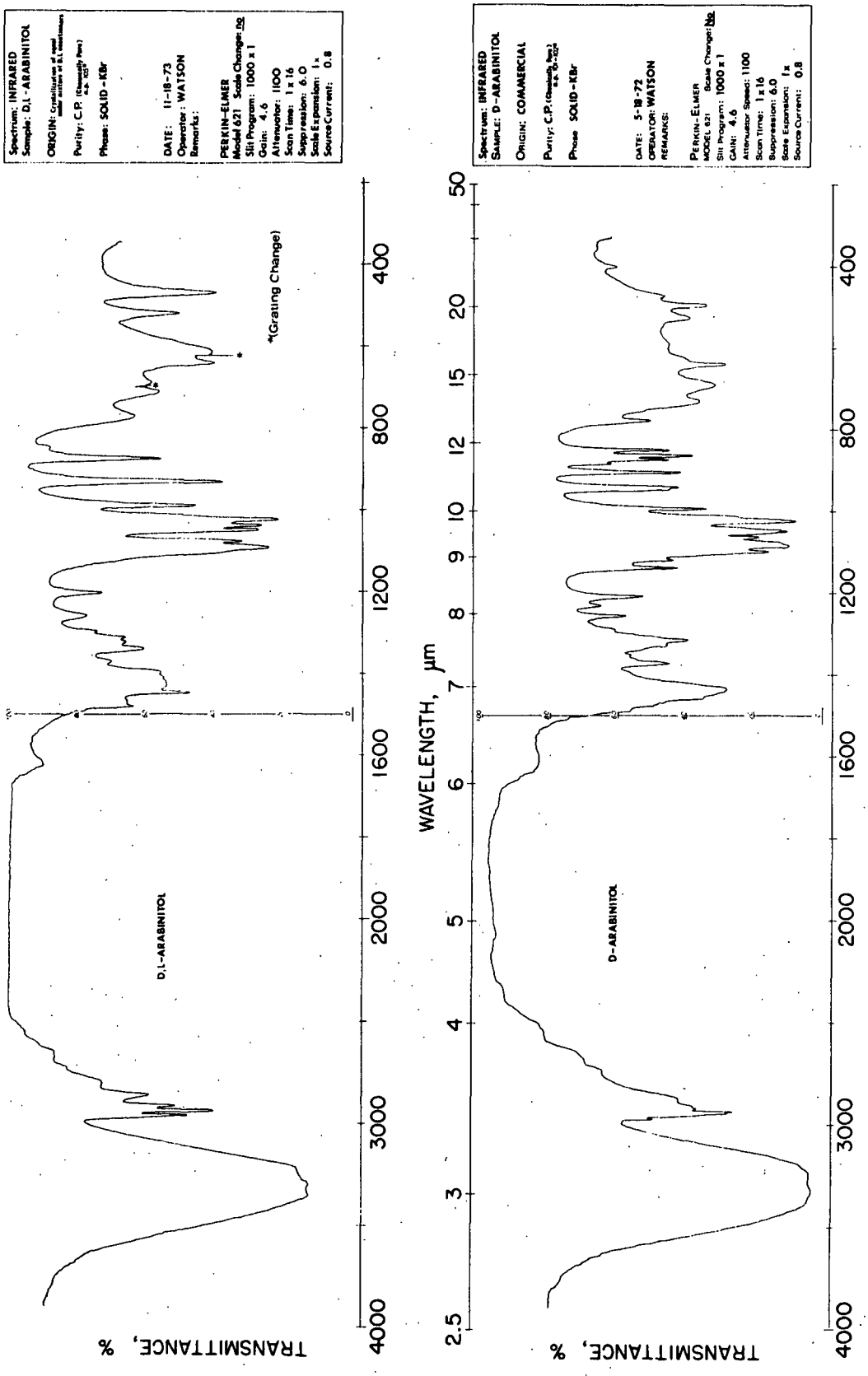

Figure 8. Infrared Spectra of D,L-Arabinitol and D-Arabinitol

TABLE IV

VIBRATIONAL SPECTRA OF D-ARABINITOL AND D,L-ARABINITOL

D-Arabinitol (Solid)		D,L-Arabinitol (Solid)	
$\Delta\nu$, Raman, cm^{-1}	ν, IR, cm^{-1}	$\Delta\nu$, Raman, cm^{-1}	ν, IR, cm^{-1}
	3350(vs)[a]		3350(vs)
	3330(vs,b)		3295(vs,b)
	3320(vs,b)		3215(vs,b)
2990(w,sh)			
2977(m)	2971(w)		
		2966(vs)	
	2957(m,sh)		
2947(vs)	2945(s)	2945(vs)	2945(vs)
2939(vs)	2939(s)		
2920(s,sh)	2921(m)	2920(vs)	2919(s)
2910(vs,b)	2906(m)		
2882(m,sh)			
		2877(sh)	2870(sh)
		2868(w,b)	2865(m,b)
1494(s)	1491(w,sh)	1486(s)	1481(m)
1464(s,sh)	1462(m,sh)[pr]		1465(m,sh)[pr]
1454(s)	1450(m,sh)[pr]	1454(s)	1448(s)
1440(w,sh)	1440(s,b)[pr]		1425(m,b)[pr]
		1406(m)	
1395(vw,b)	1395(vvw)		1395(m,sh)[pr]
1375(s)	1372(m)	1375(m)	1372(w)
1357(s)	1352(vvw)	1342(s)	1340(m)
1333(vs)	1330(m,sh)		
		1323(vw,b)	1325(m)
	1314(m)		1312(m)
1304(s)	1304(w,sh)	1302(w)	1298(w)
1294(m)	1293(vw,sh)		
1280(m)	1280(vw)		
1268(s,sh)	1268(vw,sh)	1271(s)	
1260(vs)	1259(w)	1262(m)	1265(w,sh)

TABLE IV (Continued)

VIBRATIONAL SPECTRA OF D-ARABINITOL AND D,L-ARABINITOL

D-Arabinitol (Solid)		D,L-Arabinitol (Solid)	
$\Delta\nu$, Raman, cm^{-1}	ν, IR, cm^{-1}	$\Delta\nu$, Raman, cm^{-1}	ν, IR, cm^{-1}
1237(w)[pr]	1234(vw)[pr]	1230(s)	
1213(w)[pr]	1211(w)[pr]	1209(w)	1205(m)
1143(vs)	1140(m)		
		1133(vs)	1132(w,sh)
1124(m)	1122(m)		
		1115(m)	
1109(m)	1102(s)	1110(m,sh)	1109(s,sh)
1089(m,sh)	1088(vs)		1090(vs)
1086(m)	1085(vs,sh)	1084(m)	1081(vs)
1069(w)	1069(s)		
1057(vs)	1055(s,sh)	1061(vs)	1055(sh)
1049(sh)	1050(vs)		1053(vs)
		1040(m)	1040(vs)
		1035(m,sh)	
1028(w)	1028(vs)	1025(w,sh)	1025(vs)
1016(m)	1015(s,sh)		
997(m)	995(m)	996(s)	990(vs)
951(s)	950(m,sh)		
945(m,sh)	943(m)		
		938(s)	933(vs)
909(w)	905(m)		
887(vs)	885(m)	882(vs)	878(s)
878(vs)	877(m)		
867(s)	866(m)		
855(s)	855(m)	855(s)	850(w)
782(m)	780(w)	782(vw)	773(m,b)
736(w,b)	735(m,b)		
		708(s,b)	712(s,b)
697(m,b)	692(m,b)		694(s,b)
647(m)	643(s)	647(m)	642(vs)

TABLE IV (Continued)

VIBRATIONAL SPECTRA OF D-ARABINITOL AND D,L-ARABINITOL

D-Arabinitol (Solid)		D,L-Arabinitol (Solid)	
$\Delta\nu$, Raman, cm^{-1}	ν, IR, cm^{-1}	$\Delta\nu$, Raman, cm^{-1}	ν, IR, cm^{-1}
595(vvw)[pr]	595(vw,b)		
540(vw)	538(vvw)	540(w,sh)	535(vw,sh)
528(m)	526(m)	528(m)	522(s)
491(s)	495(m)		
472(s)	470(m)	478(vs)	470(s)
405(vvw)	400(vvw)	406(vw)	400(vw)
363(m)			
			350(vw)
334(m)		330(vvw)	330(m,b)
325(w)			
		303(m,sh)	300(w)
295(s)			
		284(s)	
275(w,sh)			
		267(m,sh)	
235(w)		235(w,sh)	
		227(m,b)	
		215(w,sh)	

[a] Conventional symbolism indicating relative intensity: vs = very strong; s = strong; m = medium; w = weak; v = very; b = broad; sh = shoulder.

[pr] Poor resolution.

Wilson, et al. (16) have described in detail the essential elements of the theory behind the NC analysis of molecular vibrations. The mathematical treatment of the vibrations is initiated by defining the kinetic and potential energies of a model in terms of a suitable set of coordinates. The model is generally specified to consist of (1) point masses representing the atoms and (2) force constants which represent the intramolecular forces holding the atoms in an equilibrium configuration.

From the kinetic and potential energies of the model it is then possible to derive the differential equations which describe the vibrational motion of the model. The simultaneous solutions to these differential equations result in a set of algebraic equations. In terms of internal coordinates, these equations, in matrix form, may be expressed as

$$(\underset{\sim}{GF} - \lambda_k \underset{\sim}{E})\, \underset{\sim}{l}_k = 0 \qquad (1)$$

where $\underset{\sim}{G}$ = the inverse kinetic energy matrix

$\underset{\sim}{F}$ = force constant matrix

λ_k = frequency parameters = $4\pi^2\nu_k^2$ (where ν_k^2 is a fundamental frequency of the oscillator)

$\underset{\sim}{E}$ = unit matrix

$\underset{\sim}{l}_k$ = is a column vector of the amplitudes of the various displacement coordinates in the kth vibration.

There are three components in Equation (1):

(1) the structure of the molecular model,

(2) the force constants,

(3) the vibrational frequencies.

The $\underset{\sim}{G}$ matrix is easily derivable from known structural data. Thus, in systems where the force constant matrix (i.e., the $\underset{\sim}{F}$ matrix) is known, the solution to the vibrational problem is straightforward. The $3n-6$ frequency parameters (or $3n-5$ for linear molecules) can be evaluated directly. The eigenvalues, λ_k, are the roots of the secular determinant (i.e., characteristic equation)

$$\det (\underset{\sim}{GF} - \lambda_k \underset{\sim}{E}) = 0 \qquad (2)$$

Equation (2) is the vibrational secular equation. Solving this equation is fundamental to the NC analysis process.

In the present instance, however, the elements of the $\underset{\sim}{F}$ matrix are unknown. They may be obtained by a method of successive iterations beginning with approximations to the force constants in the $\underset{\sim}{F}$ matrix. The calculated frequency parameters (i.e., eigenvalues of $\underset{\sim}{GF}$) will not be equal to those derived by experiment. The differences between the observed and calculated frequencies form a basis for determining better approximations of the force constant parameters in the $\underset{\sim}{F}$ matrix.

The basic framework used for the NC analyses was based on the Wilson $\underset{\sim}{GF}$ method (16) and Pitzner's (1) modification of programs developed by Schachtschneider (18,19). It involves a sequence of iterations in which a set of force constant parameters, Φ_i, are adjusted to reduce the least-squares deviation between observed frequencies, $\lambda_{obs.}$, and calculated frequencies, $\lambda_{cal.}$, such that

$$Q^r = \sum_k P_k [\lambda_{k(obs.)} - \lambda_{k(cal.)}]^2. \qquad (3)$$

In Equation (3), Q^r is the value of the sum of the squared residuals after the rth iteration. P_k is an element of an arbitrary weighting matrix P. The sum Q is a "function" of the independent force constant parameters. That is, if any parameter Φ_i is varied, a change in Q will result. Therefore, we can consider the parameters Φ_i as independent "variables" and Q is a "function" of these "variables."

A nonlinear least-squares refinement method developed by Fletcher-Powell (22) (FP) and employed by Pitzner (1) in his study of the 1,5-AHP's was used. Gans (24) has also used the FP minimization algorithm successfully. The main features of the NC analyses and nonlinear least-squares refinement of the force constants are shown in Fig. 9. The flow diagram can be divided in four basic parts:

(1) Data input,

(2) Solving the secular equation,

(3) Refining the initial constants using the FP method, and

(4) Results.

DATA INPUT

The Internal Coordinates Chosen for the NC Analyses

These coordinates were defined in accordance with the suggestions of Decius (25). The three types of internal valence coordinates used to describe the vibrational displacements were: (1) valence bond stretching; (2) valence angle bending; and (3) torsion. For the pentitols, 65 internal coordinates were defined to describe each molecule. Since each of these molecules has 60 internal degrees of freedom, there are 5 implied redundancies. These are local and removable, but they are included to facilitate the construction of a

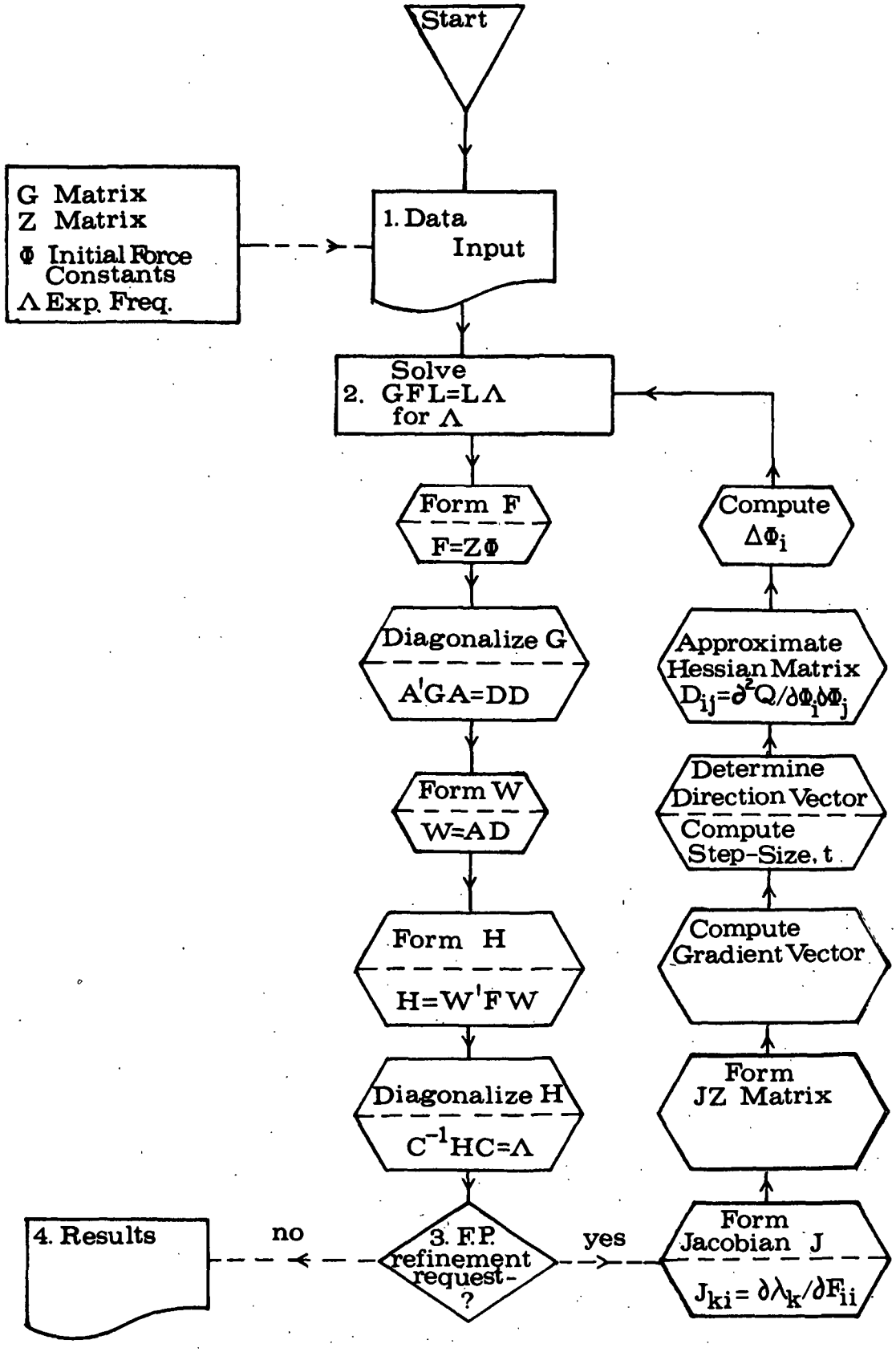

Figure 9. General Flow Diagram for the Basic Force Constant and Normal Coordinate Calculations

simplified valence quadratic force field. There are 21 valence bond stretching coordinates, 35 valence bond angle bending coordinates, and 9 torsional coordinates.

A total of 52 internal coordinates were used to describe erythritol. These included 17 valence bond stretching coordinates, 28 valence angle bending coordinates, and 7 valence angle torsion coordinates. Since erythritol has 48 internal degrees of freedom, there are four redundancies. The significant input data appear in Appendix I. Tables XVIII-XX describe the internal coordinates for each of the four molecules.

The $\underset{\sim}{G}$ Matrix

The number of internal coordinates used to define the vibrational motion of a molecule also determines the order of its $\underset{\sim}{G}$ matrix. Thus, the $\underset{\sim}{G}$ matrix of erythritol would be of lower order than the $\underset{\sim}{G}$ matrices of the other alditols. Of general significance is the fact that the $\underset{\sim}{G}$ matrix depends only on the masses of the atoms and the geometry of the molecule. Also, the $\underset{\sim}{G}$ matrix is always symmetric and always positive definite, that is, its eigenvalues are all real and positive.

More formally, the $\underset{\sim}{G}$ matrix is defined in terms of the atomic masses and a transformation matrix commonly referred to as the $\underset{\sim}{B}$ matrix. The $\underset{\sim}{B}$ matrix is defined in the following expression

$$\underset{\sim}{S} = \underset{\sim}{B}\underset{\sim}{X} \qquad (4)$$

where $\underset{\sim}{S}$ = internal displacement coordinates expressed as a vector

$\underset{\sim}{X}$ = cartesian displacement coordinates expressed as a vector.

The $\underset{\sim}{B}$ matrix is rectangular with $3n$ columns and as many rows as there are internal coordinates. The $\underset{\sim}{G}$ matrix is usually given as

$$\underset{\sim}{G} = \underset{\sim}{B}\underset{\sim}{M}^{-1}\underset{\sim}{B}' \qquad (5)$$

where $\underset{\sim}{M}^{-1}$ = diagonal matrix of order $3n$ whose elements are the inverses of the atomic masses each being present 3 times

$\underset{\sim}{B}'$ = transpose of the $\underset{\sim}{B}$ matrix.

The specific details of the $\underset{\sim}{G}$ matrix development are presented elsewhere by Wilson, et al. (16).

To determine the $\underset{\sim}{G}$ matrix it is necessary to calculate the cartesian coordinates of the "atoms" in the alditol models. These coordinates were computed from the internal coordinates. The structural data necessary for these computations is specified in Appendix I. The bond lengths and bond angles of xylitol, ribitol, erythritol and D-arabinitol are specified in Tables XXI-XXIV. The "atoms" in each of these molecular models were numbered in the manner depicted in Fig. 21.

The coordinates of ribitol and xylitol are based on their respective crystal structures determined by Jeffrey, et al. (26,27) using x-ray diffraction techniques. As previously mentioned, the structural data for D-arabinitol was based on the structure of the D isomer in the D,L crystal (20). However, the structural data for erythritol was obtained from several sources. The bond distances and angles of all coordinates not involving hydrogen atoms were taken from the structural data of Bekoe and Powell (23). The remaining internal coordinates were estimated by averaging the appropriate coordinates from the crystal structures of the other alditols.

In all cases an average bond length of 0.97 A was used for OH coordinates, 1.093 A for methylene CH coordinates, and 1.120 A for the methine CH coordinates. These distances are longer than those reported for the alditols, but are consistent with thermodynamic and neutron diffraction data. Likewise, an average value of 110.0° was used for all COH bond angles and 109.0° for all CCH bond angles. These values represent averages taken from neutron diffraction studies on α-D-glucose (28), β-D-glucose (29), and D-tartaric acid (30).

The resulting $\underset{\sim}{G}$ matrices of xylitol, ribitol, erythritol, and D-arabinitol are reported in Tables XXV-XXVIII, respectively. Each $\underset{\sim}{G}$ matrix is unique. There are, for example, 855 nonzero elements in the $\underset{\sim}{G}$ matrices of ribitol, xylitol, and D-arabinitol. Of these there are 806 elements in the $\underset{\sim}{G}$ matrix of ribitol that have significantly different values than corresponding elements in the $\underset{\sim}{G}$ matrix of xylitol, and 803 elements which are different than corresponding elements in the $\underset{\sim}{G}$ matrix of D-arabinitol.

The $\underset{\sim}{Z}$ Matrix

Before solving the vibrational secular equation, explicit form must be given to the $\underset{\sim}{F}$ matrix. The force field selected for use in this study is empirical and is an extension of the fields developed by Pitzner (1), Snyder and Schachtschneider (8), and Snyder and Zerbi (9). The field is called a "Simplified Valence Quadratic Force Field" (SVQFF) after Pitzner.

For reasons of convenience, both in the solution of Equation (2) and in the nonlinear refinement of the force constants, the $\underset{\sim}{F}$ matrix is not evaluated directly. A transformation matrix is used instead. The $\underset{\sim}{Z}$ matrix, which is sometimes referred to as the constraint matrix, is defined by the expression

$$F_{ij} = \sum_k Z_{ijk} \Phi_k \qquad (6)$$

where the F_{ij} terms represent elements of the $\underset{\sim}{F}$ matrix. The $\underset{\sim}{Z}$ matrices for each of the alditol compounds are reported in Tables XXIX-XXXIII.

Whereas the $\underset{\sim}{Z}$ matrix is a mathematical formalism, the $\underset{\sim}{F}$ matrix is an integral part of a mathematical expression for an important physical quantity, the potential energy V. For small values of atomic displacement the potential energy in terms of internal coordinates is

$$V = \frac{1}{2}\sum_{k,l}^{3n-6} F_{kl}S_kS_l \qquad (7)$$

where S_k and S_l represent internal displacement coordinates. Actually, the upper limit on the series expansion [Equation (7)] is determined by the total number of internal coordinates used to describe the model and not the $3n-6$ degrees of freedom. Equation (7) is derived from a Taylor series expansion of V as a function of the internal displacement coordinates S_k:

$$2V = 2V_o + 2\sum_k (\partial V/\partial S_k)_o S_l + \sum_{k,l} (\partial^2 V/\partial S_k \partial S_l)_o S_k S_l + \ldots \text{ higher terms}$$

$$= 2V_o + 2\sum_k F_k S_l + \sum_{k,l} F_{kl} S_k S_l + \ldots \text{ higher terms.} \qquad (8)$$

If the potential energy is chosen to be zero at the equilibrium configuration, then $V_o = 0$. In this configuration all the S_k's are zero because the atoms are all in their equilibrium positions. Thus, the potential energy must be at a minimum or

$$2\sum_k F_k S_l = 0 \qquad (9)$$

since $(\partial V/\partial S_k)_o = 0$.

Also, for small amplitudes of vibration, the higher order terms can be neglected so that the potential energy is

$$V = \frac{1}{2} \sum_{k,l} F_{kl} S_k S_l .$$

The $\underline{\underline{F}}_{kl}$ terms represent quadratic force constants and are the elements of the $\underset{\sim}{F}$ matrix.

In a polyatomic molecule, the number of quadratic force constants greatly exceeds the number of frequencies. A general quadratic force field (GQFF) would include all possible $\underline{\underline{F}}_{kl}$ terms (since $\underset{\sim}{F}$ is a symmetric matrix $\underline{\underline{F}}_{kl} = \underline{\underline{F}}_{lk}$). The SVQFF is derived from the GQFF by assuming that many of the $\underline{\underline{F}}_{kl}$ terms are zero and by grouping force constants which are likely to have similar values together. The assumption to assign many of the interaction terms a zero value is based on the likelihood that the potential interactions between nonconjugated bonds with no common nucleus are very small. The effect is to reduce the number of independent force constants, $\underline{\Phi}_i$, necessary to describe the force field of large, complex molecules.

Table V defines the 59 force constant parameters used to specify the SVQFF of the alditol models. Each constant is defined in terms of an internal coordinate or interacting pairs of internal coordinates sharing common atoms. The first 21 constants in Table V are referred to as "diagonal" terms because, as elements, they occupy positions along the diagonal of the symmetric $\underset{\sim}{F}$ matrix. The remaining 43 constants are "off-diagonal" or cross terms.

There are 8 valence bond stretching constants in Table V. Each stretching constant is associated with a particular atomic grouping. There are, however, only two basic types of atomic groupings: (A) the methine (C-C(H)-OH) and (B)

TABLE V

THE SIMPLIFIED VALENCE QUADRATIC FORCE FIELD (SVQFF)
APPROXIMATION CONTAINING 59 INDEPENDENT TERMS

No.	Description[a] (Diag. Terms)	Atomic Grouping	Coordinates Involved	Common Atoms	Values: Alditols Final	Alditols Initial	Error[b]	1,5-AHP's[c]	Others
			Stretch		(mdyn./A)				
1	O'H	C-CH_2-O-H	O-H	--	6.275(0.0)[de]	6.275		0.0	
2	OH	C-C(H)-O-H	O-H	--	6.197(0.0)[e]	6.197		6.283	6.440[f]
3	C'H	C-CH_2-O-H	C-H	--	4.591(-0.13)	4.597	0.016	4.597	4.626[g]; 4.554[h]
4	CH	C-C(H)-O-H	C-H	--	4.593(0.09)	4.589	0.019	4.589	4.688[g]; 4.588[h]
5	C'O	C-CH_2-O	C-O	--	5.088(0.12)	5.082	0.013	0.0	
6	CO	C-C(H)-O	C-O	--	5.046(-0.16)	5.054	0.013	5.103	
7	C'C	C-CH_2-O	C-C	--	4.268(0.49)	4.247	0.013	0.0	
8	CC	C-C(H)-O	C-C	--	4.227(-0.47)	4.247	0.011	4.247	4.261[g]; 4.337[h]
			Bend		[mdyn.A/(rad.)^2]				
9	HC'H	C-CH_2-O	HCH	--	0.474(4.64)[e]	0.452	0.004	0.452	0.471[g]; 0.550[h]
10	HC'C	C-CH_2-O	HCC	--	0.786(-2.04)	0.802	0.007	0.792	0.752[g]; 0.656[h]
11	HCC	C-C(H)-O	HCC	--	0.689(-5.95)	0.730	0.012	0.725	0.718[g]; 0.656[h]
12	HC'O	C-CH_2-O	HCO	--	0.850(1.17)	0.840	0.006	0.0	
13	HCO	C-C(H)-O	HCO	--	1.112(9.44)	1.007	0.021	0.963	
14	C'OH	C-CH_2-O-H	COH	--	0.704(-8.24)	0.762	0.011	0.0	0.760[f]
15	COH	C-C(H)-O-H	COH	--	0.646(-11.16)	0.718	0.011	0.735	0.760[f]
16	C'CC	C-C(H)O-CH_2-O	CCC	--	1.097(4.19)	1.051	0.012	0.0	
17	CCC	C-C(H)O-C(H)-O	CCC	--	1.061(-0.19)	1.063	0.013	1.056	1.071[g]
18	CC'O	C-CH_2-O	CCO	--	1.355(12.40)	1.187	0.031	0.0	
19	CCO	C-C(H)-O	CCO	--	1.274(8.32)	1.168	0.003	1.180	
			Torsion		(mdyn./rad.)				
20	-CC-		C-C		0.042(19.05)	0.034	0.002	0.027	
21	-CO-		C-O		0.055(-3.64)	0.057	0.0	0.028	
	(Off-diagonal)		(Interacting)						
			Stretch-Stretch		(mdyn./A)				
22	CHCC	generalized[i]	CH,CC	C	-0.039(0.0)[e]	-0.039		-0.027	
23	CHCO	"	CH,CO	C	0.015(0.0)[e]	0.015		0.016	
24	CCCC	"	C-C,C-C	C	0.200(46.50)	0.107	0.019	0.107	0.101[g]
25	CCCO	"	C-C,C-O	C	0.212(65.09)	0.074	0.023	0.107	
			Stretch-Bend		(mdyn./rad.)				
26	SB35	generalized	C-O,COH	CO	-0.156(27.56)	-0.113	0.009	0.357	
27	SB36	"	O-H,COH	CO	0.238(0.0)[e]	0.238		0.006	
28	SB32	"	C-H,HCO	CH	-0.157(0.0)[e]	-0.157		-0.167	
29	SB37	"	C-O,HCO	CO	0.368(-3.53)	0.381	0.012	0.388	
30	SB30	"	C-C,CCO	CC	0.363(13.22)	0.315	0.008	0.381	
31	SB31	"	C-C,CCO	CO	0.575(-2.26)	0.588	0.013	0.664	
32	SB33	"	C-C,CCC	CC	0.539(10.02)	0.485	0.001	0.485	0.417[g]

See end of table for footnote.

TABLE V (Continued)

THE SIMPLIFIED VALENCE QUADRATIC FORCE FIELD (SVQFF)
APPROXIMATION CONTAINING 59 INDEPENDENT TERMS

No.	Description[a] (Diag. Terms)	Atomic Grouping	Coordinates Involved	Common Atoms	Values: Alditols Final	Alditols Initial	Error[b]	1,5-AHP's	Others
			Stretch-Bend		(mdyn./rad.)				
33	SB29	generalized	C-H,CCH	CH	-0.107(-99.06)	-0.213	0.012	-0.167	
34	SB34	"	C-H,HCH	CH	-0.160(0.0)[e]	-0.160		-0.167	
35	SB28	"	C-C,CCH	CC	0.344(-32.27)	0.455	0.006	0.481	0.478[g]; 0.328[h]
			Bend-Bend		[mdyn.A/(rad.)^2]				
36	BB61	generalized	HCH,CCH	CH	0.026(-11.54)	0.029	0.009	0.025	
37	BB60	"	CCH,CCC	CC	-0.238(48.74)	-0.122	0.013	-0.094	-0.031[g]
38	BB55	"	CCH,HCO	CH	0.150(8.67)	0.137	0.006	0.135	0.115[g]
39	BB54	"	HCH,HCO	CH	-0.027(0.0)[e]	-0.027		0.0	
40	BB52	"	CCH,CCO	CC	-0.110(56.36)	-0.048	0.011	-0.094	
41	BB53	"	HCO,HCO	CO	-0.012(0.0)[e]	-0.012		-0.005	
42	BB59	"	HCO,CCO	CO	-0.097(-22.68)	-0.119	0.013	-0.094	
43	BB46	"	CCO,CCO	CO	0.063(33.33)	0.042	0.012	0.052	
44	BB47	"	CCO,CCC	CC	-0.098(135.71)	0.035	0.025	0.052	
45	BB41	HC-CH(trans)	CCH,CCH	CC	0.077(0.0)[e]	0.077		0.049	0.121[g]; 0.127[h]
46	BB49	HC-CC(trans)	HCC,CCC	CC	-0.041(0.0)[e]	-0.041		-0.047	0.049[g]
47	BB58	HC-OH(trans)	HCO,COH	CO	0.042(0.0)[e]	0.042		0.016	
48	BB56	CC-OH(trans)	CCO,COH	CO	-0.052(69.23)	-0.016	0.013	0.010	
49	BB42	CC-CC(trans)	CCC,CCC	CC	-0.022(40.91)	-0.013	0.012	-0.014	-0.011[g]
50	BB45	OC-CO(trans)	CCO,CCO	CC	0.004(425.00)	-0.013	0.013	-0.014	
51	BB62	CC-CO(trans)	CCO,CCC	CC	-0.027(51.85)	-0.013	0.010	-0.014	
52	BB40	HC-CH(gauche)	CCH,CCH	CC	-0.021(0.0)[e]	-0.021		-0.002	0.004[g];-0.005[h]
53	BB48	HC-CC(gauche)	HCC,CCC	CC	-0.167(5.39)	-0.158	0.006	-0.106	-0.052[g]
54	BB50	HC-CO(gauche)	HCC,CCO	CC	-0.123(-119.51)	-0.270	0.012	-0.238	
55	BB57	HC-OH(gauche)	HCO,COH	CO	0.036(0.0)[e]	0.036		0.0	
56	BB64	CC-OH(gauche)	CCO,COH	CO	-0.027(37.04)	-0.017	0.012	0.010	
57	BB43	CC-CC(gauche)	CCC,CCC	CC	-0.047(53.19)	-0.022	0.013	-0.024	0.011[g];-0.024[h]
58	BB44	OC-CO(gauche)	CCO,CCO	CC	0.070(125.71)	-0.018	0.024	-0.024	
59	BB63	CC-CO(gauche)	CCO,CCC	CC	-0.105(81.90)	-0.019	0.006	-0.024	

[a] I.e., the descriptive code for the force constant terms as they appear in the potential energy distributions.

[b] The standard error in the force constants, $\sigma(\Phi_i)$, is estimated from a matrix developed in the refinement which approximates the variance-covariance matrix.

[c] Values taken from Pitzner (1).

[d] The values in parentheses correspond to the percentage difference between the final force constants (Φ^a) and the initial force constants (Φ^b): % difference = $\frac{100(\Phi^a - \Phi^b)}{\Phi^a}$.

[e] Not included in the final refinement.

[f] Values taken from Vasko (3,13).

[g] Values taken from Snyder and Zerbi (9).

[h] Values taken from Snyder and Schachtschneider (8).

[i] I.e., the interaction constant applies equally to both methylene and methine atomic groupings.

the methylene ($C-CH_2-OH$). These are depicted in Fig. 10 and are appropriately designated in Table V.

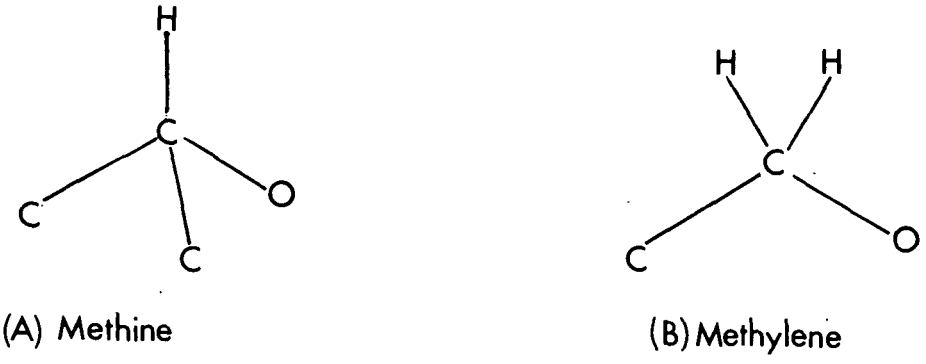

(A) Methine (B) Methylene

Figure 10. Different Atomic Groupings Defined

A similar distinction is made for the constants which relate to valence angle bending, but not for the torsion constants or the interaction constants. However, a distinction is made between a "trans" and a "gauche" bend-bend interaction when they are centered on adjacent carbon atoms. Figure 11 illustrates how some of the possible interaction force constants are defined. Only nearest neighbor interactions are considered. This implies that all stretch-stretch interaction constants must contain a common atom and all stretch-bend and bend constants must contain two common atoms.

SOLVING THE SECULAR EQUATION

There are many methods for solving secular equations. However, for large molecules digital computers and methods amenable to machine computation must be used. To compute the eigenvalues, λ_k, of the secular determinant it is necessary to separate the $\underset{\sim}{GF}$ matrix product from the $\lambda_k \underset{\sim}{E}$ product in Equation (1) such that

$$\underset{\sim}{GF}\underset{\sim}{l}_k = \lambda_k \underset{\sim}{E}\underset{\sim}{l}_k. \qquad (10)$$

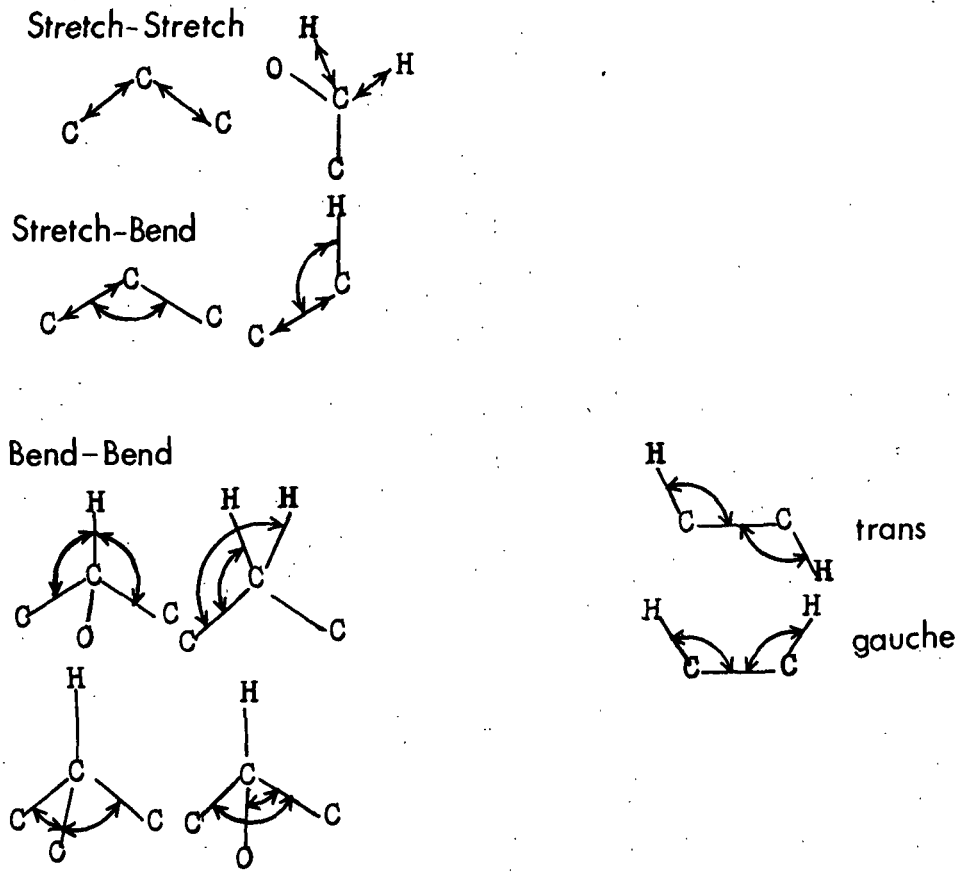

Figure 11. Some Interaction Force Constants Defined

There will be equivalent expressions for each λ_k. These equations can be combined. The vibrational equation can then take the form

$$\underset{\sim}{GFL} = \underset{\sim}{L\Lambda} \tag{11}$$

where $\underset{\sim}{\Lambda}$ is a diagonal matrix of the frequency parameters, λ_k, and $\underset{\sim}{L}$ is the transformation from normal coordinates, $\underset{\sim}{Q}$, to internal coordinates, $\underset{\sim}{S}$, such that

$$\underset{\sim}{S} = \underset{\sim}{LQ}. \tag{12}$$

Equation (11) can be solved by successive diagonalization using a digital computer. Although the product $\underset{\sim}{GF}$ is not a symmetric matrix, it can be diagonalized by diagonalizing the two symmetric $\underset{\sim}{G}$ and $\underset{\sim}{F}$ matrices. The basic steps are shown in Fig. 9. The details are presented by Schachtschneider (7,18,19).

The $\underset{\sim}{G}$ matrix is first diagonalized by an orthogonal transformation to give

$$\underset{\sim}{A}'\underset{\sim}{G}\underset{\sim}{A} = \underset{\sim}{D}\underset{\sim}{D} \tag{13}$$

or

$$\underset{\sim}{G} = \underset{\sim}{A}\underset{\sim}{D}\underset{\sim}{D}\underset{\sim}{A}' \tag{14}$$

where $\underset{\sim}{A}$ is the orthogonal eigenvector matrix of $\underset{\sim}{G}$, and $\underset{\sim}{D}$ is a diagonal matrix whose elements are the square roots of the eigenvalues of $\underset{\sim}{G}$. A transformation matrix $\underset{\sim}{W}$ defined as

$$\underset{\sim}{W} = \underset{\sim}{A}\underset{\sim}{D} \tag{15}$$

is then formed and applied to the $\underset{\sim}{F}$ matrix. A symmetric matrix $\underset{\sim}{H}$ results.

$$\underset{\sim}{H} = \underset{\sim}{W}'\underset{\sim}{F}\underset{\sim}{W}. \tag{16}$$

The $\underset{\sim}{H}$ matrix is symmetric since $\underset{\sim}{A}$ is orthogonal and $\underset{\sim}{D}$ is diagonal. To solve the secular equation, $\underset{\sim}{H}$ must then be diagonalized. The Jacobi method is used. The result may be expressed as

$$\underset{\sim}{C}^{-1}\underset{\sim}{H}\underset{\sim}{C} = \underset{\sim}{C}^{-1}\underset{\sim}{W}'\underset{\sim}{F}\underset{\sim}{W}\underset{\sim}{C} = \underset{\sim}{\Lambda} \tag{17}$$

where $\underset{\sim}{\Lambda}$ is the diagonal matrix of frequency parameters.

To calculate the normal coordinate associated with each normal mode, the $\underset{\sim}{L}$ matrix must be computed. Recall that the $\underset{\sim}{L}$ matrix is the transformation from normal coordinates to internal coordinates. Multiplying Equation (17) from the left by first $\underset{\sim}{C}$ and then $\underset{\sim}{W}$ results in the following expression

$$\underset{\sim}{W}\underset{\sim}{W}'\underset{\sim}{F}\underset{\sim}{W}\underset{\sim}{C} = \underset{\sim}{W}\underset{\sim}{C}\underset{\sim}{\Lambda}. \tag{18}$$

Since $\underset{\sim}{W}\underset{\sim}{W}' = \underset{\sim}{G}$, Equation (18) becomes

$$\underset{\sim}{GFWC} = \underset{\sim}{WC}\Lambda. \tag{19}$$

Comparing Equations (11) and (19) it is obvious that the $\underset{\sim}{L}$ matrix may be defined as

$$\underset{\sim}{L} = \underset{\sim}{WC}. \tag{20}$$

The eigenvalues which result from Equation (17) are directly related to the fundamental frequencies. The frequencies of the three alditol molecules selected for the refinement procedure were calculated using Pitzner's force constants developed for the 1,5-AHP's (see Table V). The frequencies are listed in Table VI.

OPTIMIZATION OF THE FORCE CONSTANT PARAMETERS

The objective of the refinement is to minimize the least squares deviation between the observed and calculated frequency parameters. In the process an initial set of force constants are optimized using the Fletcher-Powell minimization algorithm. As shown in Fig. 9 the first step in the refinement results in the formation of $\underset{\sim}{J}$, the Jacobian matrix having elements $(\partial\lambda_{\underline{k}}/\partial F_{\underline{ii}})^{\underline{r}}$. The $\underset{\sim}{J}$ matrix is computed indirectly from the $\underset{\sim}{L}$ matrix defined in Equation (20), since

$$J_{ki} = L_{ik}^2 \cong \partial\lambda_k/\partial F_{ii}. \tag{21}$$

The three general steps of the Fletcher-Powell algorithm are as follows:

(1) Compute a gradient vector $\underset{\sim}{g}^{\underline{r}}$ having elements $g_{\underline{i}}^{\underline{r}} = (\partial Q/\partial\Phi_{\underline{i}})^{\underline{r}}$, where $g_{\underline{i}}^{\underline{r}}$ represents the $\underline{i}$th element of the gradient vector after $\underline{r}$ iterations.

(2) Determine a direction along which to make a desired move.

(3) Compute a step-size, $\underline{t}$, and move in the desired direction.

TABLE VI

CALCULATED FREQUENCIES FOR THE ALDITOL MODELS
BASED ON PITZNER'S FINAL FORCE CONSTANTS
LISTED IN TABLE V

Ribitol, ν, cm^{-1}		Xylitol, ν, cm^{-1}		Erythritol, ν, cm^{-1}	
3356	1158	3356	1145	3356	1130
3356	1100	3356	1118	3356	1089
3356	1080	3356	1094	3356	1059
3356	1059	3356	1068	3355	1008
3355	1028	3356	1058		
2979	1021	2978	983	2950	865
				2947	779
2960	963	2975	956	2925	686
2938	939	2938	934	2903	583
2924	878	2924	896		
2915	846	2914	860	2877	494
2898	729	2882	767	2870	441
2876	566	2880	574	1550	412
				1495	368
1485	489	1445	463		
1456	467	1444	399	1374	277
1427	390	1438	366	1322	262
1403	323	1411	327	1314	250
1393	291	1386	292	1298	247
1362	255	1358	266		
				1296	234
1348	249	1324	262	1284	226
1299	244	1306	251	1266	153
1287	242	1299	250	1250	136
1280	222	1288	230		
1270	215	1266	201	1223	121
1255	191	1262	181	1213	106
				1182	78
1242	176	1249	172	1137	42
1238	159	1237	159		
1221	120	1233	142		
1210	105	1207	97		
1208	80	1187	75		
1164	61	1181	70		

The calculation of the $\underline{J}$ matrix and the subsequent formation of the $\underline{JZ}$ matrix are necessary steps in the computation of the gradient vector. In matrix notation $\underset{\sim}{g}^r$ may be written as

$$\underset{\sim}{g}^r = -2(\underset{\sim}{J}^r\underset{\sim}{Z})'\underset{\sim}{P}\overline{\Delta\lambda}^r \qquad (22)$$

where $\overline{\Delta\lambda^r}$ is defined to be a matrix of the elements $\Delta\lambda_i^r = |\lambda_{k(obs.)} - \lambda_{k(cal.)}^r|$.

From Equation (22) it is evident that when $\underset{\sim}{g}^r$ is zero, either $\overline{\Delta\lambda^r}$ is zero, and the experimental frequencies are fitted exactly, or $(\underset{\sim}{J}^r\underset{\sim}{Z})'$ is singular and Q, the sum of the squared residuals, is not and cannot be zero.

The increment added to the force constants, $\Delta\overline{\Phi}^r$, after each iteration is calculated indirectly from the following expression

$$\Delta\overline{\Phi}^r = - (\underset{\sim}{D}^r)^{-1}\underset{\sim}{g}^r \tag{23}$$

where $\underset{\sim}{D}^r$ is a Hessian matrix having elements

$$D_{ij} = \partial^2 Q/\partial\Phi_i\partial\Phi_j. \tag{24}$$

The approach used in the Fletcher-Powell method to calculate $\Delta\overline{\Phi}^r$ approximates the Hessian matrix $\underset{\sim}{D}^r$ at each iteration. Essentially, a positive definite matrix, $\underset{\sim}{H}^r$, which is initially an identity matrix, is updated at each iteration.[4]

The procedures for approximating $\underset{\sim}{D}^r$ at each iteration are discussed by Fletcher and Powell (22). However, it can be readily seen from Equation (23) that if $\underset{\sim}{H}^1$ is initially an identity matrix the direction of movement will be along the negative gradient $(-\underset{\sim}{g}^r)$ as in the method of steepest descent. As $\underset{\sim}{H}^r$ approached $\underset{\sim}{D}^r$, the Hessian matrix, the direction of movement is different from the path of steepest descent and an approximation to the Hessian in the neighborhood of the optimum is generated. The use of the Hessian, or an approximation to the Hessian, indicates an attempt to use second-order information. The

[4]Where the $\underset{\sim}{H}$ matrix is to be distinguished from the $\underset{\sim}{H}$ in Equation (16).

method of steepest descent which is utilized by linear least squares techniques, like that of Snyder-Schachtschneider, uses only gradient or first-order information.

To approach $\underline{\underline{D}}^{r}$ a direction vector must be found and a step-size, $\underline{t}_{\underline{m}}$, calculated at each iteration. The latter calculation occurs in three stages. The first estimates the magnitude of $\underline{t}_{\underline{m}}$, the second determines an interval containing $\underline{t}_{\underline{m}}$, and the third cubically interpolates the value of $\underline{t}_{\underline{m}}$.

The Initial Force Constants

There are no decisive methods for selecting an initial set of force constants. At the outset, some modifications in Pitzner's SVQFF were made in anticipation of some differences between the constants describing these two molecular systems. As mentioned previously, the valence bond constants associated with the methylene atomic groupings in the alditols were distinguished from those associated with the methine atomic groupings. In addition, some changes in the off-diagonal bend-bend interactions were made. Both Snyder, et al. (9) and Pitzner grouped a number of related interaction constants together (i.e., their values were assumed to be similar). In the SVQFF for the alditols, the nearest neighbor bend-bend interaction constants were separated. Distinctions were not, however, made with regard to the atomic groupings associated with the various types of interaction constants.

Pitzner noted that the contribution of the CO stretch-bend interactions to the 1,5-AHP force field was a major difference between the force fields of THP and the 1,5-AHP compounds. In view of this observation, a series of trial adjustments were made to those constants associated with the methylene atomic groupings (i.e., the terminal carbon atoms). Independent adjustments to the stretch-bend

and bend-bend interaction constants associated with the skeletal coordinates were made also. In the process of exploring how perturbations to the values of these constants affected the computed frequency distributions, a new set of initial constants evolved. The values of the initial constants used in final refinement are given in Table V.

Termination of the Force Constant Refinement

The refinement is terminated if either of the following two conditions are satisfied. The first condition requires that all the corrections to the force constants, $\Delta\Phi_i$, be less than or equal to an arbitrary constant of 0.0001. The second condition requires that the ratio of the successive weighted sums of squares of the residuals be greater than a fractional constant of 0.995. In order to check against premature convergence, the latter condition may be required to be met several times before actual termination is initiated.

RESULTS

If one of the criteria for convergence is satisfied, the secular equation [i.e., Equation (11)] is solved one last time, as shown in Fig. 9. The final refinement[5] terminated after 17 perturbations after having satisfied the first condition (i.e., all corrections to the force constants were less than 0.0001). In this calculation 128 observed frequencies (from ribitol, xylitol and erythritol) were used to adjust 45 independent force constants. The 17 perturbations consumed approximately 7 1/2 hours of IBM/44 360 CPU time. Both the initial and final set

[5]The final refinement represents only one of a series of refinements. The success of any refinement was determined by a number of criteria defined by the constraints placed on the refinement process. The three most important constraints were: (1) an improved correlation between the experimental and calculated frequencies; (2) a plausible potential energy distribution; and (3) reasonable changes in the values of the force constant parameters.

of force constants, and a comparison of the two, are given in Table V along with the estimates of standard error.[6] The estimated errors must be viewed as upper limits, however, because they are derived from the diagonal elements of the final $\underset{\sim}{H}^{r}$ matrix and only approximate the least squares variance-covariance matrix. The approximation is known to be a poor one unless the number of iterations approaches the number of parameters undergoing adjustment (31).

The vibrational frequencies, the potential energy distributions, and the cartesian displacement coordinates for each molecule have been calculated. The less important data have necessarily been excluded from the text of this thesis but can be generated from the data presented. Since, the cartesian displacement coordinates provide complementary information about the molecular vibrations they are excluded. The potential energy distribution is defined as the way in which the displacement of each internal coordinate contributes to the potential energy of each normal vibration. The relative contribution of the displaced internal coordinates to the total potential energy associated with each normal coordinate are given in Appendix III.[7] The fractional contribution of each force constant, Φ_k, is also evaluated (see Appendix III).[8] The information derived from these distributions describe the vibrations and formulate the bases for the spectral interpretations given.

---

[6] Error estimates do not exist for those constants held fixed during the refinement. The OH constants were not refined. Also interaction constants found to be insensitive to the data were excluded. Error estimates on these latter constants would be meaningless.

[7] The % contribution = $\underset{\sim}{L}^{2}_{ik}\underset{\sim}{F}_{ii}/\lambda_k$.

[8] The % contribution = $\underset{\sim}{J}\underset{\sim}{Z}_{ijk}\Phi_k/\lambda_k$.

Ribitol

The frequencies calculated from the final set of force constants given in Table V are listed in Table VII and assigned to corresponding experimental frequencies. The average error between the calculated and experimental frequencies is 9.0 cm^{-1}.[9] The approximate motions which describe each of the calculated modes are also given in Table VII. The more ambiguous motions are illustrated in Fig. 12. These descriptions are based on the potential distribution associated with each calculated mode. The dominant internal coordinates and potential constants are given in Table XXXV.

Xylitol

The calculated frequencies, their respective assignments and band interpretations are listed in Table VIII. The average error between the calculated and experimental frequencies is 9.4 cm^{-1}. The dominant internal coordinates and potential constants are given in Table XXXVI.

Erythritol

The calculated frequencies, their respective assignments and interpretations are tabulated in Table IX. The average error is 9.6 cm^{-1}. The dominant internal coordinates and potential constants are given in Table XXXVII.

[9] The average error (mean deviation) is a term commonly used in the literature to represent the average difference between the calculated and assigned experimental frequencies. The OH stretching frequencies were excluded from the error computation. The Raman frequencies were used whenever possible due to the poor resolution of many of the infrared bands.

TABLE VII

INTERPRETATION OF THE VIBRATIONAL SPECTRUM OF RIBITOL

Band Assignment				
Experimental		Calculated	Difference[a]	Spectral Interpretation, approximate motion
Δν, Raman, cm^{-1}	ν, IR, cm^{-1}	ν, cm^{-1}	cm^{-1}	
		3351.8		OH stretch (str.)
	3340(vs,b)[b]	3351.8		OH str.
	3250(vs,b)	3330.8		OH str.
		3330.8		OH str.
		3330.1		OH str.
	2972(s)	2968.4	3.6	asymmetric (asym.) methylene CH str.
2965(s)	2960(vs)	2949.1	15.9	asym. methylene CH str.
2949(vs)		2934.0	15.0	methine CH str.
2928(s,sh)[c] 2922(s)	2928(vs)	2922.8	2.2	methine CH str.
	2913(sh)	2914.7	-1.7	methine CH str.
2900(s)		2901.7	-1.7	symmetric (sym.) methylene CH str.
2887(s,sh)	2893(s,sh)	2880.8	6.2	sym. methylene CH str.
2858(vw)[d]	2853(w,b)[d]			
		1482.6		methylene CH_2 scissor coupled with methylene CH_2 wag
1469(s)	1467(s)	1471.5	-2.5	methylene CH_2 scissor coupled with methylene CH_2 wag
1452(s)	1458(s)	1452.0	0.0	methine CH deformation (op and ip bend)[e]
1433(w,b)	1422(m,b)	1426.6	6.4	methine CH deformation coupled with OH ip bend
1378(w,b)		1381.1	-3.1	methine CH ip bend
	1364(m)	1368.1	-4.1	methine CH op bend
1342(s)	1344(m)	1353.7	-11.7	methine CH deformation coupled with methylene CH_2 wag
	1328(m)	1331.4	-3.4	OH ip bend coupled with CH deformation; methylene CH_2 wag and twist

TABLE VII (Continued)

INTERPRETATION OF THE VIBRATIONAL SPECTRUM OF RIBITOL

Band Assignment				
Experimental		Calculated	Difference[a]	Spectral Interpretation, approximate motion
$\Delta\nu$, Raman, cm^{-1}	ν, IR, cm^{-1}	ν, cm^{-1}	cm^{-1}	
1317(vw,b)		1312.5	4.5	CH deformation coupled with methylene CH_2 twist; OH ip bend
1295(m,sh)		1295.3	-0.3	CH ip bend coupled with methylene CH_2 twist
1289(m)	1289(w)	1292.3	-3.3	CH ip bend coupled with OH ip bend
1270(s)		1268.9	1.1	OH ip bend
1265(sh)	1265(w)	1265.0	0.0	OH ip bend coupled with methylene CH_2 twist
1246(m)		1252.5	-6.5	methylene CH_2 twist coupled with OH ip bend
1237(w,b)		1231.8	5.2	methylene CH_2 twist coupled with OH ip bend
1222(w,b)		1213.8	8.2	methylene CH_2 twist coupled with OH ip bend
	1209(w)	1202.1	6.9	OH ip bend coupled with methylene CH_2 twist
1135(s)	1133(m)	1154.0	-19.0	CC str. coupled with some OH ip bend
1118(s)	1117(s)	1138.5	-20.5	CC str. coupled with some CO str.
1092(w,sh)	1098(vs)	1084.8	7.2	OH ip bend coupled with methylene CH_2 rock and twist and CC str.
1078(s)	1074(s)	1073.2	4.8	CC str. coupled with CO str. and OH ip bend
1066(s)	1068(sh)	1057.8	8.2	CO str. coupled with CC str., OH ip bend, methylene CH_2 rock and twist
1054(s)[c] 1050(s)	1049(m) 1045(m)	1046.8	5.2	CO str. and CC str. coupled with OH ip bend, methylene CH_2 deformation
1037(m)	1032(vs)	1004.3	32.7	CO str. coupled with CC str., and OH ip bend

TABLE VII (Continued)

INTERPRETATION OF THE VIBRATIONAL SPECTRUM OF RIBITOL

Band Assignment				
Experimental		Calculated	Difference[a]	Spectral Interpretation, approximate motion
$\Delta\nu$, Raman, cm^{-1}	ν, IR, cm^{-1}	ν, cm^{-1}	cm^{-1}	
948(s)[c]	948(w)	969.2	-18.2	CO str. coupled with methylene CH_2 rock and twist, OH ip bend
915(w)	912(s)	935.7	-20.7	CO str. coupled with OH ip bend, CC str., and methylene CH_2 rock and twist
893(vs)	888(vs)	870.0	23.0	CC str. coupled with CO str. and OH ip bend
860(vs)	859(s)	852.3	11.7	CO str., CC str., coupled with some OH ip bend
749(s)	748(s)	758.6	9.6	CO op bend coupled with CC and CO str.
695(vvw,b)[d]	692(m,b)[d]			
628(m,b)	624(s,b)	609.7	18.3	CO op bend coupled with CC skeletal bend
575(vvw,b)[d]	574(s,vb)[d]			
529(s)	529(m,sh)	524.0	5.0	CO deformation coupled with CC skeletal bend
478(m)	470(m,sh)	490.6	-12.6	CO op bend coupled with some CC str., CC skeletal bend
458(m)	453(m,sh)	426.3	31.7	CO deformation coupled with OH op bend
388(vw)		380.7	7.3	OH op bend coupled with CO deformation (ip and op)
351(m)		347.0	4.0	OH op bend
		339.3		OH op bend
		333.4		OH op bend
327(m)		326.7	0.3	OH op bend
310(w,b)		305.5	4.5	OH op bend coupled with CC skeletal torsion; CO deformation; CC skeletal bend

TABLE VII (Continued)

INTERPRETATION OF THE VIBRATIONAL SPECTRUM OF RIBITOL

Band Assignment				
Experimental		Calculated	Difference[a]	
$\Delta\nu$, Raman, cm^{-1}	ν, IR, cm^{-1}	ν, cm^{-1}	cm^{-1}	Spectral Interpretation, approximate motion
274(m,b)		266.7	7.3	CO deformation coupled with OH op bend; CC skeletal torsion
234(w,b)		252.9	-18.9	CO deformation coupled with CC skeletal bend
209(m)		218.6	-9.6	CC skeletal torsion coupled with CC skeletal bend
202(m)		192.3	9.7	CC skeletal torsion coupled with CC skeletal bend
		174.9		mainly CC skeletal torsion
		124.8		
		116.0		
		85.1		
		71.4		
		Average error =	9.01	

[a] Difference = obs. freq. (Raman) - calc. freq.

[b] Conventional symbolism indicating relative intensity: vs = very strong; s = strong; m = medium; w = weak; v = very; b = broad; sh = shoulder.

[c] Apparent correlation field splitting; the approximate midpoint between the split bands is used in the difference calculation.

[d] Suspected overtone or combination band.

[e] Deformation denotes a less specific valence angle bend. (Ip = in-plane and op = out-of-plane.)

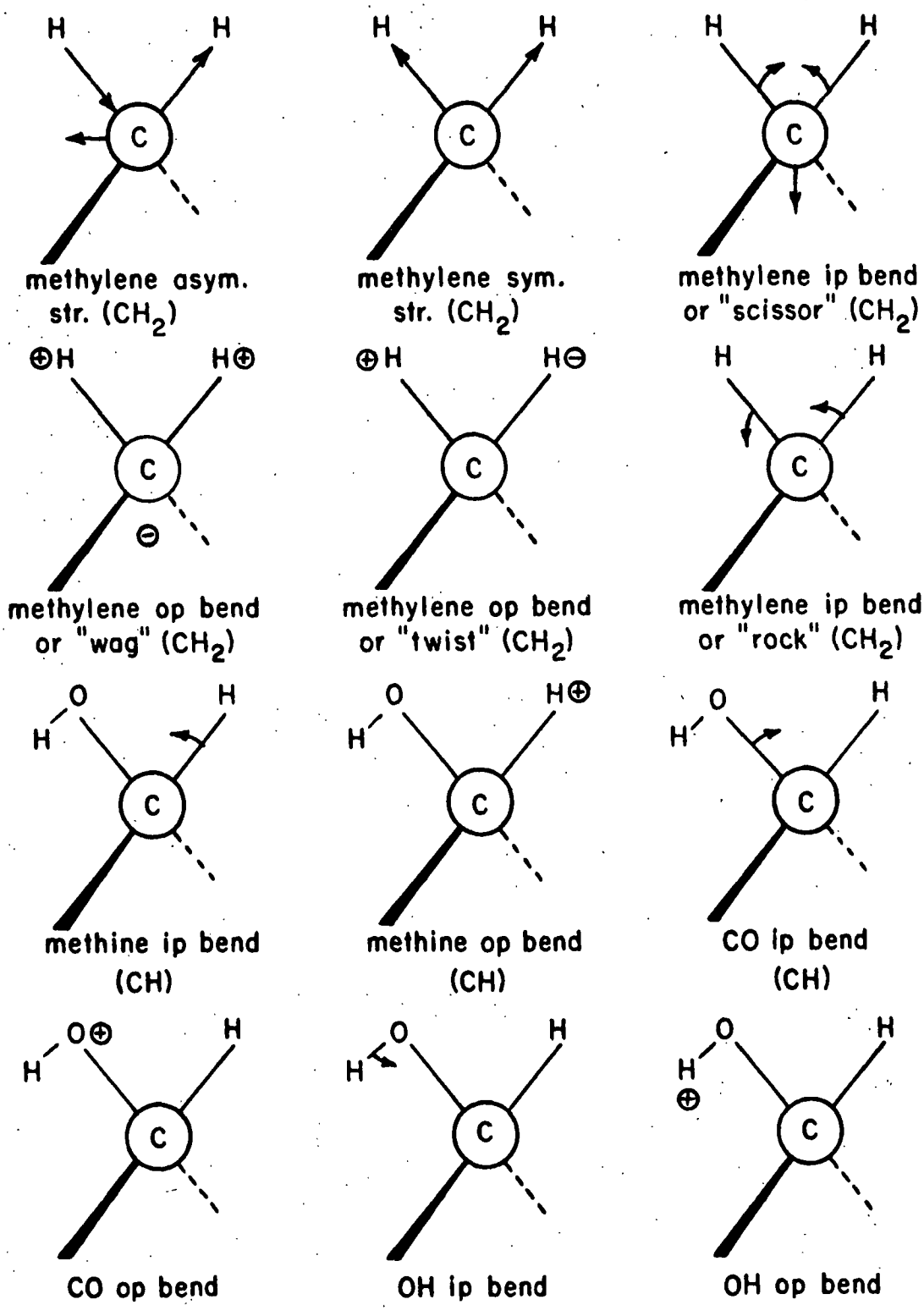

Figure 12. The Descriptions of Several of the Atomic Group Vibrations Referred to in Tables VII-X. (⊕ and ⊖ Indicate Movement Perpendicular to the Plane of the Page.) (Ip = In-Plane and op = Out-of-Plane)

TABLE VIII

INTERPRETATION OF THE VIBRATIONAL SPECTRUM OF XYLITOL

Band Assignment				
Experimental		Calculated	Difference[a]	Spectral Interpretation, approximate motion
$\Delta\nu$, Raman, cm^{-1}	ν, IR, cm^{-1}	ν, cm^{-1}	cm^{-1}	
3435	3420(vs,b)[b]	3351.6		OH stretch (str.)
3362	3360(vs,b)	3351.5		OH str.
3302	3290(vs,b)	3330.8		OH str.
		3330.4		OH str.
		3330.3		OH str.
2998(s)	2997(s)	2966.9	31.1	asymmetric (asym.) methylene CH str.
2972(w)	2972(m)	2963.9	8.1	asym. methylene CH str.
2957(vs)	2955(m)	2934.2	22.8	methine CH str.
2948(s)	2945(s)	2922.9	25.1	methine CH str.
2915(m)	2916(vs)	2914.1	0.9	methine CH str.
2900(vs)		2884.3	15.7	symmetric (sym.) methylene CH str.
2889(sh)		2882.7	6.3	symmetric methylene CH str.
1464(vs)	pr	1463.3	0.7	methylene CH_2 scissor coupled with methylene CH_2 wag
1452(sh)		1462.5	-10.5	methylene CH_2 scissor coupled with methylene CH_2 wag
1440(vw)	pr	1439.6	0.4	CH op bend coupled with methylene CH_2 deformation[e]
1424(sh)	pr	1435.2	-11.2	methine CH deformation coupled with methylene CH_2 deformation, OH ip bend
1407(w)	1409(s)	1396.8	10.2	methine CH op bend, methylene CH_2 wag, OH ip bend
1374(w)	1374(s)	1362.1	11.9	methine CH ip and op bend coupled with some methylene CH_2 wag

TABLE VIII (Continued)

INTERPRETATION OF THE VIBRATIONAL SPECTRUM OF XYLITOL

Band Assignment				
Experimental		Calculated	Difference[a]	Spectral Interpretation, approximate motion
$\Delta\nu$, Raman, cm^{-1}	ν, IR, cm^{-1}	ν, cm^{-1}	cm^{-1}	
1352(vw,b)	1351(s)	1355.7	-3.7	methine CH op and ip bend coupled with OH ip bend and methylene CH_2 wag
1346(w,sh)		1347.8	-1.8	methine CH op bend
1335(w)	1331(vw)	1323.8	11.2	methine CH ip bend coupled with OH ip bend
1319(m)	1312(s)	1320.8	-1.8	methine CH ip bend; some OH ip bend
1308(m)	1305(sh)	1297.0	11.0	OH ip bend coupled with CH op bend
1298(w)		1295.5	2.5	methine CH ip and op bend coupled with OH ip bend
1281(s)	1280(s)	1274.3	6.7	methylene CH_2 twist coupled with OH ip bend
1243(m)	1248(m)	1245.2	-2.2	methylene CH_2 twist coupled with OH ip bend; methine CH op bend
1231(w)[pr]		1233.9	-2.9	OH ip bend coupled with methylene CH_2 twist
1225(w)[pr]		1213.5	11.5	OH ip bend coupled with methylene CH_2 twist
1219(w)[pr]	1218(vw)	1199.2	19.8	methylene CH_2 twist coupled with OH ip bend
1122(sh)	1124(vs)	1114.0	8.0	CC str. coupled with some OH ip bend
1110(s)	1111(vs)	1109.5	0.5	CC str. coupled with some OH ip bend
1094(vs)[c] 1089(sh)	1094(vs)[c] 1087(vs)	1087.3	4.7	CC str. coupled with CO str. and OH ip bend
1073(vs)	1076(sh)	1070.0	3.0	OH ip bend coupled with CO str., methylene CH_2 twist and rock
1061(vs)	1067(vs)	1059.6	1.4	CC str. coupled with CO str. OH ip bend and methylene CH_2 twist and rock

TABLE VIII (Continued)

INTERPRETATION OF THE VIBRATIONAL SPECTRUM OF XYLITOL

Band Assignment				
Experimental		Calculated	Difference[a]	Spectral Interpretation, approximate motion
$\Delta\nu$, Raman, cm^{-1}	ν, IR, cm^{-1}	ν, cm^{-1}	cm^{-1}	
1032(vw)		1028.9	3.1	CO str., CC str. coupled with OH ip bend, methylene CH_2 rock and twist
1007(m)	1010(vs)	1009.8	-2.8	CO str., CC str. coupled with methylene CH_2 deformation
960(vw)		974.8	-14.8	CO str., coupled with OH ip bend, CC str.
921(m)[c] 914(m)		928.8	-10.8	CO str., coupled with OH ip bend, methylene CH_2 rock and twist, CC str.
889(s)	887(s)	893.3	-4.3	CO str., CC str. coupled with OH ip bend, methylene CH_2 rock and twist
858(vs)	860(vs)	842.8	15.2	CO str., CC str. coupled with OH ip bend
750(vvw)	742(vs) 698(sh)[d]	773.1	-23.1	CO op bend
600(vvw)	598(s) 563(s)[d]	613.5	-13.5	CO op bend
520(w)	520(vs)	511.0	9.0	CO op bend coupled with CC skeletal bend
464(w)		437.0	27.0	CO op bend coupled with OH op bend, CC skeletal bend
428(vs)	433(w)	398.9	29.1	CO op bend coupled with OH op bend
385(w)		371.3	13.7	OH op bend coupled with CO op bend
360(vs)		360.7	-0.7	OH op bend coupled with CO op bend
		349.8		OH op bend
		335.4		OH op bend coupled with some CO op bend
		334.1		OH op bend

TABLE VIII (Continued)

INTERPRETATION OF THE VIBRATIONAL SPECTRUM OF XYLITOL

Band Assignment				
Experimental		Calculated	Difference[a]	Spectral Interpretation, approximate motion
$\Delta\nu$, Raman, cm^{-1}	ν, IR, cm^{-1}	ν, cm^{-1}	cm^{-1}	
324(m)		321.0	3.0	OH op bend
297(w)				
277(w)		275.9	-2.9	CO ip bend coupled with OH op bend, CC skeletal torsion
243(vw)		241.2	1.8	CO bend deformation coupled with OH op bend; CC skeletal torsion CC skeletal bend
226(w)		215.5	10.5	CC skeletal torsion
207(m)		197.9	9.1	CC skeletal torsion
		172.2		mainly skeletal torsion modes
		144.0		
		102.3		
		87.9		
		74.5		
		Average error =	9.41	

[a] Difference = obs. freq. (Raman) - calc. freq.

[b] Conventional symbolism indicating relative intensity: vs = very strong; s = strong; m = medium; w = weak; v = very; b = broad; sh = shoulder.

[c] Apparent correlation field splitting; the approximate midpoint between the split bands is used in the difference calculation.

[d] Suspected overtone or combination band.

[e] Deformation denotes a less specific valence angle bend. (Ip = in-plane and op = out-of-plane.)

[pr] Poor spectral resolution.

TABLE IX

INTERPRETATION OF THE VIBRATIONAL SPECTRUM OF ERYTHRITOL

Band Assignment				
Experimental		Calculated	Difference[a]	Spectral Interpretation, approximate motion
$\Delta\nu$, Raman, cm^{-1}	ν, IR, cm^{-1}	ν, cm^{-1}	cm^{-1}	
		3351.7		OH stretch (str.)
		3351.6		OH str.
	3285(b)[b]	3331.0		OH str.
	3250(b)	3330.9		OH str.
2972(vs)	2975(vs)	2974.1	-2.1	asymmetric (asym.) methylene CH str.
2963(vs)	2965(vs)	2964.5	-1.5	asym. methylene CH str.
2930(s)	2935(s)	2921.7	8.3	methine CH str.
2919(m)	2918(vs)	2909.9	9.1	methine CH str.
2903(vs)	2902(m)	2872.3	30.7	symmetric (sym.) methylene CH str.
	2890(sh)	2867.5	22.5	sym. methylene CH str.
1469(s)	1469(m)	1498.0	-29.0	methylene CH_2 deformation (scissor and wag)
1450(w)	1456(s)	1457.8	0.2	methylene CH_2 deformation (scissor and wag)[e]
1415(w)	1414(vs)	1418.2	-3.2	methine CH ip bend; CH op bend
1373(w)	1375(w,sh)	1369.8	3.2	methine CH ip bend coupled with OH ip bend
1366(w)	1366(m)	1353.6	12.4	OH ip bend coupled with methylene CH_2 wag
1324(vw)		1331.4	-7.4	methine CH op bend coupled with OH ip bend
1306(vw)	1307(w)	1320.2	-14.2	methylene CH_2 wag and twist coupled with OH ip bend; CH op bend
1273(m)	1271(s)	1276.4	-4.4	OH ip bend coupled with CH ip bend
	1254(s)	1250.0	4.0	methylene CH_2 twist coupled with OH ip bend; methine CH op bend
1245(sh)		1245.2	0.2	methylene CH_2 twist

TABLE IX (Continued)

INTERPRETATION OF THE VIBRATIONAL SPECTRUM OF ERYTHRITOL

Band Assignment				
Experimental		Calculated	Difference[a]	Spectral Interpretation, approximate motion
$\Delta\nu$, Raman, cm^{-1}	ν, IR, cm^{-1}	ν, cm^{-1}	cm^{-1}	
1236(m)		1230.7	5.3	methine CH op bend coupled with methylene CH_2 twist and wag; OH ip bend
	1216(m)	1205.3	10.7	methine CH ip and op bend; some CC str.
1121(m)	1121(vw)	1148.8	-27.8	OH ip bend; CC str. coupled with some CH_2 twist and rock
1107(s)		1128.4	-21.4	CC str. coupled with methylene CH_2 twist; OH ip bend
1068(w)	1078(vs)	1065.5	2.5	CO str., OH ip bend
	1053(vs)	1060.5	-7.5	CO str.
1040(m)[c] 1030(m)	1038(sh)	1030.2	4.8	CO str., OH ip bend
	968(vs)	973.0	-5.0	CO str., OH ip bend, CC str.
918(vs)	918(vw)	891.2	26.8	CC str., CO str. coupled with some methylene CH_2 rock
874(vs)[c] 862(s)	880(vs)[c] 865(s)	837.8	30.2	CC str., CO str. coupled with some methylene CH_2 rock
	709(sh)			
698(vs)	692(vs)[c] 672(sh)	699.2	-1.2	CC str. coupled with CC skeletal bend
	620(vs)	611.5	8.5	CO op bend; some CC str.
		545.0		CO op bend
486(m)	488(m)	485.4	0.6	CO op bend, CC skeletal bend and some OH op bend
	431(m)[c] 422(m)	431.4	-4.4	methylene CH_2 deformation (mainly op) coupled with OH op bend, CC skeletal bend
383(m)	378(vw)	378.3	4.7	CO op (ip also) coupled with OH op bend

TABLE IX (Continued)

INTERPRETATION OF THE VIBRATIONAL SPECTRUM OF ERYTHRITOL

Band Assignment				
Experimental		Calculated	Difference[a]	Spectral Interpretation, approximate motion
$\Delta\nu$, Raman, cm^{-1}	ν, IR, cm^{-1}	ν, cm^{-1}	cm^{-1}	
		370.2		OH op bend coupled with some CC skeletal torsion
350(vw)		348.2	1.8	OH op bend
		335.4		OH op bend
312(w)		327.4	-15.4	OH op bend
263(m)		273.5	-10.5	CO op bend coupled with methylene CH_2 op bend
245(w)		242.0	3.0	CC skeletal bend coupled with CC skeletal torsion
		158.2		mainly skeletal torsion and bending modes
		149.3		
		125.7		
		91.6		
		75.4		
		48.9		
		Average error =	9.84	

[a] Difference = obs. freq. (Raman) - calc. freq.

[b] Conventional symbolism indicating relative intensity: vs = very strong; s = strong; m = medium; w = weak; v = very; b = broad; sh = shoulder.

[c] Apparent correlation field splitting; the approximate midpoint between the split bands is used in the difference calculation.

[d] Deformation denotes a less specific valence angle bend. (Ip = in-plane and op = out-of-plane.)

D-Arabinitol

The normal modes of D-arabinitol were calculated[10] using the constants modeled from ribitol, xylitol, and erythritol without any additional refinement. The calculated frequencies and the approximate motions describing each mode are given in Table X. In Table X both the calculated frequencies of D-arabinitol and the observed frequencies (Raman and IR) of D-arabinitol and D,L-arabinitol are given. The average errors are 7.9 and 9.5 cm^{-1}, respectively. The dominant internal coordinates and potential constants are given in Table XXXVII.

[10] The calculated frequencies are based on the structure of D-arabinitol as it exists in the D,L mixed crystal (20).

TABLE X

AN INTERPRETATION OF THE VIBRATIONAL SPECTRA OF D AND D,L-ARABINITOL

D-Arabinitol		Band Assignments			D,L-Arabinitol		
Δν, Raman, cm^{-1}	ν, IR, cm^{-1}	Difference[b] cm^{-1}	Calculated[a] ν, cm^{-1}	Difference[b] cm^{-1}	Δν, Raman, cm^{-1}	ν, IR, cm^{-1}	Spectral Interpretation, approximate motion
	3350(vs)[c]		3351.7			3350(vs)[c]	OH stretch (str.)
			3351.5				OH str.
	3330(vs,b)		3330.8			3295(vs,b)	OH str.
	3220(vs,b)		3330.8			3215(vs,b)	OH str.
			3330.8				OH str.
2990(w,sh)[d]							
2977(m)	2971(w)	-5.8	2982.8	-16.8	2966(vs)		asymmetric (asym.) CH str.
	2957(m,sh)	1.0	2956.0				asym. CH str.
2947(vs)[cs] 2939(vs)	2945(s)[cs] 2939(s)	9.1[e]	2933.9	11.1[e]	2945(vs)	2945(vs)	CH str.
2920(s,sh)	2921(m)	-1.3	2921.3	-1.3	2920(vs)	2919(s)	CH str.
2910(vs,b)	2906(m)	-3.6	2913.6				CH str.
2882(m,sh)		-14.2	2896.2	-19.2	2877(sh)	2870(sh)	symmetric (sym.) CH str.
			2864.8	3.2	2868(w,b)	2865(m,b)	sym. CH str.
1494(s)	1491(w,sh)	18.0	1476.0	10.0	1486(s)	1481(m)	methylene CH_2 scissor and some wag
1464(s,sh)	1462(m,sh)[pr]	2.6	1461.4	3.6		1465(m,sh)[pr]	methylene CH_2 scissor and some wag
1454(s)	1450(m,sh)[pr]	12.3	1441.7	12.3	1454(s)	1448(s)	methine CH ip and op bend
1440(w,sh)	1440(s,b)[pr]	7.6	1432.4	-7.4		1425(m,b)[pr]	methine CH ip bend coupled with OH ip bend
1395(vw,b)[d]	1395(vvw)[d]				1406(m)[d]	1395(m,sh)[d]	
1375(s)	1372(m)	-7.4	1382.4	-7.4	1375(m)	1372(w)	methine CH op bend
1357(s)	1352(vvw)	-12.9	1369.9	-27.9	1342(s)	1340(m)	methine CH op bend
1333(vs)	1330(m,sh)	-0.6	1333.6	-10.6	1323(vw,b)	1325(m)	methine CH ip and op bend
	1314(m)	-10.5	1324.5	-12.5		1312(m)	methine CH op coupled with OH ip bend; methylene CH_2 wag and twist
1304(s)	1304(w,sh)	5.0	1299.0	3.0	1302(w)	1298(w)	methine CH ip bend coupled with some methylene CH_2 wag and twist
1294(m)	1293(vw,sh)	0.8	1293.2				OH ip bend coupled with methine CH op and ip bend
1280(m)	1280(vw)	-5.1	1285.1				OH ip bend coupled with methine CH ip bend
1268(s,sh)	1268(vw,sh)	-2.6	1270.6	0.4	1271(s)		methine CH ip bend coupled with OH ip bend; methylene CH_2 twist
1260(vs)	1259(w)	-1.1	1261.1	0.9	1262(m)	1265(w,sh)	methine OH ip bend coupled with methine OH ip bend

See end of table for footnotes.

TABLE X (Continued)

AN INTERPRETATION OF THE VIBRATIONAL SPECTRA OF D AND D,L-ARABINITOL

D-Arabinitol		Band Assignments			D,L-Arabinitol		Spectral Interpretation, approximate motion
		Difference[b]	Calculated[a]	Difference[b]			
Δν, Raman, cm^{-1}	ν, IR, cm^{-1}	cm^{-1}	ν, cm^{-1}	cm^{-1}	Δν, Raman, cm^{-1}	ν, IR, cm^{-1}	
1237(w)[pr]	1234(vw)[pr]	-9.3	1246.3	-16.3	1230(s)		methylene CH_2 twist and wag; some OH ip bend
			1219.1				methylene CH_2 twist and wag
1213(w)[pr]	1211(w)[pr]	5.0	1208.0	1.0	1209(w)	1205(m)	methylene CH_2 twist and wag; some OH ip bend
			1190.7				OH ip bend coupled with methine CH ip and op bend
1142(vs)	1140(m)	2.0	1141.0	-8.0	1133(vs)	1132(w,sh)	CC str., CO str. coupled with OH ip bend
1124(m)	1122(m)	8.1	1115.9	-0.9	1115(m)		CC str. coupled with methylene CH_2 rock and twist
1109(m)	1102(s)	1.0	1108.0	2.0	1110(m,sh)	1109(s,sh)	methylene CH_2 rock and twist coupled with CO str., OH ip bend
1089(sh)[cs] 1086(m)	1088(vs)[cs] 1085(vs,sh)	5.7[e]	1082.3	1.7	1084(m)	1090(vs)[cs] 1081(vs)	CC str., CO str.
1069(w)[d]	1069(s)[d]						
1057(vs)[cs] 1049(s,sh)	1055(s,sh)[cs] 1050(vs)	-17.2[e]	1070.2	-9.2	1061(vs)	1055(sh)[cs] 1053(vs)	CO str., CC str. coupled with OH ip bend
1028(w)	1028(vs)	8.7	1019.3	17.7	1040(m)[cs] 1035(m)	1040(vs)	CO str. coupled with OH ip bend; methylene CH_2 rock
1016(m)	1015(s,sh)	5.7	1010.3	14.7	1025(w,sh)	1025(vs)	CO str., CC str. coupled with methine OH ip bend
997(m)	995(m)	27.3	969.7	26.3	996(s)	990(vs)	CC str., CO str.
951(s)[cs] 945(m,sh)	950(m,sh) 943(m)	10.3[e]	937.7	0.3	938(s)	933(vs)	CO str., some CC str. coupled with OH ip bend
909(w)[d]	905(m)[d]						
887(vs)[cs] 878(vs)	885(m) 877(m)	13.2[e]	896.2	14.2	882(vs)	878(s)	CC str., CO str.
867(s)[cs] 855(s)	866(m) 855(m)	1.3[e]	858.7	-3.7	855(s)	850(w)	CO str., CC str. coupled with some methine CH op bend; OH ip bend
782(m)[d]	780(w)[d]				782(vw)[d]	773(m,b)[d]	
736(w,b)[d]	735(m,b)[d]						
697(m,b)	692(m,b)	-21.1	718.1	-10.1	708(s,b)	712(s,b)[cs] 694(s,b)	CO op bend coupled with CO str., CC str. and CC skeletal bend
647(m)	643(s)	20.6	626.4	23.6	649(m)	642(vs)	CO op bend coupled with some methine CH op bend; CC skeletal bend
595(vvw)[d]	595(vw,b)[d]		?590.6				
540(vw)[d]	538(vvw)[d]				540(w,sh)[d]	535(vw,sh)	
528(m)	526(m)				528(m)	522(s)	CO op bend
491(s)	495(m)	10.5	480.5	-2.5	478(vs)	470(s)	CO op bend coupled with CC skeletal bend; some CC str., CO str.
472(s)	470(w)		?430.1				CO op and ip bend coupled with CC skeletal torsion; OH op bend

See end of table for footnotes.

TABLE X (Continued)

AN INTERPRETATION OF THE VIBRATIONAL SPECTRA OF D AND D,L-ARABINITOL

D-Arabinitol		Band Assignments			D,L-Arabinitol		Spectral Interpretation, approximate motion
		Difference[b]	Calculated[a]	Difference[b]			
Δν, Raman, cm^{-1}	ν, IR, cm^{-1}	cm^{-1}	ν, cm^{-1}	cm^{-1}	Δν, Raman, cm^{-1}	ν, IR, cm^{-1}	
405(vvw)[d]	400(vvw)[d]				406(vw)[d]	400(vw)[d]	
			372.3				OH op bend coupled with CO op and ip bend
363(m)		3.8	359.2	-9.2		350(vw)	OH op bend coupled with some CO ip bend
			341.1				OH op bend
334(m)		2.2	331.8	-1.8	330(vvw)	330(m,b)	OH op bend coupled with methine deformation
325(w)		-3.6	328.6	-25.6	303(m,sh)	300(w)	OH op bend
295(s)		-7.2	302.2	-18.2	284(s)		OH op bend coupled with CO ip and op bend; CC skeletal bend
275(w,sh)		7.0	268.0	-1.0	267(m,sh)		CO deformation coupled with OH op bend; CC skeletal bend
235(w)		-14.7	249.7	-14.7	235(w,sh)		CO deformation coupled with CC skeletal bend and torsion; OH op bend
					227(m,b)		
			211.2	3.8	215(w,sh)		CC skeletal torsion; CO deformation
			195.9				mainly skeletal torsion and bending modes
			149.2				
			135.3				
			111.7				
			80.6				
			74.7				
	Average error =	7.91		9.52			

[a] The calculated frequencies are based on the structural data for D-arabinitol as it exists in the mixed crystal (20).

[b] Difference = obs. freq. (Raman) - calc. freq.

[c] Conventional symbolism indicating relative intensity: vs = very strong; s = strong; m = medium; w = weak; v = very; b = broad; sh = shoulder.

[d] Suspected overtone or combination bend.

[cs] Apparent correlation field splitting.

[e] Difference calculation is based on an approximate midpoint between the split bands.

[pr] Indicates poor spectral resolution.

DISCUSSION OF RESULTS

GENERAL COMMENTS

Three criteria have been used to evaluate the success of the NC analyses:

1. The extent to which the observed spectra and the calculated spectra correlate.
2. The transferability of the SVQFF to related molecular systems.
3. The extent to which the constraints imposed on the analyses are satisfied.

In general, the fit to the experimental frequencies of ribitol, xylitol, and erythritol was quite good for molecules as complex as the alditols. As shown in Tables VII-IX, the average errors are 9.0, 9.4, and 9.7 cm^{-1} for ribitol, xylitol, and erythritol, respectively (this excludes the unassigned OH bands). The overall average error is 9.1 cm^{-1}. The overall average error is slightly higher for the alditols than for the 1,5-AHP compounds (6.3 cm^{-1}). The fit is, however, comparable to that obtained for the aliphatic ethers (9) (average error 10.4 cm^{-1}).

The average error is not the only criterion for judging the quality of the fit. For example, Vasko, et al. (3,13) report an average error of 10.0 cm^{-1} in comparing their data on the calculated and observed frequencies of the α-D-glucose molecule. However, between 1400-1250 cm^{-1} they observe 6 bands and predict 12, and between 800-600 cm^{-1} 7 bands are observed and only 3 are calculated. Thus, the average error is not always indicative of the extent to which the calculated spectra actually match the observed distribution of bands. Average error depends on the nature of the assignment.

Figure 13 compares the results of the final refinement. Both the calculated and experimentally observed frequencies of each alditol used in the refinement are plotted. In all cases the computed spectra approximate the observed spectra quite well. There are a few experimental bands (usually weak in intensity) which could not be correlated with calculated frequencies. It is suggested that these bands do not represent fundamental modes.

In the spectra of ribitol, for instance, the experimentally observed bands at 2858 cm^{-1} (R,IR)[11], 695 cm^{-1} (R,IR), and 575 cm^{-1} (R,IR) have not been assigned as fundamental modes. These bands do not appear in Fig. 13 but are designated in Table VII. There are also several instances of apparent correlation field splitting of fundamental vibrations (an effect produced by the intermolecular coupling of molecules in the unit cell). These have been designated in Table VII and Fig. 13.

The bands at 2858 and 695 cm^{-1} are suspected of being either overtone or combination bands because of their low intensities in both the Raman and infrared. The 695 cm^{-1} is poorly resolved in the IR because it appears as a shoulder on the broad band at 624 cm^{-1}. The band at 575 cm^{-1}, though barely visible in the Raman is quite strong in the IR. It is possible that this band is an overtone whose intensity is enhanced as a result of Fermi resonance. Fermi resonance is a phenomenon that may occur when two vibrational energy levels (usually one fundamental and one overtone) have nearly the same energy and are symmetrically suited. In such cases, the intensity of the overtone is enhanced and becomes almost if not equally as strong as the fundamental. In addition,

[11](R,IR) denotes that the band is both Raman and infrared active. In such cases, the Raman frequency is given.

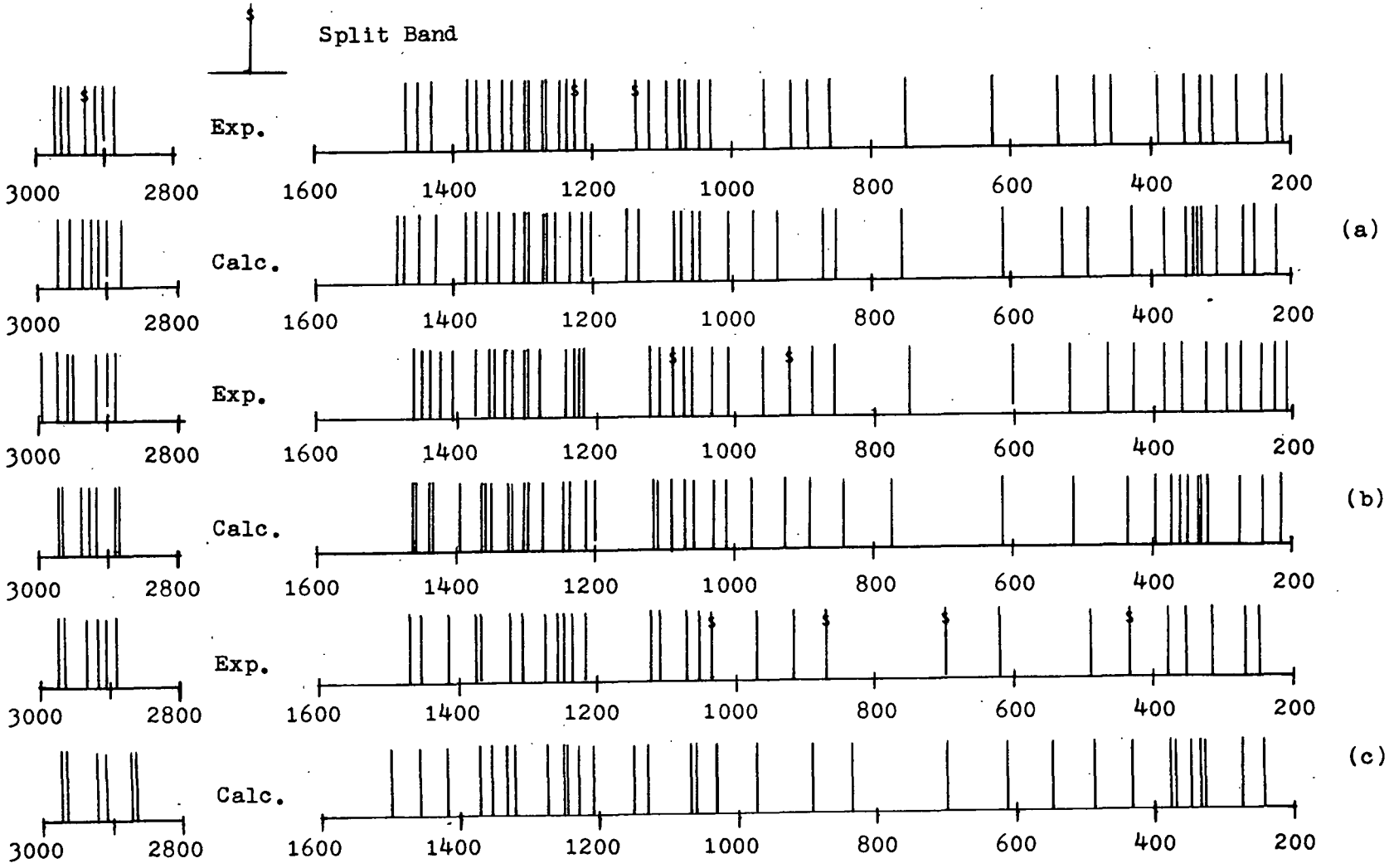

Figure 13. A Comparison of Calculated and Assigned Experimental Frequencies: (a) Ribitol, (b) Xylitol, (c) Erythritol

the two levels "repel" one another, so that the one with the greater energy moves to a higher frequency, and the one with the lower energy moves to a lower frequency (32). The 575 cm^{-1} is located between two fundamentals, one at 624 cm^{-1} and the other at 529 cm^{-1}.

The situation is similar in the case of xylitol. The observed bands at 695 cm^{-1} (IR), 563 cm^{-1} (IR), and 297 cm^{-1} (R) have not been assigned as fundamentals. Neither of the first two bands are Raman active. The 695 cm^{-1} band is extremely weak and appears as a poorly resolved shoulder on the strong fundamental at 742 cm^{-1}. The 563 cm^{-1} band is fairly strong in the IR but is located between two fundamentals, one at 598 cm^{-1} (IR) and the other at 520 cm^{-1} (R,IR). Crystal field splitting of several fundamentals is also suggested and the appropriate bands have been designated in Fig. 13 and in Table VIII. In the erythritol spectra there are no suspected overtone or combination bands. Instances of apparent field splitting are designated in Fig. 13 and Table IX.

Comparison of the calculated and observed distributions in Fig. 13 with these factors in mind, shows that the fit in the case of ribitol is not quite as good as the fit obtained to the spectra of the other two alditols. The fit between the observed and calculated spectra of xylitol is perhaps the best. It is noteworthy that in the case of 1,5-anhydroribitol (1,5-AHR), studied by Pitzner (1), the correlation between the observed and computed distributions was not nearly as good as the fit obtained between the experimental and calculated modes in the other 1,5-AHP's. Although the average error was 7.6 cm^{-1} as compared to the overall error of 6.3 cm^{-1}, there were 9 observed bands between 1150 and 650 cm^{-1} which could not be correlated with calculated modes. However, this does not necessarily suggest a trend.

Careful examination of the observed and calculated spectra plotted in Fig. 13 shows that in each instance there are characteristic gaps in the distribution of the bands between 1500-400 cm^{-1}. Essentially the alditol spectra are structured into well-defined groups of bands in this particular region. The first characteristic gap occurs between 1200-1150 cm^{-1}. The potential distributions indicate that this gap is an apparent transition point between valence angle bending coordinates involving at least one hydrogen atom, and skeletal stretching vibrations. Another characteristic void occurs between approximately 850-750 cm^{-1} in all the spectra. It is widest for erythritol (170 cm^{-1}) and equal for xylitol and ribitol (108 cm^{-1}). The potential distributions indicate that above the gap skeletal stretching vibrations dominate while below the gap skeletal bending vibrations predominate.

The calculated distributions do, however, deviate somewhat from the observed distributions below 400 cm^{-1}. The deviation results from the fact that there are more calculated bands than observed bands in each of the spectra. The most logical explanation for this is that the predicted bands simply cannot be resolved. Many of the calculated modes are close to accidental degeneracy in this region. This may account, in part, for both the larger widths and asymmetric contours of many of the bands in this region. Two additional factors also combine to make band resolution more difficult. First, many of the low energy vibrational bands may be inherently too weak to be observed in either the Raman or IR. Secondly, higher backgrounds interfere with the resolution of the weaker bands. Rayleigh scattering interferes at low wavelengths in the Raman causing the base line to increase sharply in this region. In the infrared KBr absorption begins to occur at about 350 cm^{-1}.

Aside from the fact that both the observed and computed band distributions agree quite well for each of the alditol models, their respective force fields were identical. Thus, the observed differences in the frequencies between the pentitol compounds must result primarily from differences in their $\underset{\sim}{G}$ matrices. Unlike the 1,5-AHP's, the bond angles and bond lengths are not all the same and thus they contribute to the differences in the respective $\underset{\sim}{G}$ matrices. However, the dominant structural differences result from both conformational and configurational differences among the isomers in the case of the pentitols. Thus, the frequency variations in their spectra must then be attributed primarily to the changes in the coupling of vibrations that result from these structural differences.

The results also indicate that most of the vibrations in the molecules studied arise, to a first approximation, from the isolated molecule, apart from its environmental surroundings. The fact that a good fit to the observed spectra of erythritol was obtained using the same field substantiates this observation. Erythritol differs from the pentitol models in size, complexity (there are 8 molecules per unit cell as opposed to 4 per unit cell in each of the other alditols), and vibrational degrees of freedom. However, it is important to emphasize that these findings do not necessarily imply that this approximation can be applied to all molecules. They do complement the work of Pitzner (1) and thereby add support to the notion that a key factor in understanding the vibrational spectra of other carbohydrate molecules, such as the pentoses and hexoses, will depend primarily upon the properties of the isolated molecule treated as a vibrating unit in the crystal lattice.

The sensitivity of the calculated modes to structural differences brought about by changes in the conformation of the molecular model is shown in Fig. 14.

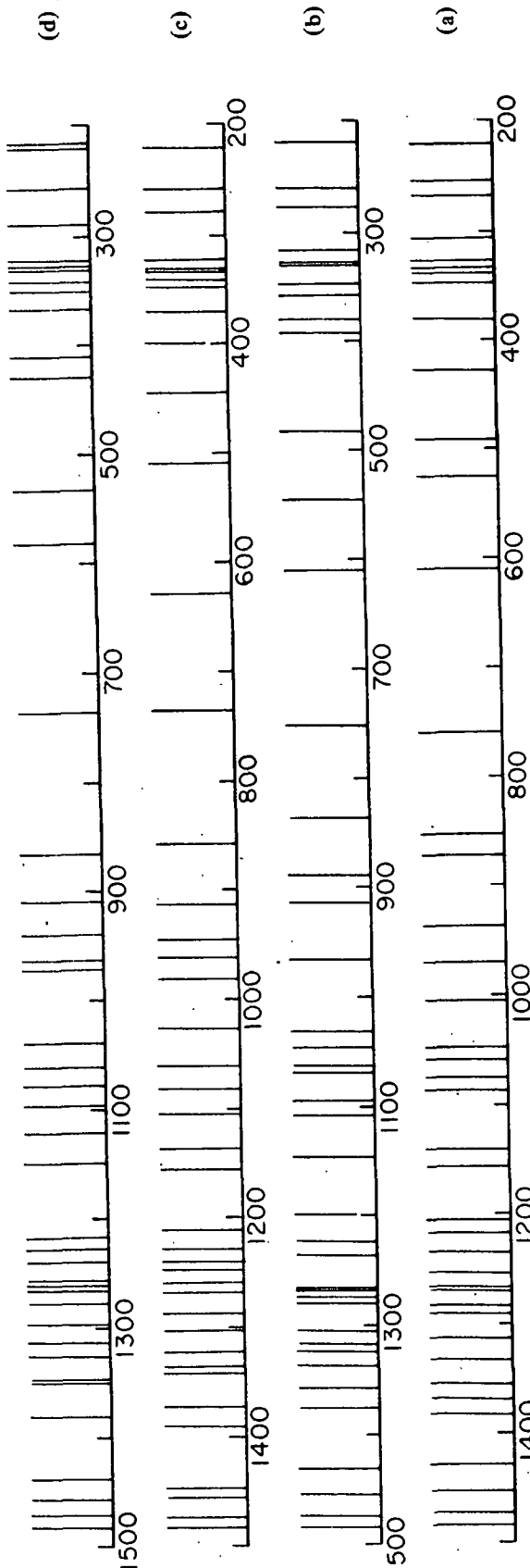

Figure 14. Calculated Frequencies of Ribitol in Alternate Conformations: (a) Reported Conformation (26), (b) Conformation C(I), (c) Conformation C(II), and (d) Conformation C(III)

The calculated distribution of frequencies in the spectrum of ribitol between 1500-200 cm^{-1} is shown in Fig. 14(a) as are the distributions calculated from three other conformational isomers of ribitol. In conformation C(I) the ribitol model is in an extended chain conformation similar to erythritol and D-arabinitol. This conformation was formed by a 120° rotation (counter-clockwise) about C(3)-C(4) which results in a syn-axial interaction between C_2O and C_4O (see Fig. 21, Appendix I). No other structural changes were made. Conformation C(II) was formed by a rotation about C(1)-C(2) so that the terminal hydroxyl group on C(1) was in a conformation identical to that of xylitol. The final conformation C(III) was formed by combining the structural changes made to form C(I) and C(II). The frequencies calculated for each of the three isomers are listed in Table XI.

From Fig. 14 and Table XI it is evident that the sensitivity of the bands in the ribitol spectrum to these conformational changes is greatest between 1150-200 cm^{-1}. Comparing the Raman spectrum of ribitol in solution with that of the solid (shown in Fig. 2) indicates that the most significant changes in the distribution of bands occur in this same region. The possible conformations of ribitol in solution are numerous indeed. However, the data presented in Fig. 14 suggest that changes in the distribution of bands in solid-state vibrational spectra which occur upon solution result, in part, from the structural differences among the various conformational isomers. The structural differences among the isomers result in significant changes in the vibrational coupling associated with the fundamental modes.

TABLE XI

CALCULATED FREQUENCIES OF RIBITOL IN THREE ALTERNATE CONFORMATIONS

Structural Model[a], ν, cm^{-1}		Conformation C(I), ν, cm^{-1}		Conformation C(II), ν, cm^{-1}		Conformation C(III), ν, cm^{-1}	
3351	1138	3351	1108	3351	1135	3351	1120
3351	1048	3351	1095	3351	1103	3351	1094
3330	1073	3330	1068	3330	1080	3330	1078
3330	1057	3330	1060	3330	1059	3330	1060
3330	1046	3330	1043	3330	1025	3330	1038
2968	1004	2968	1030	2966	980	2966	971
2949	969	2949	963	2949	960	2949	963
2934	935	2933	922	2933	945	2932	939
2922	870	2922	888	2922	910	2922	909
2914	852	2914	834	2914	856	2913	865
2901	758	2901	748	2901	733	2901	735
2880	609	2880	607	2883	626	2883	581
1482	524	1482	543	1482	506	1482	531
1471	490	1471	483	1471	441	1471	428
1452	426	1449	395	1453	396	1456	409
1426	380	1427	379	1445	368	1439	367
1381	347	1373	356	1389	347	1380	349
1368	339	1355	346	1370	339	1350	340
1353	333	1334	329	1340	333	1348	332
1331	326	1322	328	1336	331	1324	328
1312	305	1314	315	1320	320	1312	322
1295	266	1301	273	1300	276	1296	288
1292	252	1278	257	1284	255	1276	255
1268	218	1272	217	1265	217	1266	218
1265	192	1266	192	1258	202	1260	213
1252	174	1265	147	1244	185	1257	144
1231	124	1234	135	1238	130	1239	133
1213	116	1218	115	1225	101	1226	117
1202	85	1197	95	1208	86	1216	86
1154	71	1144	68	1155	75	1147	76

[a]Based on the crystal structure determined by Kim, et al. (26).

TRANSFERABILITY OF THE SVQFF TO RELATED MOLECULES

The normal modes of D-arabinitol[12] were calculated for two reasons:

1. To test the predictive capabilities of the force constants calculated using models of ribitol, xylitol, and erythritol.
2. To possibly resolve the uncertainty as to whether the structure of the D isomer in the D,L crystal is the same as its structure in the optically active D isomer.

The calculated frequencies are plotted in Fig. 15 as are the experimental frequencies in the spectra of both D and D,L-arabinitol. These frequencies are compared in Table X also. From Fig. 15 it is evident that the calculated frequencies approximate the observed frequencies in both the D and D,L forms quite well. The results suggest that the model force field in Table V is well suited to this class of compounds. The ability to transfer these constants to D-arabinitol suggests that the field does have physical significance, includes sufficient interaction terms, and should provide an adequate approximation to the spectra of other related alditols.

COMPARISON OF THE D AND D,L-ARABINITOL SPECTRA

As a matter of interest, a racemic mixture of the D and L isomers was prepared. The spectra (R and IR) of the mixed crystal form were compared with the observed spectra of the D isomer. If the molecular vibrations below 3000[13] were totally independent of the crystalline environment (which was

---

[12] Recall that the calculated frequencies are based on the structure of D-arabinitol as it exists in the D,L mixed crystal (20).

[13] In the following discussion, the spectral bands will be referred to by their frequencies in wave numbers.

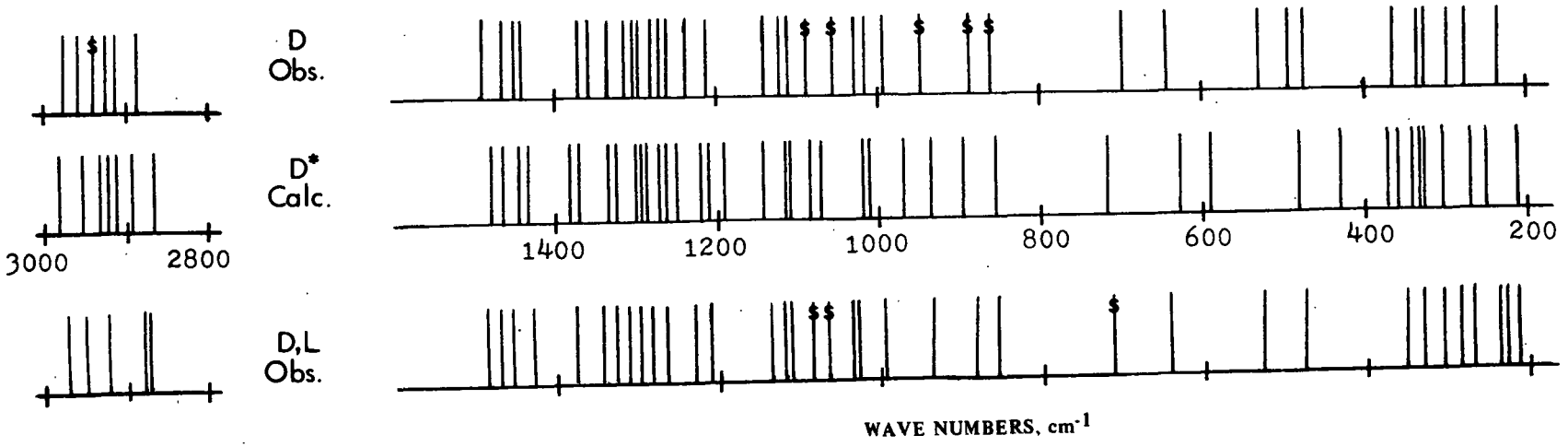

*Based on the structure of the D molecule in the D,L crystal

$ split band

Figure 15. A Comparison of the Calculated Frequencies of D-Arabinitol with the Experimental Frequencies of D and D,L-Arabinitol

certainly not expected to be the case), then the spectra of the mixed crystal should be identical to either isomer, provided that the molecular conformations remain the same (which is not necessarily the case). Consequently, such a comparison would provide some insight into the effects of the unit cell geometry and intermolecular interactions on vibrational spectra.

A similar comparison was made by Pitzner (1) on 1,5-anhydro-D,L-arabinitol and its L isomer. Pitzner noted that the D,L spectra correlated fairly well with that of the optically active L isomer, but that a number of the D,L bands were shifted in frequency from corresponding bands in the spectra of the L isomer. He noted that suspected differences in the geometry of their unit cells and/or differences in the intermolecular hydrogen bonding could possibly explain the differences in the spectra of the two forms.

From Fig. 7 and 8 it is apparent that differences do occur between the spectra of the D,L mixed crystal and the optically active D isomer of arabinitol. These differences have been classified into 5 types:

1. Differences in the frequencies of the observed fundamentals.
2. Differences in the relative intensities of the observed bands.
3. Differences relating to the Raman or IR activity of the fundamental modes.
4. Apparent differences in the number of suspected overtone or combination bands.
5. Apparent differences in the number of vibrational splitting effects (correlation field splitting).

In Table X the computed frequencies of D-arabinitol were correlated with the experimentally observed bands in the spectra of both the D and D,L forms. An element of trial remains in these correlations and their validity must in part be judged on the basis of all the results obtained from the NC analyses.

However, using these calculated frequencies an interpretation of the arabinitol spectra was made.

Based on the assignments made in Table X it was possible to compare the observed bands in the arabinitol spectra. It is evident that a number of bands in the D spectra are shifted in frequency from similar bands in the D,L spectra. These shifts result in noticeable changes in the distribution of observed bands in Fig. 15. However, judging from the data presented in Table X and the distributions plotted in Fig. 15, the changes in the distributions are not comparable to the types of differences that occur among the pentitol spectra. Comparing the arabinitol spectra, there are, in fact, only 5 assigned bands in the Raman spectrum of the D isomer (1440, 1357, 697, 363, 295) that differ in frequency by more than 10 cm^{-1} from corresponding bands in the D,L mixed crystal. Of these 5 bands, two differ in frequency by only 11 cm^{-1} and none differ by more than 15 cm^{-1}. Furthermore, of the 41 bands compared between 2980 and 300, only 16 of the observed bands differ by more than 7 cm^{-1}.

The shifts in some of these frequencies are large enough to suggest that there may be minor conformational differences in the terminal methylene hydroxyl groups in the structure of the isolated D isomer. However, no major differences in conformation are indicated. In the case of ribitol, altering the conformation of the molecular model substantially affected the distribution of bands in the calculated spectrum. Comparatively large shifts in the band distributions occurred between 1030-350 (see Fig. 14 and Table XI). Skeletal stretching and bending modes are active in this region indicating that the coupling of vibrations involving the carbon and oxygen atoms are especially sensitive to structure. Relatively minor differences between the arabinitol spectra occur in this region. Thus, these shifts are suggested to result from either changes in the pattern

of intermolecular bonding between the two crystalline forms, or minor conformational differences.

There are four other types of observed differences that are also significant. First, there are major differences in the band intensities. For example, the relative intensities of the D-arabinitol bands between 1400-1200 and between 400-200 indicate that these bands are more intense than corresponding D,L bands. Intensity variations usually indicate changes in the nature of the bond. Variations in intermolecular bonding can influence band intensities, and therefore it is significant to note that the melting point of the D,L form (105°C) is 14.5 degrees higher than the D isomer. However, other factors are involved. For example, the D isomer is optically active, whereas the racemic mixture is not. Optical activity may influence the intensities. The consequences of optical activity, if any, on vibrational spectra have not been explored. Also, unit cell geometry may again be a factor. Because the unit cell of the D,L mixed crystal is different than that of the D isomer, differences in the intensity of the scattering may result.

Secondly, though most every band in the D isomer is active in both the Raman and IR there are a few instances in the D,L spectra where mutual activity is not observed. However, in view of the weaker intensities of many of the bands in the D,L spectra the bands not observed may be inherently too weak for detection. For example, there are 7 bands between 2980 and 400 [2966(R), 1465 (IR), 1425(IR), 1312(IR), 1271(R), 1230(R) and 1115(R)] in D,L-arabinitol that are not mutually active. The 1425(IR) band is a broad, poorly resolved band of medium intensity. Corresponding bands (see Table X) in the spectra of the D isomer occur at 1440(s,b)(IR) and 1440(w,sh)(R). Judging from the relative IR intensities of these modes, it is likely that the 1425(IR) band is too

weak to be detected in the Raman spectrum of D,L-arabinitol. The same is true for the bands at 2966(R), 1271(R), 1230(R) and 1115(R) except that they are too weak for IR detection. Poor resolution may be responsible for the fact that the 1465 band is not observed in the Raman.

However, it is also possible that the mutual exclusion observed for these bands is related to the localized inversion symmetry of the D,L pairs in the crystal. When the D and L enantiomers crystallize, D,L pairs are formed and the D enantiomer is hydrogen bonded to the L enantiomer by bonds at two locations. If special selection rules resulting from the inversion symmetry are in operation, the breakdown due to anharmonicity is extensive. The majority of the bands in the D,L spectra are mutually active.

There is also a difference in the number of suspected overtone and combination bands in the spectra of the D isomer. The suspected overtone and combination bands are described in Table XII for both crystal forms. As noted above, the relative intensities of the bands between 1400-1200 and 400-200 in the D isomer were more intense than corresponding bands in the spectrum of the racemic mixture. This may account, in part, for the greater number of overtone and combination bands.

For example, in Fig. 7 there is a band at approximately 780 in both spectra. The band is more intense in D-arabinitol than in D,L-arabinitol. Clearly, no fundamentals are predicted to occur in this region. It is therefore suggested that this band is a combination band rather than a fundamental. As specified in Table XII, the suggested combination is 491(s) + 295(s) = 786 cm^{-1}. A comparison of the relative intensities of the Raman bands at approximately 295 in both spectra (see Fig. 7) reveals that the band is much more intense in the spectrum of D-arabinitol. Thus, a combination of the type suggested would likely be more intense in the D spectrum.

TABLE XII

SUSPECTED COMBINATION OR OVERTONE BANDS

Crystal	Obs. Freq., cm^{-1}		Possible Combination or Overtone
D-Arabinitol	2990(w,sh)	(R)[a]	2(1494)(s) = 2988
D-Arabinitol	1395(vw,b)	(R)(IR)	887(vs) + 528(m) = 1415
D,L-Arabinitol	1395(w,sh)	(IR)	
D-Arabinitol	1069(w)	(R)(IR)	697(m) + 363(m) = 1060
D-Arabinitol	909(w)	(R)(IR)	3(295)(s) = 885
D-Arabinitol	782(m)	(R)(IR)	295(s) + 491(s) = 786
D,L-Arabinitol	782(vw)	(R)(IR)	
D-Arabinitol	736(w,b)	(R)(IR)	2(363)(m) = 726
D-Arabinitol	595(vvw)	(R)(IR)	2(295)(s) = 590
D-Arabinitol	540(vw)	(R)(IR)	2(268)(cal.) = 536
D,L-Arabinitol	540(w,sh)	(R)(IR)	
D-Arabintiol	405(vvw)	(R)(IR)	2(196)(cal.) = 392
D,L-Arabinitol	406(vw)	(R)	

[a](R) = Raman active; (IR) = infrared active.

Another seemingly new band appears at 909 in the D spectrum. In view of the difference in the relative intensity of the 295 band in the Raman spectrum of the D isomer, there is reason to suspect that the 909 band is a possible overtone [i.e., 3(295) = 885 cm^{-1}]. The second overtone of this band is also suspected to be Raman active and to occur at 600, though its intensity is much weaker. Although it is unusual for a third overtone to be greater than a second overtone, Fermi resonance could explain the difference. The 909 band is very near a series of fundamental modes which are the strongest bands observed in the spectrum below 1500. The remaining bands suggested to be either overtones or combination bands in Table XII are all relatively weak and located near fundamental modes.

To suggest that the bands given in Table XII are, in fact, overtones and combinations of fundamental bands is done with reservation. There is no direct way to substantiate such an interpretation. It is also possible that a number of these bands result from external vibrations, coupling between external and internal modes (which would also result in combination bands of a summation or difference nature), or thermally excited second-order transitions of low energy fundamentals. Sherwood (33) notes that internal and thermally excited external vibrational coupling become especially important as the vibrations of internal and external modes approach one another in value (i.e., below 800 cm^{-1}).

Finally, the perturbations to vibrational coupling by the presence of other molecules in the same unit cell are apparently more extensive in the D isomer as evidenced by the degree of vibrational splitting in the solid state. It should be emphasized that solid-state splittings or changes in selection rules result from an interaction of a molecule with its environment. In organic substances the most common cause of solid-state effects is hydrogen bonding. Therefore, it is interesting to note that the melting point of the D isomer is 14.5 degrees lower than the D,L mixed crystal. However, factors other than the degree of hydrogen bonding are involved. The coupling together of the vibrations of different molecules within the unit cell may give vibrations which are symmetric or antisymmetric with respect to operations of the crystallographic point group (which is unknown in the case of the D isomer). Consequently, selection rules would then be an important factor. Although hydrogen bonding would be expected to be the most common type of intermolecular coupling, electronic coupling is also possible. As Gans (32) points out, the interactions of molecules in a unit cell are very poorly understood and not amenable to quantitative work, except in the simplest cases.

Apparent correlation field splitting occurs in several regions in both sets of spectra. Between 900-850 there are clearly four bands (887, 878, 867, and 855) in the D isomer. In the D,L spectrum only two bands occur in this region, which is consistent with both the calculated distribution in Table X and the observed distribution in the spectra of its configurational relatives ribitol and xylitol. Also based on the predicted band distributions it is likely that the doublets in the D isomer assigned to the calculated fundamentals at 2934, 1082, 1070, and 938 result from field splitting effects. In the D,L spectrum the corresponding bands assigned to the predicted fundamentals at 2934 and 938 are not split. However, the bands assigned to 1082, 1070, 1019 and 718 are split as Table X indicates.

INTERPRETATION OF THE ALDITOL SPECTRA

The third criterion used in this study to evaluate the quality of the NC analyses related to the extent to which the constraints on the analyses were satisfied. One important constraint stipulated that the interpretations based on the normal coordinates be consistent with the group frequency correlation charts for those regions of the spectra where the charts are applicable.

Unfortunately, the information based on group frequency correlations is of little value below 1500 cm^{-1}. At best, parallels can be drawn between group frequency charts and the calculated frequency of the major components of the normal coordinate associated with each fundamental.

The individual bands in the alditol spectra are best described by the dominant internal coordinates and potential constants associated with each mode (see Appendix III). Though discussion of the individual bands would be beneficial, it would also be impractical due to the number of bands involved

and the complexity of the normal coordinates. However, it is possible to examine the spectra in terms of the group motions described in Tables VII-X. These motions, illustrated in Fig. 12, have been used to approximately characterize the normal coordinate of each fundamental vibration. In Table XIII the calculated spectra of the alditols, 1,5-AHP's (1) and the n-paraffins (7) have been compared. The basic group vibrations have been classified in terms of the calculated normal frequencies. Table XIV is constructed similarly to compare each of the alditols in terms of their respective group motions.

The advantages of using group motions to interpret the spectral bands is that the various internal modes may be classified according to frequency. Thus, it is easier to identify trends among the spectra. It must be emphasized, however, that the vibrations of the atoms may be localized within particular atomic groupings. A band interpreted as a methine op bending mode, for instance, can involve a displacement of each of the methine CCH coordinates, although the relative amplitudes of the atoms involved are not necessarily the same.

OH AND CH STRETCHING MODES

The bands in only two regions of the spectrum can be associated with individual group motions. In the first region, between 3350-3100, hydroxyl groups are involved. As Table XIII shows, the OH stretching vibrations were calculated to occur between 3350-3300. The observed OH stretching frequencies, which are clearly sensitive to hydrogen bonding, occurred between 3350-3225. Because these vibrations are not coupled significantly with the vibrations of other groups, they are essentially independent of the rest of the bands in the spectra and were treated accordingly. No attempts were made to correlate the observed and calculated frequencies, and they were excluded from the refinement of the force constant parameters.

TABLE XIII

GROUP VIBRATIONAL MOTIONS OF THE ALDITOLS, 1,5-AHP's AND n-PARAFFINS

Group Vibrational Motions	Alditols Freq. Region	1,5-AHP's (1) Freq. Region	n-Paraffins (7) Freq. Region
Methylene OH str.	3350		
Methine OH str.	3330	3356	
CH_3 asym. CH str.			2969-2965
Methylene asym. CH str.	2985-2950	2982-2978	2929-2912
Methine CH str.	2940-2910	2946-2910	
CH_3 sym. CH str.			2884-2883
Methylene sym. CH str.	2900-2865	2882-2880	2861-2849
CH_3 op HCH bend			1466
CH_3 ip HCH bend			1473-1446
CH_3 sym. HCH bend			1385-1368
Methylene ip bend or "scissor"	1485-1457 1439-1435	1470-1460	1473-1446
Methylene op bend or "wag"	1485-1457 1439-1300	1470-1410 1388-1347	1411-1174
Methine CH ip bend (<HCO)	1450-1216	1435-1200	
Methine CH op bend (<HCC)	1450-1200	1435-1200	
Methylene op bend or "twist" Methylene ip bend or "rock"	1330-1200	1330-1220	1310-1175
OH ip bend	∿1420 1330-1200 1140-850	∿1410 1285-1200 ∿1160 ∿1075	
C-O stretching	∿1140 1110-850	1155 1110-1040 1010-900 870-850	
C-O ring stretch (C-O-C)		1130-1095 1061-1014 980-850	
C-C stretching	1154-1087 1059-840		1132-∿885
C-C ring stretch		1163-850 750 670-460	
CH_3 rocking			975-835
Methylene op bend or "twist" Methylene ip bend or "rock"	∿1148-1108 1080-1040 970-830	1163-1108 1074-930 873-850	1069-719
CCO bend (op and ip)	775-360 330-220	980-880 750-640 463-250	
CCC skeletal bending	700 600-430 302-200		533-0
Ring bending modes		750-540 480-300 ∿250	
OH op bend	430-300 268-249	285-220	
CC skeletal torsion	∿430 370-50	∿300 200-130	∿153-0

TABLE XIV

FREQUENCY CLASSIFICATION OF THE GROUP VIBRATIONAL MOTIONS OF THE ALDITOLS

Group Vibrational Motions	Ribitol Freq. Region	Xylitol Freq. Region	Erythritol Freq. Region	D-Arabinitol Freq. Region
Methylene OH str.	∿3352	∿3352	∿3352	∿3352
Methine OH str.	∿3330	∿3330	∿3330	∿3330
Methylene asym. CH str.	2968-2949	2967-2963	2974-2964	2983-2956
Methine CH str.	2934-2914	2934-2914	2921-2909	2934-2914
Methylene sym. CH str.	2902-2881	2884-2882	2872-2867	2896-2865
Methylene ip bend or "scissor"	1482-1472	1463-1462 ∿1439-1435	1498-1457	1476-1461
Methylene op bend or "wag"	1482-1471 1352-1330	1463-1462 1439-1355	1498-1457 ∿1353-1320	1476-1461 1324-1299
Methine CH ip bend (HCO)	1452-1290	∿1435 1362-1295	1418-1369 ∿1276 ∿1216	1441-1432 1333-1261
Methine CH op bend (HCC)	1452-1312	1439-1347 1297-1245	1331-1320 1250-1205	1441-1320 ∿1293 ∿1200
Methylene op bend or "twist"	1332-1245	1274-1200	∿1320	1270-1219
Methylene ip bend or "rock"	1265-1200		1250-1230	
OH ip bend	∿1426 1330-1312 1292-1150 ∿1080-850	1323-1200 1114-850	1369-1320 1270-1230 1148-970	∿1432 1324-1200 ∿1141-850
C-O stretching	∿1130 1073-850	1087-840	1065-830	∿1141 1108-850
C-C stretching	1154-1004 930-∿850	1114-1087 1059-840	1148-1128 973-837	1141-1115 1082-850
Methylene op bend or "twist"	1084	1070-1009	1148-1128	1115-1108
Methylene ip bend or "rock"	1058-1045 970-930	928-893	891-837	∿1019
CCC bend (op and ip)	750-380 305-250	775-360 330 275-240	611-485 ∿380 ∿275	720-430 375-350 302-211
CCC skeletal bending	609-490 ∿305 250-190	511-430 240-210	∿700 485-430 ∿240	∿718 625 ∿480 302-250
OH op bend	426-300 ∿266	430-320 ∿240	430-327	430-302 268-249
CC skeletal torsion	305-266 218-71	275-74	∿370 240-50	∿430 250-74

The CH stretching modes which were observed between 3000-2800 constitute the second group of localized vibrations. As Table XIII shows, the bands occur in three distinct groups: asymmetric methylene stretching, methine stretching, and symmetric methylene stretching. This pattern suggested by the potential energy distributions occurs in both the alditols and the 1,5-AHP's.

From Table XIV it is apparent that below 1500 the alditol spectra are less structured due to the coupling of vibrations associated with different group motions. Nonetheless, patterns do emerge. The region between 1500-1200 is characterized, in part, by angle bending coordinates involving at least one hydrogen atom. In contrast, bands between 1150-800 are dominated by skeletal stretching vibrations (both CC and CO), coupled with bending contributions from methylene (CH_2) and COH groups. Between 800-450 the majority of bands are characterized by angle bending coordinates not involving hydrogen atoms. Skeletal bending and CCO bending vibrations predominate in this region. Below 450 cm^{-1} skeletal bending, skeletal torsion, and OH op bending modes contribute significantly as shown in Table XIV. The dominant group motions in each of these regions will be discussed individually beginning with the methylene CH_2 bending vibrations.

CH_2 BENDING FREQUENCIES

From Table XIII it is apparent that parallels can be drawn among the spectra of the alditols, 1,5-AHP's, and the n-paraffins. In each class of compounds, the common group vibrations are located in similar regions of the spectrum. Figure 16 represents a diagrammatic summary of the likely frequency ranges of various types of vibrations in polymethylene compounds. The information in Fig. 16 is based on a discussion of the spectra of the planar

zigzag polymethylene-type compounds by Sheppard (34). For the most part, the interpreted frequency ranges are based on group frequency correlations among the spectra of related molecules. The dashed lines represent regions where the assignments are the most ambiguous.

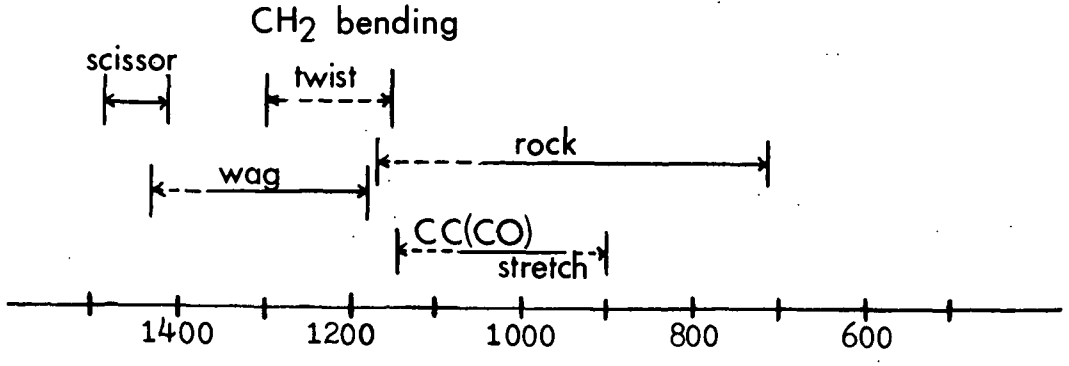

Figure 16. Frequency Ranges of Various Types of Vibrations in Polymethylene Compounds

It is apparent from Table XIII that the calculated distribution of CH_2 bending motions in the n-paraffins accurately match the distribution patterns shown in Fig. 16. Figure 16 suggests that the methylene ip (scissoring) bending modes are pure vibrations (i.e., uncoupled) and occur exclusively between 1480-1440 in polymethylene compounds. The distribution of bands associated with methylene op bending (wag and twist) overlap and are suggested to occur between 1450-1150. The bands associated with asymmetric methylene ip bending (rock), shown to have the widest distribution, occur between 1170-720. However, Fig. 16 does not indicate the extent to which these group motions are coupled.

Schachtschneider and Snyder (7) found that the various CH_2 vibrations do couple. In particular, the potential distributions associated with the CH_2 wagging modes indicated that these vibrations were coupled to other methylene bending vibrations and to CC stretching vibrations as well. Similar coupling

patterns for these vibrations are predicted for both the alditols and 1,5-AHP's. However, in both cases the coupling is more extensive. In the alditols, for example, methine CH ip and op bending and OH ip bending are substantially coupled to the CH_2 deformations which occur between 1400 and 1200. To further complicate matters, both CO and CC stretching vibrations are found to couple somewhat with these vibrations. In all cases, however, the angle bending vibrations involving at least one hydrogen atom predominate in this region.

METHINE CH BENDING

The methine CH angle bending vibrations contribute to the potential distribution most heavily between 1450-1200 in the alditols and between 1435-1200 in the 1,5-AHP's as shown in Table XIII. For the most part these methine deformations are confined to this relatively narrow region as both Tables XIII and XIV indicate.

COH BENDING

The COH ip bending vibrations are calculated to couple extensively to group motions between 1450-800 as shown in Table XIV. To help support the assignments and interpretations based on the NC analyses, the deuterated spectra of ribitol, xylitol, and erythritol were measured. The fundamentals predicted to have substantial OH ip bending contribution were expected to be affected by deuterium substitution.

Five kinds of changes in the spectra of these compounds were observed after deuterium exchange with the hydroxyls:

1. Bands disappeared completely.
2. The relative intensities of bands were reduced, but the bands did not disappear.

3. The relative intensities of bands increased.

4. The frequencies of a number of bands shifted to higher or lower levels.

5. New bands appeared.

A mode is considered to be characteristic whenever it corresponds to a vibration of a particular type of bond or bond angle. Therefore, when a characteristic COH frequency decreases in intensity upon deuteration, a COD mode should be observed at a lower frequency in the spectrum. The first and fifth kinds of observed changes, mentioned above, exhibit this type of behavior. Bands that disappear upon deuteration can readily be associated with OH related vibrations. However, new bands which appear in the spectra upon deuteration cannot always be associated with COD related vibrations. This point will be discussed in greater detail later. Intensity changes are difficult to interpret as are the observed shifts in frequency. These effects are undoubtedly related to changes in the nature of both the bonds and the vibrational coupling. The fact that change does occur, however, is sufficient to establish the contribution of the hydroxyl proton to the overall motion.

In ribitol, for example, displacement of COH coordinates contribute substantially to the potential associated with the following calculated frequencies: 1426, 1331, 1312, 1295, 1292, 1268, 1265, 1252, 1231, 1213, and 1202 (see Table VII). In each instance the observed bands assigned to these frequencies are affected by deuteration. The observed Raman bands assigned to fundamentals at 1426, 1312, 1231, and 1213 disappear completely with deuteration. Furthermore, the relative intensities of the two bands assigned to frequencies 1268 and 1265 are considerably reduced. At 1268 the methylene COH contribution is approximately 53%, and 47% at 1265 (see Table XXXIV). In most other instances the coupling of COH vibrations is such that this kind of characterization is

not possible. The results from deuteration studies on other aliphatic hydroxy compounds support the likelihood of this assignment (35). In 1-propanol methylene, OH bending occurs at 1275, in ethylene glycol at 1274, in glycerol at 1268, and in diethylene glycol at 1283 and 1267. In glucose (13) the mode most often assigned to the CH_2OH group occurs at 1278. The observed bands at 1295(m,sh) and 1289(m) assigned to 1295(calc.) and 1292(calc.), respectively, are shifted in frequency somewhat and their relative intensities increase. The remaining two bands in this group, assigned to frequencies 1331 and 1202, are low intensity bands observed in the IR only. Infrared spectra on deuterated samples were not utilized in most cases (erythritol is the exception) due to the poor resolution obtained and the difficulty caused by H_2O contamination during pellet formation.

In the next region between 1200-800, which is dominated mostly by CC and CO stretching vibrations, assignment of COH frequencies by isotopic substitution is especially difficult. The spectral resolution is complicated by a number of factors. First, the bands are noticeably broader (see Fig. 17). Some lines decrease in intensity but do not disappear, and the presence of additional bands in the spectra begin to interfere with existing bands. Furthermore, even though repeated crystallization from the deuterated solvent improves the degree of deuteration, complete (i.e., 100%) exchange is unlikely. Consequently, the observed spectrum in Fig. 1 represents a superposition of the scattering from both ribitol and deuterated ribitol. Because substantial changes are observed it is very difficult to directly correlate the bands in the ribitol spectrum with bands in the spectrum of the isotopically substituted sample. In spite of these difficulties, the effects observed upon deuteration are reasonably consistent with the predicted coupling of OH ip vibrations with the skeletal stretching modes.

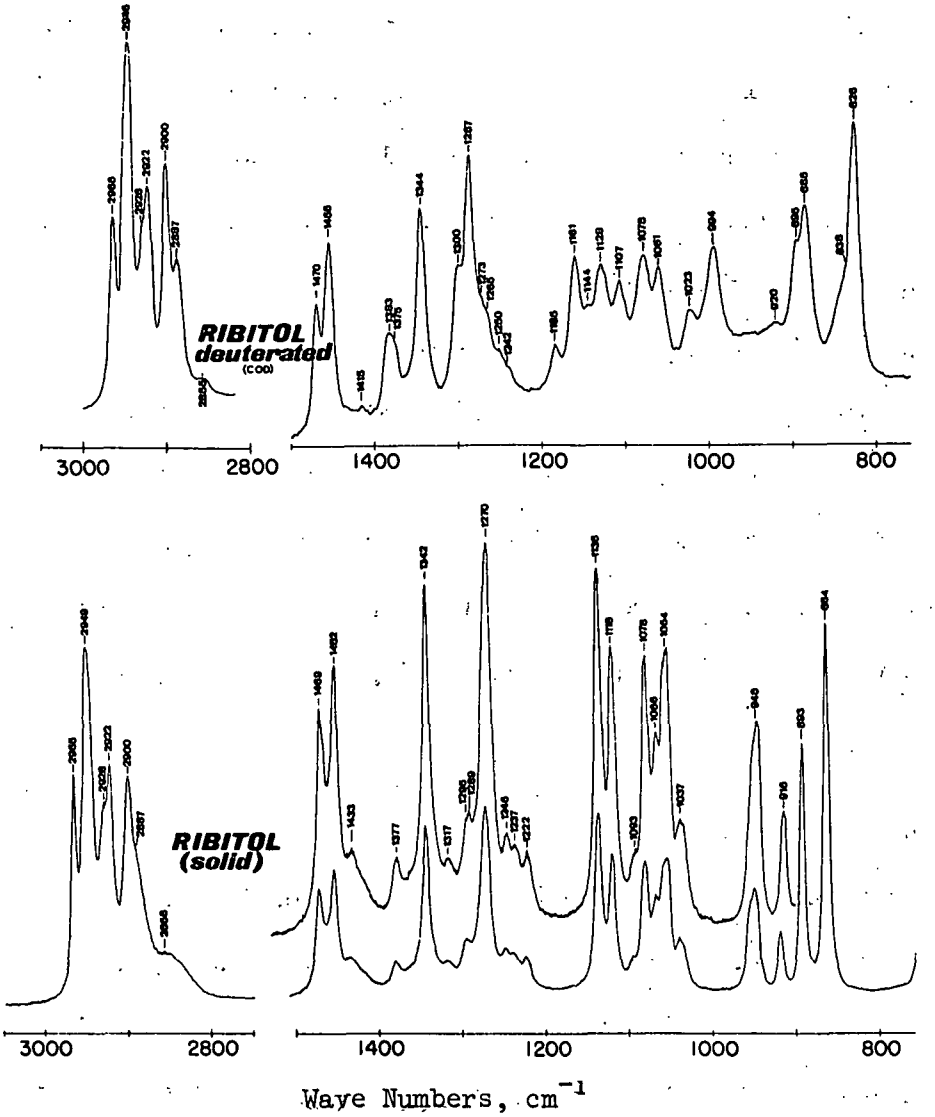

Figure 17. Raman Spectra of Ribitol

For example, in Fig. 17 the Raman bands observed at 1135 and 1118 are shifted slightly in frequency and the intense 1054 band disappears. This latter band which is assigned to the calculated fundamental at 1047 shows substantial OH bending contribution to the associated normal coordinate. The band at 1093 is not present in the deuterated spectrum, but may well be hidden in the background. The bands at 1037 and 948 disappear completely. The intensity of the 915 band is reduced, a shoulder appears on the band at 893, and the 864 band has apparently shifted to 828 (a change of 56 cm^{-1}). In addition, at least 3 new bands (1185, 1161, 1144) appear in the void characteristic of the pentitols

between 1200 and 1150. The band at 1161 is particularly strong. Two other new bands appear in the deuterated spectrum also, one at 1023 and the other at 994.

The xylitol spectra are similarly structured with respect to COH ip vibrations. Table XIV shows that COH vibrations are predicted to be most active in two regions between 1330-1200 and between 1115-850. From Fig. 4, however, it is apparent that the xylitol bands between 1410 and 1381 are affected by isotopic substitution. For example, the observed band at 1407, which is assigned to the calculated fundamental at 1396, disappears. The associated normal coordinate shows that the principal motions are the methine and methylene CH and COH bending vibrations. Though resolution in the xylitol spectrum is extremely poor between 1380 and 1335, three bands have been identified at 1374(w,sh), 1352(vw,b), and 1346(w,sh) and are assigned to 1362, 1355, and 1347, respectively. The intensities of these bands are affected by deuteration as shown in Fig. 4. Of the three bands, the band assigned to 1355 shows a 15% COH bending contribution as compared to 5% for the 1362 band. As predicted, deuteration confirms that all the normal modes between 1330-1200 involve substantial contribution from coupled COH ip bending vibrations. Characteristically, the methylene COH bending vibrations occur at 1297 and 1274.

Between 1200 and 800 the skeletal stretches show significant coupling with COH bending vibrations. Though resolution is even more of a problem in xylitol than in ribitol, the relative intensities of the bands assigned to 1109, 1059, 928, and 893 are all reduced, which is consistent with the extensive coupling of CO stretch and COH bending motions predicted by the potential distributions of these modes. New bands appear in the deuterated spectrum at 1176(w), 1157(w,sh), 1137(s), 1120(m), 1040(sh), 942(vw), 930(vw), 905(sh) and 880(vw). Frequency shifts and intensity changes occur also. The band assigned to 1029

which is initially very weak in the Raman increases substantially upon deuteration. Furthermore, the band observed at 858(vs) apparently shifts to 840, though the relative intensity is essentially unchanged.

In erythritol, bending motions involving hydroxyl protons are similarly distributed. The relative intensities of the bands observed at 1456(s) and 1366(m) increased after deuteration as shown in Fig. 18.

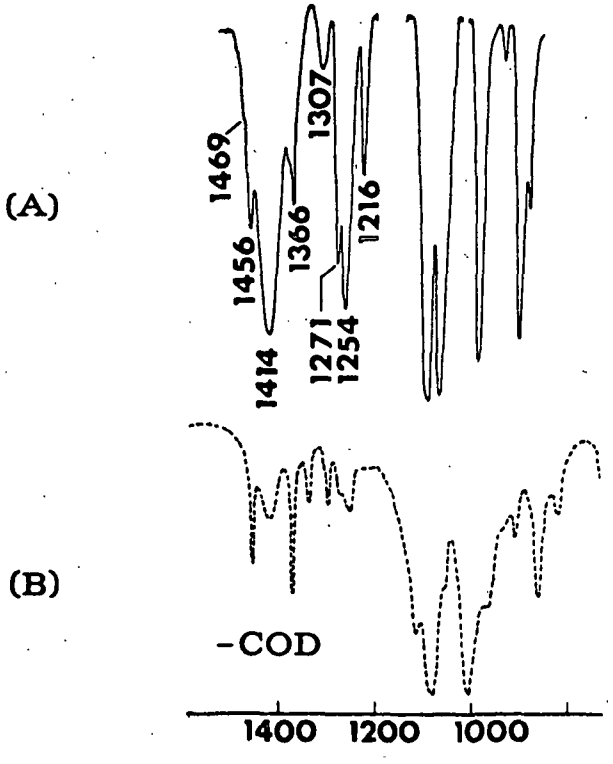

Figure 18. Infrared Spectra of Erythritol
(A) Solid; (B) Deuterated

The 1456(s) band, primarily a methylene HCH bending mode, is assigned to the mode calculated at 1457 and shows an 8% methylene COH ip bending contribution. Methylene wag (21%) and COH ip bending (24%) both contribute to the 1366 mode. Methine and methylene COH ip bending characteristically occurs at 1276 (calc.) and 1250(calc.) also. The relative intensities of the bands assigned to these fundamentals are significantly reduced after deuteration. Another

band at 1375, which is observed in Fig. 18 as a shoulder on the 1366(s) band, disappears and the bands at 1216 and 1053 are reduced in relative intensity. New bands appear at 1115, 1008, and 820, and the majority of bands between 980-800 are all significantly shifted in frequency.

From the above discussion it is clear that the bands assigned to fundamentals involving OH ip bending vibrations are affected by deuteration. Both the experimental and calculated data indicate that COH ip bending motions are coupled substantially with other group vibrations having a broad distribution of frequencies. Furthermore, the structure of the alditol spectra with respect to COH related motions is reasonably consistent with the structure of the spectra of the aliphatic hydroxy compounds mentioned earlier (i.e., 1-propanol, ethylene glycol, glycerol, and diethylene glycol). The fact that a reasonably good fit to the observed spectra was obtained in spite of the extensive coupling of OH ip motions with skeletal stretching modes suggests that the effects of hydrogen bonding are not transmitted to the skeletal vibrations.

In view of the correlation between the bands affected by deuteration and the bands calculated to have a substantial OH ip bending component, a calculation of the frequencies of deuterium-substituted ribitol and xylitol was undertaken. The hydroxyl protons in each molecule were replaced with deuterium by making the appropriate changes in mass and constructing a new $\underset{\sim}{G}$ matrix for each compound. When an atom of a molecule is replaced by an isotopic atom of the same element, it is assumed that the changes in the potential energy function and configuration of the molecule are negligible[14]. Consequently,

[14] For evidence supporting this assumption, see Herzberg, G., Spectra of diatomic molecules. 2nd ed. Table 39, New York, Van Nostrand, 1950.

the force constants are unaffected. However, the frequency parameters, λ_k, are affected substantially as a result of the changes in both the vibrational coupling and the masses of the hydroxyl protons. Vibrational frequencies involving hydrogen atoms oscillating with large relative amplitudes will be affected more than frequencies where the hydrogen atoms are vibrating with small relative amplitudes. In the limiting case where only hydrogen atoms are moving, a replacement of all of them by deuterium should decrease the corresponding fundamentals by a factor of $1/\sqrt{2}$ (i.e., the reciprocal of the square root of the ratio of the masses).

Table XV compares the observed Raman spectrum of deuterated ribitol with the computed spectra of both ribitol and deuterated ribitol in the frequency range from 3400-600 cm^{-1}.[15] A similar comparison of the xylitol spectra is given in Table XVI.

In both cases the predicted shifts in the OH stretching frequencies correlate very well with the observed shifts. The bands with normal coordinates possessing substantial COD ip bending are calculated to occur between 840 and 600 cm^{-1}. Many of the new bands observed in the deuterated spectra occur between 940 and 840 cm^{-1}. Thus, it is apparent that the predicted shifts are somewhat lower than the observed shifts. However, an exact correlation was not anticipated. Whereas the OH stretching vibrations involve primarily the hydroxyl protons, the OH bending vibrations are extensively coupled. The extent of shifting will depend on the exact form of the normal coordinate (i.e., the exact nature of the coupling). Clearly, the results from the NC analyses can only approximate the nature of the coupling. Further discr-

[15] The calculated frequencies of deuterated ribitol and xylitol are listed in Appendix IV.

TABLE XV

CALCULATED AND OBSERVED SPECTRA OF
DEUTERIUM SUBSTITUTED RIBITOL

Obs. (COD), $\Delta\nu$, cm^{-1}	Calc. (COD), ν, cm^{-1}	Calc. (COH), ν, cm^{-1}	Obs. (COD), $\Delta\nu$, cm^{-1}	Calc. (COD), ν, cm^{-1}	Calc. (COH), ν, cm^{-1}
		3351	1265(sh)	1263	1265
		3351	1250(w)		1252
		3330	1242(w,sh)	1244	
		3330			1231
		3330		1224	
					1213
2965(s)	2968	2968			1202
2949(vs)	2949	2949			
2928(s,sh)	2933	2934	1185(m,b)	1186	
2922(s)	2922	2922		1182	
	2914	2914	1161(s)		1154
	2901	2901	1144(m)	1145	1138
	2880	2880	1128(s)	1132	
				1125	
2485(sh)	2440		1107(m,b)	1094	1095
2459(s)	2440		1078(s)		1068
2429(s,vb)	2425		1061(m)		1060
	2425				1043
2415(sh)	2423			1036	1030
			1023(m)	1017	
	1481	1482	994(s)	988	
1470(m)	1468	1471		976	969
1455(s)	1444	1452			935
		1426	920(w,b)		
1415(vvw)	1408		895(sh)		
			885(s)	881	
1383(m,b)	1376	1381			870
	1362	1368			852
1344(s)	1346	1353	838(sh)	837	
		1331	826(vs)		
1300(s,sh)	1312	1312		786	
			743	751	758
	1297	1295		733	
1287(vs)	1291	1292		715	
1273(m,sh)		1268			

TABLE XVI

CALCULATED AND OBSERVED SPECTRA OF DEUTERIUM-SUBSTITUTED XYLITOL

Obs. (COD), $\Delta\nu$, cm^{-1}	Calc. (COD), ν, cm^{-1}	Calc. (COH), ν, cm^{-1}	Obs. (COD), $\Delta\nu$, cm^{-1}	Calc. (COD), ν, cm^{-1}	Calc. (COH), ν, cm^{-1}
		3352		1276	1274
		3352	1247(w)	1253	1245
		3330		1230	1233
		3330		1225	1213
		3330			1199
	2967	2967	1176(w)		
	2963	2963		1166	
	2934	2934	1157(w,sh)		
	2923	2922	1137(s)	1146	
	2914	2914	1126(sh)	1127	
	2884	2884	1120(m)		1114
	2882	2882		1103	1109
			1087(s)		1087
2545(w)	2440		1075(s,sh)	1063	1070
2500(m)	2439				1060
2428(w)	2425		1040(sh)	1036	1028
2405(w)	2423		1030(m)	1011	1009
2360(w,b)	2423				
			998(m)	997	
1465(vs)	1459	1463		982	975
1454(m,sh)	1453	1462	942(vvw)		
	1432	1439	930(vvw)		928
	1425	1435	905(sh)		
		1396	893(w)		893
1380(m)	1383		880(vw)		
1364(s)	1352	1362	853(m,sh)	858	
1353(m,sh)	1343	1355	840(vs)		842
	1342	1347		832	
		1323		794	
		1320		763	773
1309(s)	1306		738(vvw)	737	
		1297		717	
1288(m)	1289	1295	575(vvw,b)	591	613

discrepancies in the shifting result from the fact that the observed frequencies are influenced by cubic and quartic terms in the potential energy. The effects of hydrogen bonding also perturb the coupling of these vibrations with other group motions.

In spite of the observed discrepancies, the trends between the calculated and observed data in Tables XV and XVI are revealing. For example, one of the most important differences in the spectra of the deuterated pentitols was the appearance of a series of bands between 1200-1140 cm^{-1}. No bands are observed in this region in the spectra of the unsubstituted alditols. However, the calculations in Tables XV and XVI show that the agreement between the calculated and observed spectra of the deuterated pentitols is quite good in this region. In fact, if one allows for the fact that some proton exchange occurred during sample preparation, the correlation between the deuterated spectra and the calculated spectra of both the substituted and unsubstituted pentitols is very good between 1185-975 cm^{-1}. The potential distributions associated with the bands calculated between 1200-1140 cm^{-1} indicate that these "new" bands are not COD related vibrations. They are, in fact, predominately skeletal stretching vibrations which exhibit very little (less than 10%) coupling with COD components. Consequently, "new" bands which appear in the vibrational spectra after deuteration cannot necessarily be correlated with COD related vibrations. The calculated distributions do indicate, however, that the new bands which occur between 900-800 cm^{-1} are likely to be COD related vibrations. The weak intensity of these bands relative to the bands between 1200-1100 cm^{-1} suggests that it is also quite possible that some of the COD bands may be inherently too weak for detection.

CO AND CC STRETCHING

In the alditols, it is apparent from Table XIV that between 1150-800 extensive coupling occurs among the skeletal stretching, OH ip bending, and methylene twisting and rocking vibrations. The presence of the skeletal CC and CO stretching components in this region is consistent with the interpretive trends based on group frequency correlations. In Fig. 16, for instance, the CH_2 rock and CC stretching bands are shown to overlap extensively. However, overlapping of the bands does not necessarily imply coupling of the internal modes. Snyder and Schachtschneider (8) found the coupling of the CC stretch, methylene rock, and methylene twist to be extensive. In the case of the n-paraffins the coupling is also influenced by the methyl rocking modes in this region. For example, in n-pentane (gauche) the calculated fundamental at 1107 contained the following components: methyl rock (32%), CC stretch (24%), methylene twist (17%), and methylene rock (14%). Figure 16 suggests that methylene twisting and rocking appear in two regions, the twisting between 1311-1170 and the rocking between 1061-721. In contrast, Schachtschneider and Snyder (7) found that methylene rocking and twisting components are coupled in both regions to each other and to methyl rocking and skeletal stretching components as well.

In spite of the extensive coupling in this region the bands in the alditol spectra are for the most part characterized by CC and CO stretching vibrations. An analogous situation occurs in the spectra of the 1,5-AHP's where a number of vibrations in this region involve ring stretching vibrations (1).

The mixing of the CC and CO stretching components, which is clearly evident from the potential distributions in Appendix III, shows the result

of having similar bonds and similar masses in a chainlike molecule. In a carbon chain molecule there will not be one characteristic CC frequency. Coupling will occur between the equivalent bonds which leads to a splitting of the characteristic frequency. The stronger the coupling between these bonds, the larger the splitting, and the wider the frequency distribution. The CC and CO force constants are of similar magnitude and the masses of the carbon and of oxygen atoms are comparable. Thus, the vibrations of the atoms in these atomic groupings would be expected to be highly mixed. For example, in paraffin molecules the CC stretching vibrations often give weak bands in the IR because the changes in the dipole moments associated with these bonds are relatively small. However, in molecules such as the straight-chain alcohols, the intensity of the various skeletal bands is greater. The coupling of the more polar CO bond with the CC stretching components is the attributed cause of the increase in the relative intensities of these bands (34).

The skeletal vibrations of the alditols encompass the entire CC and CO bond network, and not just the vibrations of the carbon atoms in the backbone. Figure 19 compares the basic structures of xylitol and ribitol with respect to the relative orientations of the carbon and oxygen atoms. These molecules are configurational isomers. The only structural differences occur in the relative orientations of O_{13} and O_6. However, based on geometric considerations, changing the orientation of O_{13} and O_6 in xylitol is likely to affect the coupling of the skeletal vibrations throughout the entire molecule.

In xylitol there are two intersecting planes that contain a zigzag arrangement of successive CC and CO bonds. The first plane, which contains 6 atoms and 5 successive bonds, is formed by O_6, C_1, C_2, C_3, C_4 and O_{16} shown in Fig. 19. The second contains 5 atoms and 4 successive bonds and is defined

by O_{13},C_3,C_4,C_5, and O_{19}. The different orientations of the O_{13} and O_6 atoms in ribitol reduce both the total number of atoms and successive bonds in each plane by one.

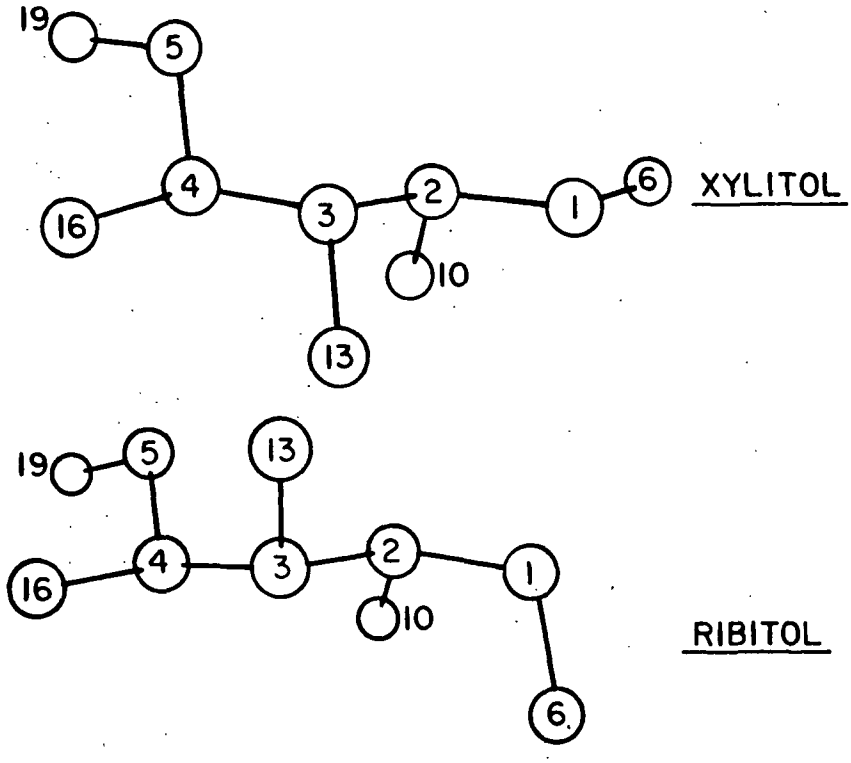

Figure 19. Basic Backbone Structure of Xylitol and Ribitol

There is a strong possibility that the degree of interaction between successive bonds is reduced by the reorientation of these atoms to positions outside either of the intersecting planes. Thus, the manner in which the vibrations in xylitol and in ribitol couple will be markedly different.

It is interesting to note that a similar geometric difference occurs between the α- and β-glucose molecules which are configurationally different at the anomeric site. The beta form of glucose consists of five similar bond types all lying approximately in an extended, planar, zigzag arrangement across the ring oxygen atom. Only four such bonds exist in the alpha form (see Fig. 20).

Again, from simple geometric considerations the nature of vibrational coupling present in the beta form would be expected to be different than in the alpha form. In both of these instances there is little doubt that other and perhaps even more significant changes in the coupling, which are not envisioned as easily, do occur.

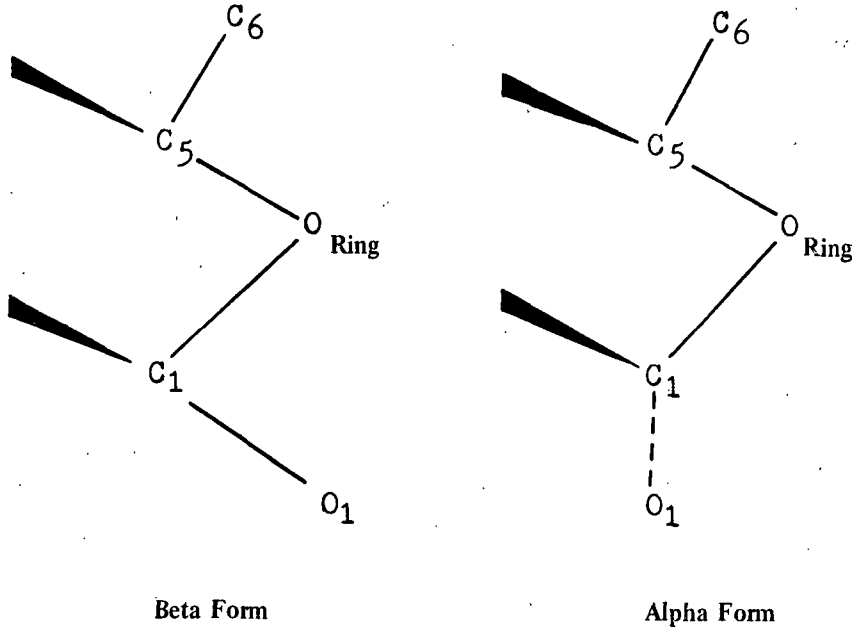

Figure 20. Configurations of α- and β-Glucose

Another aspect concerning the skeletal vibrations deserves to be emphasized also. While the results of the analyses indicate that CC motions couple with the other CC and CO vibrations, the coordinates involved indicate that the vibrations are quite often localized. For example, the intense ribitol band observed at 1078(s)(R) has been assigned to the calculated fundamental at 1073 in Table VII and is interpreted as primarily a CC and CO stretching mode. As indicated in Appendix III, the coordinates involved show that the motion is localized primarily on atomic groups adjacent to C(2) (see Fig. 19). The dominant components in the normal coordinate are: C1C2(17%), C20(12%), COH2(24%), and C4C5(16%). Likewise in the 1138 band the coordinates involved are: C1C2(25%), C2C3(22%), C10(6%), and C30(5%). However, there were no perceptible patterns in

the nature of the coupling which could be related to the structural differences among the pentitols. Each fundamental was unique with respect to the components involved. The nature of the coupling suggests that any detailed interpretation of the vibrational spectra of molecules as complex as the alditols must involve analyses of their respective normal coordinates.

CC STRETCHING MODES IN THE ALDITOLS AND 1,5-ANHYDROPENTITOLS

Part of the rationale for studying both the 1,5-AHP's and the pentitols focused on their obvious geometric differences. Table XIII shows that a difference is predicted in the structure of their spectra with respect to the distribution of CC stretching modes. Ring CC stretching vibrations are predicted to occur between 1160-850 in the 1,5-AHP's. Also, they are predicted to couple very heavily with both the ring bending vibrations (or ring breathing modes as they are sometimes called) and CCO bending vibrations which occur in many of the modes between 750-300. The situation is apparently different in the alditols. Although the skeletal stretching and bending components do couple, the contribution of the CC stretching components to the potential distributions associated with the bands in this region is small in comparison. It is suggested that the difference in the coupling is a manifestation of the ring structure. When a side of one angle is deformed within a closed ring structure all angles must necessarily be deformed. Because the ring behaves as a vibrating entity, the closed structure appears to affect the extent of coupling between the stretching and bending components. These calculations involving the pentitols suggest that a factor to be confronted in going from the 1,5-AHP's to more complex pyranoses may be in understanding how the additional atomic groups perturb this coupling pattern.

LOW ENERGY BANDS

Interpretation of the vibrational spectra of the alditols below 800 cm^{-1} is complicated by a number of factors. First, few interpretive guidelines exist in this region. Almost every kind of motion not found between 1500-900 has been associated with bands in this lower region. More specifically, this region reportedly contains bending modes of pyranose rings (38) and of CH groups at the asymmetric carbon atoms in pyranose rings (5,38); nonplanar bending vibrations of hydroxyl groups (i.e., OH op bending) (37); stretching vibrations of hydrogen bonds (39), and below 150, lattice modes have been reported (33). Secondly, many of the low energy vibrational bands have, in general, relatively weak intensities and asymmetric band contours, most likely caused from either overlapping or from solid-state perturbations. Thus, larger measurement errors are expected.

Aside from these factors, however, there are a number of bands in the spectra of the alditols between 800-500 for which there are no corresponding fundamentals. It has been suggested earlier that these bands do not represent fundamental modes. In the initial stages of the analyses the presence of additional bands posed a difficult problem with regard to the actual assignments (i.e., matching calculated and observed frequency distributions). For example, when Pitzner's SVQFF approximation, described in Table V, was initially applied to ribitol, only two bands, one at 729 and the other at 566, were predicted between 800 and 490 (see Table VI). Actually, five bands are observed in the Raman spectrum at 749, 695, 628, 575, and 529. In the IR spectrum of ribitol, bands occur at 692, 624, 574, and 529. Similar situations exist in the spectra of xylitol and erythritol. Pitzner (1) assigned the bands at 873, 776, and 683 in the 1,5-anhydroribitol (1,5-AHR) spectrum to either overtones or combinations.

Because these 1,5-AHR bands were either very weak or nonexistent in the Raman his assignment is plausible.

However, the preponderance of bands in this region of the alditol spectra, for which there were no predicted fundamentals, suggested that Pitzner's field was not an adequate first approximation for the compounds in this region. This is understandable in view of the structural differences between these two classes of compounds. Because there is no direct means to determine which, if any, of the bands in this region are fundamentals, the results from a series of refinements, using the FP method, were analyzed. The final assignments appear in Table XVII.

Each refinement was based on a different combination of band assignments in an attempt to improve the overall distribution of frequencies in this region. By comparing the various refinements it was possible to determine which of the unassigned bands in each of the various molecules were most likely to be overtones, combinations, or higher order transitions of low energy fundamentals. Also, because the potential distributions indicated that skeletal CCO and CCC bending vibrations were likely to be dominant in this region, various combinations of appropriate next nearest neighbor interaction constants were introduced. The field was expanded to accommodate 69 SVQFF constants in the refinement. However, in all cases, these additional constants had little affect on the band distribution in this region. As a result, the final field contained only 59 constants and no next nearest neighbor interaction constants.

Table XVII shows that three of the five unassigned bands in ribitol appear to be fundamentals, namely the bands at 749(s)(R), 628(m)(R), and 529(s)(R), which incidentally are the strongest Raman bands in the group.

TABLE XVII

A COMPARISON OF THE OBSERVED FREQUENCIES AND CALCULATED FREQUENCIES FROM 750 TO 350 CM^{-1}

Ribitol			Xylitol		
Obs. Freq.			Obs. Freq.		
Raman	IR	Calc. Freq.	Raman	IR	Calc. Freq.
749(s)	749(s)	758	750(w)	749(vs)	773
695(vvw,b)	695(s,sh)		--	698(vvw,sh?)	
628(m)	630(vs,b)	610	600(vw)	598(s)	613.5
575(vvw,b)	575(vs,b)		--	563(s)	
529(s)	529(s,sh)	522	520(w)	520(vs)	511
478(s)	475(m)	490	464(m)	--	437
458(m)	458(m)	426	428(vs)	433(w)	398
388(vw)	--	380	385(vw)	--	371
351(m)	--	347	360(vs)	--	360

Erythritol		
Obs. Freq.		
Raman	IR	Calc. Freq.
698(vs)	692(vs,b)[a] 675	699
--	620(vs)	612
--	?	545
486(s)	490(w)	485
--	431(m)[a] 422	431
383(s)	376(vw)	378
		370
350(w)	--	348

[a]Suspected correlation field splitting.

The other two bands at 695(vvw,b)(R) and 575(vvw,b)(R) do not appear to be fundamentals. In xylitol, three of the five bands are assigned as fundamentals. In erythritol, all the observed bands in this region appear to be fundamental modes.

Table XIV indicates that the majority of bands between 800-450 are characterized by CCO bending vibrations and to a lesser extent by skeletal stretching and bending vibrations. Below 450 skeletal bending, skeletal torsion, and OH op bending modes predominate. Some coupling with methine CH and methylene CH_2 deformations was noted, but the relative contribution was small in comparison to the dominant vibrational motions (see Tables VII-X).

A COMPARISON OF CYCLIC AND ACYCLIC FORCE CONSTANTS

As Table V shows, there are no large or unreasonable kinds of force constants. The values of the related constants maintain a high degree of consistency in different systems using similar force field approximations. Also, convergence of the final values fairly close to the initial force constant values further supports the idea that this type of field is well suited to this class of compounds. These properties suggest that the field does have physical significance, includes sufficient interactions, and should be transferable to other alditol molecules such as the hexitols.

However, far more to the point is the fact that using the model field developed for ribitol, xylitol, and erythritol and structural data from a fourth molecule, D-arabinitol, a good approximation of the latter vibrational spectrum was obtained. This type of transferability has not been previously demonstrated. The ability to predict the spectra of other closely related compounds from their structure establishes the physical significance of the

field. This predictive capacity also suggests another potential use, namely, the possibility of determining the G matrix effects responsible for changes in band distributions resulting from suspected modifications in molecular structure.

Even though there are obvious differences between the pentitols and anhydropentitols, similar groupings occur at the C(2), C(3), and C(4) positions. As a general rule, force constants should be transferable (1) between similar molecules or (2) between similar groupings in different molecules (32,40). However, it is extremely difficult to know when the atomic environments are similar enough to expect transferability among the force constants.

Before comparing the force constants and before attempting to assess the extent of transferability between the similar constants, it must be emphasized that the type of model field used for the pentitols is somewhat different and more diversified than the one developed by Pitzner (1) for the 1,5-AHP's. For example, he grouped a number of internal coordinates and their interactions together in the process of defining his field. In several important instances, interactions specific to the ether linkages in the ring were grouped with interactions at other sites in the molecule. He does not, for instance, distinguish between a gauche CCO,CCO angle interaction; a gauche CCO,CCC angle interaction; a gauche CCC,CCC angle interaction; or a gauche CCC,COC angle interaction. Only one constant defines all of these skeletal bend-bend interaction coordinates. More importantly, the value of that constant will be determined by the manner in which the individual interaction constants are grouped. Thus, it is difficult to compare the force constants for the alditols and 1,5-AHP's because they do not share a common basis of development.

Although the difference in the total number of independent parameters does not suggest a very significant difference in the diversity of the two fields, the variation in the atomic groupings of the individual molecule determines the actual number of necessary constants. None of the off-diagonal interaction constants for the alditol molecules are grouped together, and the distinction in the two types of environments associated with the diagonal constants has already been noted.

However, in view of the similarity in the atomic groupings at the C(2), C(3), and C(4) positions, an effort was made to compare the diagonal constants associated with these groupings. The results are given in Table XVIII. In spite of the fact that these constants do not share a common basis of development, the $\Delta\Phi_{\underline{ab}}$ values show that the methine stretching constants (i.e., no. 2, 4, 6, and 8) are nearly equal. The largest deviation occurs between the CO and OH constants. Also, comparing $\Delta\Phi_{\underline{a}}$ with $\Delta\Phi_{\underline{ab}}$, in Table XVIII, shows that the degree of difference between the methine and methylene stretching constants within an alditol ($\Delta\Phi_{\underline{a}}$) is nearly equal to the difference between the acyclic and cyclic methine stretching constants ($\Delta\Phi_{\underline{ab}}$). Since the difference is small in both instances, this implies (1) that the effects of the methine and methylene environments on these stretching constants are negligible, and (2) that changing from a cyclic to acyclic environment does not significantly affect these constants.

Comparing the $\Delta\Phi_{\underline{a}}$ values for valence angle bending shows that the methylene force constants are different from the methine force constants in every case. Furthermore, the $\Delta\Phi_{\underline{a}}$ values are greater than $\Delta\Phi_{\underline{ab}}$ values in the majority of cases. This suggests that the bending constants which have the greatest environmental similarity are the closest to being transferable.

TABLE XVIII

A COMPARISON OF THE SVQFF DIAGONAL FORCE CONSTANTS FOR THE ALDITOLS WITH THE 1,5-ANHYDROPENTITOLS

21 Force Constants i		$\Phi(i)$	Final Φ_a / Acyclic Alditols	Delta[a] Φ_a, %	Final Φ_b / Cyclic 1,5-AHP's	Delta[b] Φ_{ab} / Comparison (Φ_a with Φ_b), %
	Stretch (mdyn./A)					
1	(methylene)	C'H	4.5905	-0.06	4.5969	-0.14
2	(methine)	CH	4.5933		4.5890	+0.09
3	(methylene)	C'C	4.2680	+0.98		
4	(methine)	CC	4.2277		4.2466	-0.47
5	(methylene)	C'O	5.0876	+0.83		
6	(methine)	CO	5.0459		5.1033	-1.14
7	(methylene)	O'H	6.2752	+1.27		
8	(methine)	OH	6.1968		6.2833	-1.40
	Bend [mdyn.A/(rad.)^2]					
9		HCH	0.4738		0.4520	+4.60
10	(methylene)	HC'C	0.7861	+14.1	0.7920	-0.75
11	(methine)	HCC	0.6889		0.7251	-5.25
12	(methylene)	HC'C	0.8504	-23.5		
13	(methine)	HCO	1.1120		0.9629	+13.41
14	(methylene)	C'OH	0.7042	+8.9		
15	(methine)	COH	0.6462		0.7345	-13.66
16	(methylene)	C'CC	1.0972	+3.4		
17	(methine)	CCC	1.0610		1.0557	+0.50
18	(methylene)	C'CO	1.3546	+6.4		
19	(methine)	CCO	1.2735		1.1801	+7.33
	Torsion (mdyn./rad.)					
20		-CC-	0.0421		0.0268	+36.34
21		-CO-	0.0548		0.0283	+48.36

[a] Delta $\Phi_a = \dfrac{(\Phi_{methylene} - \Phi_{methine})}{\Phi_{methine}} \times 100.$

[b] Delta $\Phi_{ab} = \dfrac{(\Phi_a - \Phi_b)}{\Phi_a} \times 100.$

The obvious exceptions are the CCO and COH related constants. However, these comparisons are made with reservation in view of the fact that the two fields were defined and developed differently, especially with regard to the various bend-bend interaction constants.

CONCLUSIONS

The major conclusions of this thesis derive from and are represented by the success of the normal coordinate analyses. The results of the analyses demonstrate that the vibrational spectra of the pentitols and erythritol can be understood in terms of a relatively simple force field. The spectral interpretations developed in the analyses are supported by a number of factors. First, the agreement between the computed and experimental frequency distributions was good. Secondly, the location of the group vibrational motions was consistent with similar calculations on other carbohydrate compounds. Also, the calculated locations of the various group motions parallel the information from group frequency correlations. Finally, the bands assigned to calculated fundamentals involving OH related bending vibrations are shifted by deuteration.

The major differences among the pentitol spectra result primarily from changes in the vibrational coupling caused by the structural differences among the isomers. This suggests that most of the vibrations in the molecules studied arise, to a first approximation, from the isolated molecule, apart from its environmental surroundings. Although interactions among the molecules in the unit cell were detected the effects on the spectra were localized in particular bands. The effects of hydrogen bonding appear to be secondary and are not transmitted to the skeletal stretching vibrations. The overall band distribution is most sensitive to the interactions between the vibrations of the atoms within the molecule.

The vibrational spectra of D,L-arabinitol were presented and compared to the spectra of the D isomer. Differences in the spectra of the two compounds were noted. The nature of these differences suggests that any differences in the conformation of the D isomer in either of these two compounds are minor. As a result, the differences in their observed spectra were attributed to suspected differences in the geometry of their unit cells and/or differences in the intermolecular hydrogen bonding.

The force field developed using ribitol, xylitol, and erythritol was shown to be capable of predicting the vibrational spectrum of D-arabinitol. This type of transferability has not been previously demonstrated. The ability to predict the spectra of other closely related compounds from their structure suggests that the field does have physical significance, includes sufficient interactions, and should be transferable to other alditol molecules such as the hexitols. This predictive capability also suggests another potential use. It should be possible to determine the $\underset{\sim}{G}$ matrix effects responsible for changes in band distributions resulting from suspected modifications in molecular structure.

NOMENCLATURE

A	Angstrom
1,5-AHP	1,5-anhydropentitol
1,5-AHR	1,5-anhydroribitol
asym.	asymmetric
$\underset{\sim}{B}$	internal coordinate transformation matrix $\underset{\sim}{S} = \underset{\sim}{B}\underset{\sim}{X}$
calc.	calculated
cm^{-1}	wave numbers
CPU	central processing unit
$\underset{\sim}{D}$	Hessian matrix
diag.	diagonal
diff.	difference
dist.	distribution
exp.	experimental
$\underset{\sim}{F}$	force constant matrix
F_{ij}	element of $\underset{\sim}{F}$ matrix
FP	Fletcher-Powell
freq.	frequency
$\underset{\sim}{G}$	inverse kinetic energy matrix
Φ_i	ith force constant parameter
ip	in-plane
IR	infrared
$\underset{\sim}{J}$	Jacobian matrix
KBr	potassium bromide
L	eigenvector matrix
mdyn.	millidyne
NC	normal coordinate

obs.	observed
op	out-of-plane
$\underset{\sim}{P}$	arbitrary weighting matrix
PE	potential energy
P_k	kth element of weighting matrix $\underset{\sim}{P}$
Q	sum of the squared residuals
Q^r	sum of squared residuals after r iterations
rad.	radian
$\underset{\sim}{S}$	internal coordinates expressed as a vector
S_k	kth internal displacement coordinate
SVQFF	Simplified Valence Quadratic Force Field
sym.	symmetric
THP	tetrahydropyran
V	potential energy
$\underset{\sim}{X}$	cartesian displacement coordinates expressed as a vector
$\underset{\sim}{Z}$	tranformation matrix $\underset{\sim}{F} = \underset{\sim}{Z}\Phi$
λ_i	ith eigenvalue or frequency parameter
$\underset{\sim}{\Lambda}$	eigenvalue matrix containing elements λ_{ii}
ν	frequency

ACKNOWLEDGMENTS

I wish to sincerely thank Dr. Rajai H. Atalla, Chairman of my Advisory Committee, for his continued personal interest, support, and guidance throughout the course of this investigation.

I also wish to gratefully acknowledge the other members of the Committee, Dr. Donald C. Johnson and Dr. Gary A. Baum for helping to create the atmosphere that made this thesis possible.

Many people have contributed both directly and indirectly to the successful completion of this thesis. I am indebted to each of them. In particular, I wish to acknowledge Messrs. F. R. Sweeney, D. E. Beyer, and G. J. Subert for their help in preparing tables and illustrations for this manuscript. I also wish to thank Messrs. J. J. Bachhuber and J. O. Church for their computer programming assistance.

I am deeply indebted to The Institute of Paper Chemistry for the financial support which made this study possible.

Finally, my most sincere appreciation goes to my wife, Bev, whose faith, patience, encouragement, and assistance made the completion of this investigation possible.

LITERATURE CITED

1. Pitzner, J. L. An investigation of the vibrational spectra of the 1,5-anhydropentitols. Doctoral Dissertation. Appleton, Wis., The Institute of Paper Chemistry, 1973. 402 p.

2. Spedding, H., Adv. Carbohyd. Chem. 19:23(1964).

3. Vasko, P. D., Blackwell, J., and Koenig, J. L., Carbohyd. Res. 23:407(1972).

4. Higgins, H. G., Stewart, C. M., and Harrington, K. J., J. Polymer Sci. 51:59(1961).

5. Tipson, R. S. NBS Monograph No. 110, 1968.

6. Marchessault, R. H., Pure Appl. Chem. 5:107(1962).

7. Schachtschneider, J. H., and Snyder, R. G., Spectrochim. Acta 19:117(1963).

8. Snyder, R. G., and Schachtschneider, J. H., Spectrochim. Acta 21:169(1965).

9. Snyder, R. G., and Zerbi, G., Spectrochim. Acta 23A:391(1967).

10. Burket, S. C., and Badger, R. M., J. Am. Chem. Soc. 72:4397(1950).

11. Beckett, C. W., Pitzer, K. S., and Spitzer, R., J. Am. Chem. Soc. 69:2488 (1947).

12. Pickett, H., and Strauss, H., J. Chem. Phys. 53:376(1970).

13. Vasko, P. D. Spectroscopic and vibrational studies of carbohydrates. Doctoral Dissertation. Cleveland, Ohio, Case Western Reserve University, 1971. 127 p.

14. Pray, H. L. Normal coordinate analysis of the planar vibrations of cellulose. Doctoral Dissertation. University of Tennessee, 1972. 138 p.

15. Deeds, W. E. Doctoral Dissertation. Columbus, Ohio, Ohio State University, 1951.

16. Wilson, E. B., Jr., Decius, J. C., and Cross, P. C. Molecular vibrations. New York, McGraw-Hill Book Co., 1965. 388 p.

17. Takahashi, H., Shimanouchi, T., Fukushima, K., and Miyazawa, T., J. Mol. Spectry. 13:43(1964).

18. Schachtschneider, J. H. Technical Report No. 231-64. Emeryville, California, Shell Development Co., 1964.

19. Schachtschneider, J. H. Technical Report No. 57-65. Emeryville, California, Shell Development Co., 1965.

20. Hunter, F. D., and Rosenstein, R. D., Acta Cryst. B24:1652(1968).

21. Jeffrey, G. A., and Kim, H. S., Carbohyd. Res. 14:207(1970).

22. Fletcher, R., and Powell, M. J., Computer J. 6:163(1963).

23. Bekoe, A., and Powell, H. M., Proc. Roy. Soc. A250:301(1959).

24. Gans, P., J. Chem. Soc. 1971 (A):2017.

25. Decius, J. C., J. Chem. Phys. 16:1025(1948).

26. Kim, H. S., Jeffrey, G. A., and Rosenstein, R. D., Acta Cryst. B25:2223 (1969).

27. Kim, H. S., and Jeffrey, G. A., Acta Cryst. B25:2607(1969).

28. Brown, G. M., and Levy, H. A., Science 147:1038(1965).

29. Chu, S. S. C., and Jeffrey, G. A., Acta Cryst. B24:830(1968).

30. Okaya, Y., and Stemple, N. R., Acta Cryst. 21:237(1966).

31. Powell, M. J., Computer J. 7:303(1965).

32. Gans, P. Vibrating molecules. London, Chapman and Hall Ltd., 1971. 198 p.

33. Sherwood, P. B. A. Vibrational spectroscopy of solids. London, Cambridge University Press, 1972. 208 p.

34. Sheppard, N. Advances in spectroscopy. Vol. 1. p. 288. New York, Interscience Publishers Inc., 1959.

35. Vasko, P. D., Blackwell, J., and Koenig, J. L., Carbohyd. Res. 19:297 (1971).

36. Tasumi, M., and Shimanouchi, T., Spectrochim. Acta 20:629(1964).

37. Tipson, R. S., and Isbell, H. S., J. Res. NBS 66A:31(1962).

38. Barker, S. A., Bourne, E. J., Stacey, M., and Whiffen, D., J. Chem. Soc. 1954:171.

39. Michell, J., Aust. J. Chem. 23:833(1970).

40. Steele, D. Theory of vibrational spectroscopy. W. B. Saunders Co., 1971. 221 p.

APPENDIX I

STRUCTURAL DATA NECESSARY FOR THE NORMAL COORDINATE ANALYSES

The information reported in this appendix is as follows:

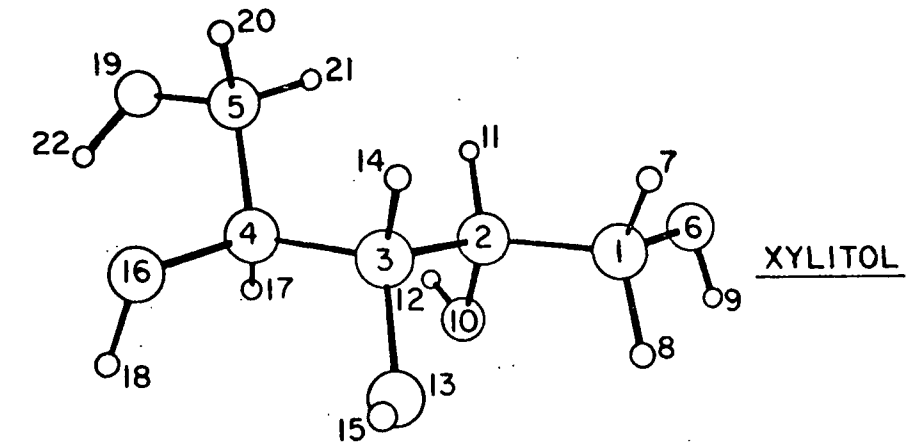

XYLITOL

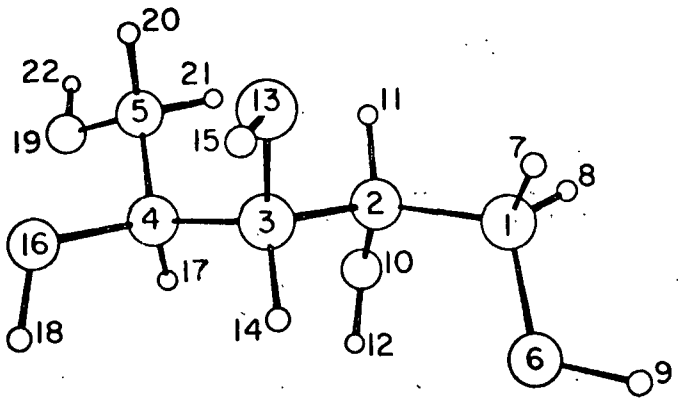

RIBITOL

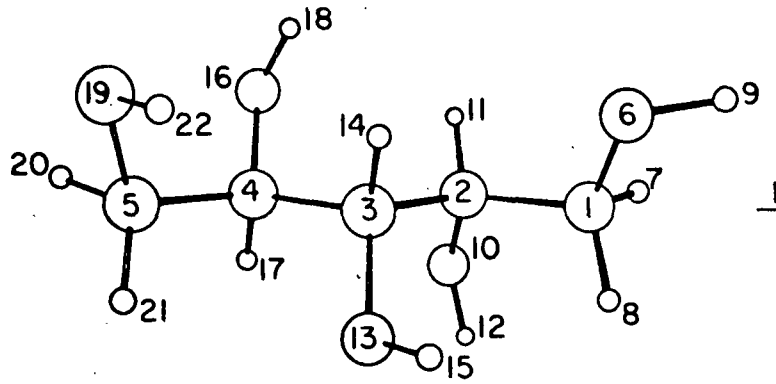

D-ARABINITOL

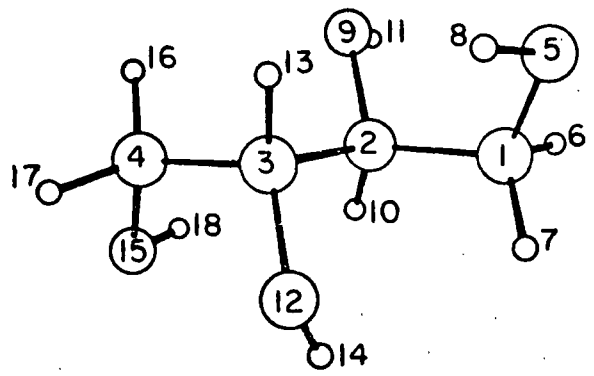

ERYTHRITOL

Figure 21. Representations of the Alditol Models

TABLE XIX

DESCRIPTION OF THE 65 INTERNAL COORDINATES
FOR XYLITOL AND RIBITOL

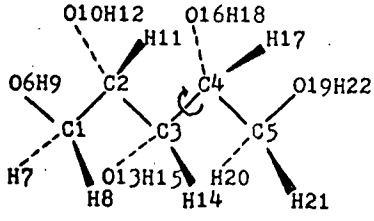

XYLITOL

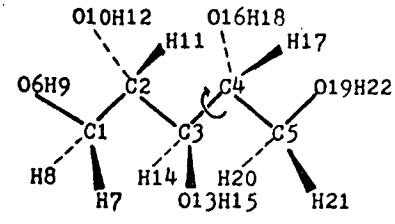

RIBITOL

Valence Bond Coordinates

	Descr.	Code		Descr.	Code		Descr.	Code		Descr.	Code
1.	C1C2	C1C2	6.	C2O10	C2O	11.	C1H8	C1H	16.	C5H21	C5H
2.	C2C3	C2C3	7.	C3O13	C3O	12.	C2H11	C2H	17.	O6H9	O1H
3.	C3C4	C3C4	8.	C4O16	C4O	13.	C3H14	C3H	18.	O10H12	O2H
4.	C4C5	C4C5	9.	C5O19	C5O	14.	C4H17	C4H	19.	O13H15	O3H
5.	C1O6	C1O	10.	C1H7	C1H'	15.	C5H20	C5H'	20.	O16H18	O4H
									21.	O19H22	O5H

Valence Bond Angle Coordinates

	Descr.	Code		Descr.	Code		Descr.	Code		Descr.	Code
22.	C1C2C3	C1CC	31.	O16C5C4	7CCO	40.	C2C1H7	1CCH	49.	C4C5H21	8CCH
23.	C2C3C4	C2CC	32.	O19C5C4	8CCO	41.	C2C1H8	'CCH	50.	H9O6C1	COH1
24.	C3C4C5	C3CC	33.	O6C1H7	H'CO	42.	C1C2H11	2CCH	51.	H12O10C2	COH2
25.	O6C1C2	1CCO	34.	O6C1H8	HC1O	43.	C3C2H11	3CCH	52.	H15O13C3	COH3
26.	O10C1C2	2CCO	35.	O10C2H11	HC2O	44.	C2C3H14	4CCH	53.	H18O16C4	COH4
27.	O10C2C3	3CCO	36.	O13C3H14	HC3O	45.	C4C3H14	5CCH	54.	H22O19C5	COH5
28.	O13C3C2	4CCO	37.	O16C4H17	HC4O	46.	C3C4H17	6CCH	55.	H7C1H8	HC1H
29.	O13C3C4	5CCO	38.	O19C5H20	HC'O	47.	C5C4H17	7CCH	56.	H2OC5H21	HC5H
30.	O16C4C3	6CCO	39.	O19C5H21	HC5O	48.	C4C5H20	CCH'			

Valence Bond Angle Torsion Coordinates[a]

	Xylitol		Ribitol	
	Descr.	Code	Descr.	Code
57.	O6C1C2C3[b]	TCC1	O6C1C2H11	TCC1
	H7C1C2O10		H7C1C2O10	
	H8C1C2H11		H8C1C2C3	
58.	H14C3C2O10	TCC2	H11C2C3H14	TCC2
	O13C3C2H11		O10C2C3O13	
	C4C3C2C1		C1C2C3C4	
59.	C5C4C3O13	TCC3	C2C3C4O16	TCC3
	O16C4C3C2		O13C3C4H17	
	H17C4C3H14		H14C3C4C5	
60.	H2OC5C4H17	TCC4	C3C4C5O19	TCC4
	H21C5C4O16		H17C4C5H20	
	O19C5C4C3		O16C4C5H21	
61.	H9O6C1H7	TC1O	H9O6C1H7	TC1O
62.	H12O10C2H11	TC2O	H12O10C2H11	TC2O
63.	H15O13C3H14	TC3O	H15O13C3H14	TC3O
64.	H18O16C4H17	TC4O	H18O16C4H17	TC4O
65.	H22O19C5H20	TC5O	H22O19C5H20	TC5O

[a]The torsional coordinates were defined for those atoms in the trans position about each bond.

[b]The torsional coordinates in this group are summed together (linear combination) to avoid the introduction of further redundancies.

TABLE XX

DESCRIPTION OF THE 52 INTERNAL COORDINATES OF ERYTHRITOL

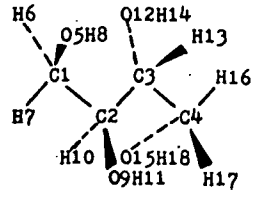

ERYTHRITOL

Valence Bond Coordinates

	Descr. Code		Descr. Code		Descr. Code
1. C1C2	C1C2	7. C4O15	C4O	13. C4H17	C4H
2. C2C3	C2C3	8. C1H6	C1H'	14. O5H8	O1H
3. C3C4	C3C4	9. C1H7	C1H	15. O9H11	O2H
4. C1O5	C1O	10. C2H10	C2H	16. O12H14	O3H
5. C2O9	C2O	11. C3H13	C3H	17. O15H18	O4H
6. C3O12	C3O	12. C4H16	C4H'		

Valence Bond Angle Coordinates

	Descr. Code		Descr. Code		Descr. Code
18. C1C2C3	C1CC	27. O5C1H7	HC1O	36. C2C3H13	4CCH
19. C2C3C4	C2CC	28. O9C2H10	HC2O	37. C4C3H13	5CCH
20. O5C1C2	1CCO	29. O12C3H13	HC3O	38. C4C3H16	CCH'
21. O9C1C2	2CCO	30. O15C4H16	HC'O	39. C4C3H17	6CCH
22. O9C2C3	3CCO	31. O15C4H17	HC4O	40. C1O5H8	COH1
23. O12C2C3	4CCO	32. C1C2H6	1CCH	41. C2O9H11	COH2
24. O12C3C4	5CCO	33. C1C2H7	'CCH	42. C3O12H14	COH3
25. O15C3C4	6CCO	34. C1C2H10	2CCH	43. C4O15H18	COH4
26. O5C1H6	H'CO	35. C2C3H10	3CCH	44. H6C1H7	HC1H
				45. H16C4H17	HC4H

Valence Bond Angle Torsion Coordinates[a]

Erythritol

	Descr. Code
46. O5C1C2H10[b] H7C1C2O9 H6C1C2C3	TCC1
47. H10C2C3H13 C1C2C3C4 O9C2C3O12	TCC2
48. H16C3C4O12 C2C3C4H17 H13C3C4O15	TCC3
49. H8O5C1C2	TC1O
50. H11O9C2H10	TC2O
51. H14O12C3H13	TC3O
52. H18O15C4C3	TC4O

[a]The torsional coordinates were defined for those atoms in the trans position about each bond.

[b]The torsional coordinates in this group are summed together (linear combination) to avoid the introduction of further redundancies.

TABLE XXI

DESCRIPTION OF THE 65 INTERNAL COORDINATES OF D-ARABINITOL

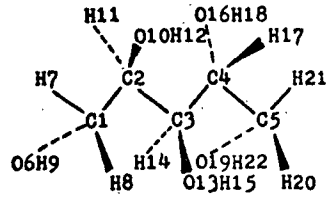

D-ARABINITOL

Valence Bond Coordinates

	Descr. Code		Descr. Code		Descr. Code		Descr. Code
1. C1C2	C1C2	6. C2O10	C2O	11. C1H8	C1H	16. C5H21	C5H
2. C2C3	C2C3	7. C3O13	C3O	12. C2H11	C2H	17. O6H9	O1H
3. C3C4	C3C4	8. C4O16	C4O	13. C3H14	C3H	18. O10H12	O2H
4. C4C5	C4C5	9. C5O19	C5O	14. C4H17	C4H	19. O13H15	O3H
5. C1O6	C1O	10. C1H7	C1H'	15. C5H20	C5H'	20. O16H18	O4H
						21. O19H22	O5H

Valence Bond Angle Coordinates

	Descr. Code		Descr. Code		Descr. Code		Descr. Code
22. C1C2C3	C1CC	31. O16C5C4	7CCO	40. C2C1H7	1CCH	49. C4C5H21	8CCH
23. C2C3C4	C2CC	32. O19C5C4	8CCO	41. C2C1H8	'CCH	50. H9O6C1	COH1
24. C3C4C5	C3CC	33. O6C1H7	H'CO	42. C1C2H11	2CCH	51. H12O10C2	COH2
25. O6C1C2	1CCO	34. O6C1H8	HC1O	43. C3C2H11	3CCH	52. H15O13C3	COH3
26. O10C1C2	2CCO	35. O10C2H11	HC2O	44. C2C3H14	4CCH	53. H18O16C4	COH4
27. O10C2C3	3CCO	36. O13C3H14	HC3O	45. C4C3H14	5CCH	54. H22O19C5	COH5
28. O13C3C2	4CCO	37. O16C4H17	HC4O	46. C3C4H17	6CCH	55. H7C1H8	HC1H
29. O13C3C4	5CCO	38. O19C5H20	HC'O	47. C5C4H17	7CCH	56. H20C5H21	HC5H
30. O16C4C3	6CCO	39. O19C5H21	HC5O	48. C4C5H20	CCH'		

Valence Bond Angle Torsion Coordinates[a]

D-Arabinitol

	Descr. Code
57. O6C1C2O10[b] H8C1C2H11 H7C1C2C3	TCC1
58. C1C2C3C4 O10C2C3H14 H11C2C3O13	TCC2
59. C2C3C4C5 H14C3C4H17 O13C3C4O16	TCC3
60. C3C4C5H20 H17C4C5O19 O16C4C5H21	TCC4
61. H9O6C1H7	TC1O
62. H12O10C2H11	TC2O
63. H15O13C3H14	TC3O
64. H18O16C4H17	TC4O
65. H22O19C5H20	TC5O

[a]The torsional coordinates were defined for those atoms in the trans position about each bond.

[b]The torsional coordinates in this group are summed together (linear combination) to avoid the introduction of further redundancies.

TABLE XXII

COMPUTER PROGRAM INPUT AND CALCULATED CARTESIAN COORDINATES FOR XYLITOL

Atoms i	j	k	l	Bond Length, D_{ij}	Bond Angle, $\sphericalangle ijk$	Dihedral Angle, $\sphericalangle(ijk - jkl)$	Mass i
1	0	0	0	0.0	0.0	0.0	12.011149
2	1	0	0	1.516999	0.0	0.0	12.011149
3	2	1	0	1.528999	110.799988	0.0	12.011149
4	3	2	1	1.535999	113.599991	-176.000000	12.011149
5	4	3	2	1.509999	111.399994	70.099991	12.011149
6	1	2	3	1.419999	111.599991	174.899994	15.999399
7	1	2	3	1.092999	0.0	56.199997	1.007970
8	1	2	3	1.092999	0.0	-64.199997	1.007970
9	6	1	7	0.970000	110.000000	-140.659988	1.007970
10	2	1	6	1.443999	109.500000	-62.399994	15.999399
11	2	1	6	1.120000	0.0	56.000000	1.007970
12	10	2	11	0.970000	110.000000	14.209999	1.007970
13	3	2	10	1.440000	108.399994	-60.299988	15.999399
14	3	2	1	1.120000	0.0	-57.799988	1.007970
15	13	3	14	0.970000	110.000000	-17.979996	1.007970
16	4	3	13	1.433000	110.199997	-49.899994	15.999399
17	4	3	2	1.120000	0.0	-51.599991	1.007970
18	16	4	17	0.970000	110.000000	-21.589996	1.007970
19	5	4	3	1.429000	112.199997	-173.199997	15.999399
20	5	4	3	1.092999	0.0	66.399994	1.007970
21	5	4	3	1.092999	0.0	-53.299988	1.007970
22	19	5	20	0.970000	110.000000	100.899994	1.007970

Atom No.	X	Y	Z	Mass
1	0.0	0.0	0.0	12.011149
2	1.516999	0.0	0.0	12.011149
3	2.059956	1.429348	0.0	12.011149
4	3.590916	1.505599	0.098186	12.011149
5	4.076804	1.087893	1.465494	12.011149
6	-0.522735	-1.315055	0.117367	15.999399
7	-0.364333	0.573257	0.856320	1.007970
8	-0.364333	0.448502	-0.927768	1.007970
9	-0.783060	-1.647739	-0.755818	1.007970
10	1.999015	-0.735363	-1.145441	15.999399
11	1.890332	-0.510319	0.924444	1.007970
12	2.700452	-1.348333	-0.874976	1.007970
13	1.612956	2.085367	-1.201427	15.999399
14	1.666511	1.978162	0.893533	1.007970
15	1.322252	2.988138	-0.997963	1.007970
16	4.033268	2.853363	-0.105132	15.999399
17	4.048431	0.848744	-0.685154	1.007970
18	4.329318	2.970715	-1.021365	1.007970
19	5.501826	1.002605	1.529322	15.999399
20	3.740887	1.814898	2.209315	1.007970
21	3.668001	0.104855	1.712807	1.007970
22	5.897627	1.518529	0.809553	1.007970

TABLE XXIII

COMPUTER PROGRAM INPUT AND CALCULATED CARTESIAN COORDINATES FOR RIBITOL

Atoms				Bond Length, D_{ij}	Bond Angle, $\measuredangle ijk$	Dihedral Angle, $\measuredangle(ijk - jkl)$	Mass i
i	j	k	l				
1	0	0	0	0.0	0.0	0.0	12.011149
2	1	0	0	1.509999	0.0	0.0	12.011149
3	2	1	0	1.533999	112.500000	0.0	12.011149
4	3	2	1	1.525000	113.899994	-171.799988	12.011149
5	4	3	2	1.518000	113.500000	62.099991	12.011149
6	1	2	3	1.426999	110.500000	-71.399994	15.999399
7	1	2	3	1.092999	0.0	46.599991	1.007970
8	1	2	3	1.092999	0.0	168.699997	1.007970
9	6	1	7	0.970000	110.000000	64.919998	1.007970
10	2	1	6	1.421000	110.399994	53.799988	15.999399
11	2	1	6	1.120000	0.0	172.299988	1.007970
12	10	2	11	0.970000	110.000000	169.019998	1.007970
13	3	2	10	1.419999	107.399994	169.799988	15.999399
14	3	2	1	1.120000	0.0	46.799988	1.007970
15	13	3	14	0.970000	110.000000	18.599991	1.007970
16	4	3	13	1.429000	109.799988	61.399994	15.999399
17	4	3	2	1.120000	0.0	-54.000000	1.007970
18	16	4	17	0.970000	110.000000	-39.939987	1.007970
19	5	4	3	1.419000	108.500000	-171.399994	15.999399
20	5	4	3	1.092999	0.0	57.299988	1.007970
21	5	4	3	1.092999	0.0	-52.699997	1.007970
22	19	5	20	0.970000	110.000000	-64.719986	1.007970

Atom No.	X	Y	Z	Mass
1	0.0	0.0	0.0	12.011149
2	1.509999	0.0	0.0	12.011149
3	2.097034	1.417231	0.0	12.011149
4	3.608407	1.459944	-0.198859	12.011149
5	4.383840	0.759569	0.902278	12.011149
6	-0.499744	0.426332	-1.266816	15.999399
7	-0.364333	0.708036	0.748727	1.007970
8	-0.364333	-1.010512	0.201921	1.007970
9	-1.467388	0.360273	-1.281031	1.007970
10	2.005319	-0.767736	-1.088338	15.999399
11	1.883332	-0.467861	0.946640	1.007970
12	1.836560	-0.305596	-1.924308	1.007970
13	1.741938	2.023935	1.233780	15.999399
14	1.572080	2.038765	-0.769752	1.007970
15	1.419998	2.925842	1.079446	1.007970
16	4.053216	2.817367	-0.238738	15.999399
17	3.878623	0.897527	-1.128952	1.007970
18	3.920060	3.184160	-1.126787	1.007970
19	5.747479	0.687029	0.516557	15.999399
20	4.129642	1.205565	1.867221	1.007970
21	3.998176	-0.255022	1.030797	1.007970
22	6.231880	0.100899	1.118809	1.007970

TABLE XXIV

COMPUTER PROGRAM INPUT AND CALCULATED CARTESIAN COORDINATES FOR ERYTHRITOL

Atoms i	j	k	l	Bond Length, D_{ij}	Bond Angle, ijk	Dihedral Angle, (ijk - jkl)	Mass i
1	0	0	0	0.0	0.0	0.0	12.011148
2	1	0	0	1.525000	0.0	0.0	12.011148
3	2	1	0	1.526999	112.299988	0.0	12.011148
4	3	2	1	1.523000	112.899994	177.599991	12.011148
5	1	2	3	1.436999	111.199997	59.399994	15.999398
6	1	2	3	1.092999	0.0	-51.599991	1.007970
7	1	2	3	1.092999	0.0	-178.099991	1.007970
8	5	1	7	0.970000	110.000000	-170.500000	1.007970
9	2	1	5	1.436999	110.899994	-59.000000	15.999390
10	2	1	5	1.120000	0.0	179.699997	1.007970
11	9	2	10	0.970000	110.000000	35.099991	1.007970
12	3	2	9	1.447000	109.500000	175.599991	15.999390
13	3	2	1	1.120000	0.0	-67.000000	1.007970
14	12	3	13	0.970000	110.000000	159.899994	1.007970
15	4	3	2	1.445000	112.399994	-64.199997	15.999390
16	4	3	2	1.129999	0.0	-171.599991	1.007970
17	4	3	2	1.129999	0.0	56.500000	1.007970
18	15	4	16	0.970000	110.000000	-167.599991	1.007970

Atom No.	X	Y	Z	Mass
1	0.0	0.0	0.0	12.011148
2	1.525000	0.0	0.0	12.011148
3	2.104427	1.412795	0.0	12.011148
4	3.626204	1.429210	-0.058751	12.011148
5	-0.519653	0.681988	1.153177	15.999398
6	-0.364333	0.640086	-0.807587	1.007970
7	-0.364333	-1.029922	-0.034167	1.007970
8	-0.078197	1.539260	1.258531	1.007970
9	2.037631	-0.638501	1.180886	15.999390
10	1.898333	-0.532753	-0.911699	1.007970
11	2.096713	-1.596533	1.040943	1.007970
12	1.552183	2.161346	-1.108379	15.999390
13	1.864355	1.914766	0.972003	1.007970
14	1.478976	1.591458	-1.889895	1.007970
15	4.135710	0.872908	-1.291210	15.999390
16	3.985834	2.489491	-0.211606	1.007970
17	4.042959	0.831241	0.804757	1.007970
18	4.092813	-0.095665	-1.260723	1.007970

TABLE XXV

COMPUTER PROGRAM INPUT AND CALCULATED CARTESIAN COORDINATES FOR D-ARABINITOL

Atoms i	j	k	l	Bond Length, D_{ij}	Bond Angle, ijk	Dihedral Angle, (ijk - jkl)	Mass i
1	0	0	0	0.0	0.0	0.0	12.011149
2	1	0	0	1.520000	0.0	0.0	12.011149
3	2	1	0	1.525000	113.299988	0.0	12.011149
4	3	2	1	1.526999	112.299988	-178.099991	12.011149
5	4	3	2	1.520000	112.899994	177.599991	12.011149
6	1	2	3	1.412999	109.099991	57.899994	15.999399
7	1	2	3	1.092999	0.0	-68.099991	1.007970
8	1	2	3	1.092999	0.0	178.099991	1.007970
9	6	1	7	0.970000	110.000000	-75.769989	1.007970
10	2	1	6	1.436999	108.399994	-178.099991	15.999399
11	2	1	6	1.120000	0.0	-66.899994	1.007970
12	10	2	11	0.970000	110.000000	-170.469986	1.007970
13	3	2	10	1.436999	110.899994	-59.000000	15.999399
14	3	2	1	1.120000	0.0	-57.799988	1.007970
15	13	3	14	0.970000	110.000000	35.139999	1.007970
16	4	3	13	1.447000	109.500000	175.599991	15.999399
17	4	3	2	1.120000	0.0	-67.000000	1.007970
18	16	4	17	0.970000	110.000000	159.969986	1.007970
19	5	4	3	1.440000	112.399994	-64.199997	15.999399
20	5	4	3	1.092999	0.0	-171.599991	1.007970
21	5	4	3	1.092999	0.0	56.500000	1.007970
22	19	5	20	0.970000	110.000000	-167.629990	1.007970

Atom No.	X	Y	Z	Mass
1	0.0	0.0	0.0	12.011149
2	1.520000	0.0	0.0	12.011149
3	2.123204	1.400631	0.0	12.011149
4	3.649257	1.374287	0.046842	12.011149
5	4.263255	2.763496	0.105989	12.011149
6	-0.462358	0.709530	1.131086	15.999399
7	-0.364333	0.384361	-0.956125	1.007970
8	-0.364333	-1.029922	0.034167	1.007970
9	-1.386180	0.476986	1.313773	1.007970
10	1.973586	-0.762480	-1.130419	15.999399
11	1.893332	-0.602641	0.867090	1.007970
12	1.578806	-0.414520	-1.945264	1.007970
13	1.774457	2.108974	-1.200665	15.999399
14	1.754073	1.966085	0.893534	1.007970
15	0.913704	2.542744	-1.091803	1.007970
16	4.084196	0.584978	1.178929	15.999399
17	4.044677	0.942603	-0.907984	1.007970
18	3.509153	0.753837	1.941631	1.007970
19	3.917804	3.465098	1.315127	15.999399
20	5.337752	2.679485	0.287760	1.007970
21	3.917211	3.351431	-0.747963	1.007970
22	3.012505	3.807799	1.252732	1.007970

TABLE XXVI

G MATRIX OF XYLITOL

i^a	j	G_{ij}	i^a	j	G_{ij}	i^a	j	G_{ij}	i^a	j	G_{ij}
1	1	0.166512	1	2	-0.029565	1	5	-0.030648	1	6	-0.027791
1	10	-0.027752	1	11	-0.027752	1	12	-0.027752	1	22	-0.050902
1	23	-0.050779	1	25	-0.054514	1	26	-0.019376	1	27	0.056156
1	28	0.024245	1	33	0.064532	1	34	0.066641	1	35	0.060765
1	40	-0.071816	1	41	-0.071816	1	42	-0.070084	1	43	0.061077
1	44	0.027125	1	50	-0.008889	1	51	-0.037364	1	55	0.072251
1	58	0.013942	1	59	-0.003875	1	61	0.059471	1	62	-0.094266
2	2	0.166512	2	3	-0.033331	2	6	-0.029766	2	7	-0.026279
2	12	-0.025608	2	13	-0.027752	2	22	-0.051305	2	23	-0.049670
2	24	0.016907	2	25	-0.051102	2	26	-0.027717	2	27	-0.053846
2	28	-0.054861	2	29	0.057257	2	30	-0.049127	2	35	0.060879
2	36	0.060542	2	40	0.028541	2	41	0.022330	2	42	0.060877
2	43	-0.070732	2	44	-0.070085	2	45	0.063028	2	46	0.030852
2	51	-0.012988	2	52	-0.040341	2	57	-0.017551	2	59	-0.012066
2	60	0.050162	2	62	0.098981	2	63	0.095647	3	3	0.166512
3	4	-0.030378	3	7	-0.028317	3	8	-0.028748	3	13	-0.022880
3	14	-0.027752	3	22	-0.049776	3	23	-0.049897	3	24	-0.051335
3	27	0.023314	3	28	0.057705	3	29	-0.054370	3	30	-0.054526
3	31	-0.025970	3	32	-0.050974	3	36	0.057845	3	37	0.063118
3	43	0.027784	3	44	0.062367	3	45	-0.071474	3	46	-0.070084
3	47	0.064590	3	48	0.020552	3	49	0.030679	3	52	-0.007554
3	53	-0.008145	3	57	-0.003723	3	58	0.015925	3	60	0.016837
3	63	-0.103540	3	64	-0.099689	4	4	0.166512	4	8	-0.024087
4	9	-0.031458	4	14	-0.028277	4	15	-0.027752	4	16	-0.027752
4	23	0.017178	4	24	-0.050466	4	29	-0.049414	4	30	0.052759
4	31	-0.020446	4	32	-0.053943	4	37	0.058142	4	38	0.066577
4	39	0.066097	4	45	0.032364	4	46	0.064213	4	47	-0.069917
4	48	-0.071816	4	49	-0.071816	4	53	-0.042761	4	54	0.050653
4	56	0.071491	4	58	0.051784	4	59	-0.016545	4	64	0.095836
4	65	0.085841	5	5	0.145758	5	10	-0.024832	5	11	-0.027263
5	17	-0.021377	5	22	-0.050826	5	25	-0.051028	5	26	-0.004251
5	33	-0.072705	5	34	-0.071972	5	40	0.062279	5	41	0.064766
5	42	0.028535	5	50	-0.060550	5	55	0.067814	5	57	-0.002444
5	58	0.004852	6	6	0.145758	6	12	-0.025929	6	18	-0.021377
6	22	0.054788	6	23	0.023760	6	25	0.023968	6	26	0.067015
6	27	-0.050852	6	28	0.025195	6	35	-0.070639	6	40	-0.051725
6	41	0.027031	6	42	0.059110	6	43	0.059529	6	44	-0.050851
6	51	-0.060550	6	57	0.020931	6	58	-0.020569	6	59	0.049064
7	7	0.145758	7	13	-0.027753	7	19	-0.021377	7	22	0.024610
7	23	0.054444	7	24	-0.049909	7	27	0.025599	7	28	-0.051668
7	29	-0.050972	7	30	0.032832	7	36	-0.070084	7	43	-0.051652
7	44	0.058976	7	45	0.057439	7	46	0.017415	7	52	-0.060549
7	57	0.048597	7	58	-0.014385	7	59	0.011859	7	60	-0.011122
8	8	0.145758	8	14	-0.027163	8	20	-0.021377	8	23	-0.050313
8	24	0.050878	8	29	0.032766	8	30	-0.050869	8	31	0.068953
8	32	0.021121	8	37	-0.070268	8	45	0.018836	8	46	0.061174
8	47	0.056510	8	48	0.031030	8	49	-0.052459	8	53	-0.060550
8	58	-0.008185	8	59	0.017127	8	60	-0.020204	9	9	0.145758
9	15	-0.026291	9	16	-0.025742	9	21	-0.021377	9	24	-0.050690
9	31	-0.002075	9	32	-0.051049	9	38	-0.072275	9	39	-0.072440
9	47	0.031623	9	48	0.064864	9	49	0.064301	9	54	-0.060550
9	56	0.067020	9	59	-0.006492	9	60	0.003107	10	10	1.075349
10	11	-0.028198	10	22	0.028785	10	25	0.052792	10	26	0.031370
10	33	-0.055962	10	34	0.060063	10	40	-0.051743	10	41	0.062236

TABLE XXVI (Continued)

G MATRIX OF XYLITOL

i^a	j	G_{ij}	i^a	j	G_{ij}	i^a	j	G_{ij}	i^a	j	G_{ij}
10	42	0.023732	10	50	-0.043281	10	55	-0.071670	10	57	-0.011789
10	58	0.045996	10	61	0.012912	11	11	1.075349	11	22	0.022520
11	25	0.055194	11	26	-0.006560	11	33	0.060999	11	34	-0.055398
11	40	0.062236	11	41	-0.051743	11	42	-0.051668	11	50	0.051464
11	55	-0.071670	11	57	0.013969	11	58	-0.049833	11	61	-0.073677
12	12	1.075350	12	22	0.050784	12	23	0.028850	12	25	0.028935
12	26	-0.024610	12	27	0.050433	12	28	-0.051796	12	35	-0.054790
12	40	0.023732	12	41	-0.051668	12	42	-0.051744	12	43	-0.051812
12	44	0.024295	12	51	0.053113	12	57	-0.003277	12	58	0.006693
12	59	-0.046964	12	62	-0.004895	13	13	1.075350	13	22	0.027356
13	23	0.050484	13	24	0.033422	13	27	-0.051336	13	28	0.051888
13	29	0.048468	13	30	0.019298	13	36	-0.054510	13	43	0.024072
13	44	-0.051337	13	45	-0.052116	13	46	-0.051585	13	52	0.051848
13	57	-0.046470	13	58	-0.001996	13	59	0.000802	13	60	-0.042950
13	63	0.006124	14	14	1.075349	14	23	0.031743	14	24	0.053932
14	29	0.017460	14	30	0.053101	14	31	-0.024453	14	32	0.032125
14	37	-0.054920	14	45	-0.050582	14	46	-0.051103	14	47	-0.051859
14	48	-0.051370	14	49	0.019278	14	53	0.051067	14	58	-0.043705
14	59	-0.000134	14	60	0.002239	14	64	0.007355	15	15	1.075349
15	16	-0.027416	15	24	0.020811	15	31	-0.007846	15	32	0.054789
15	38	-0.055281	15	39	0.059604	15	47	-0.051493	15	48	-0.051983
15	49	0.061555	15	54	-0.010453	15	56	-0.071924	15	59	0.051163
15	60	-0.016048	15	65	-0.019757	16	16	1.075348	16	24	0.031067
16	31	0.031601	16	32	0.054240	16	38	0.059385	16	39	-0.055407
16	47	0.019324	16	48	0.061554	16	49	-0.051983	16	54	-0.042975
16	56	-0.071924	16	59	-0.044765	16	60	0.012943	16	65	-0.070776
17	17	1.054595	17	25	-0.006745	17	33	-0.031989	17	34	0.038424
17	50	-0.041361	17	57	0.043890	17	61	0.008193	18	18	1.054595
18	26	0.008238	18	27	-0.009811	18	35	0.039429	18	51	-0.040674
18	57	0.031335	18	58	-0.042267	18	62	-0.003272	19	19	1.054595
19	28	-0.029992	19	29	-0.005667	19	36	0.038795	19	52	-0.040787
19	58	-0.029131	19	59	0.042952	19	63	0.004452	20	20	1.054595
20	30	-0.006122	20	31	0.009586	20	37	0.038111	20	53	-0.040986
20	59	0.043182	20	60	-0.027377	20	64	0.005206	21	21	1.054595
21	32	0.038594	21	38	-0.007772	21	39	-0.031879	21	54	-0.041101
21	60	-0.015266	21	65	-0.013432	22	22	0.169073	22	23	0.097924
22	24	-0.002494	22	25	0.098937	22	26	0.035842	22	27	-0.020798
22	28	-0.045682	22	29	0.025259	22	30	0.013639	22	33	0.030437
22	34	0.037694	22	35	-0.115782	22	36	-0.058135	22	40	-0.056653
22	41	-0.044324	22	42	-0.008954	22	43	-0.008293	22	44	-0.053382
22	45	0.029980	22	46	-0.010732	22	50	-0.001079	22	51	0.047882
22	52	0.018353	22	55	-0.066785	22	57	0.017542	22	58	-0.024268
22	59	0.006815	22	60	-0.015202	22	61	-0.012385	22	62	-0.004832
22	63	0.046800	23	23	0.170187	23	24	-0.033312	23	25	0.012887
23	26	0.004762	23	27	-0.046210	23	28	-0.022051	23	29	-0.021272
23	30	0.096761	23	31	-0.031371	23	32	-0.000430	23	35	-0.057184
23	36	-0.118049	23	37	0.026426	23	40	-0.004993	23	41	-0.007788
23	42	0.030644	23	43	-0.055889	23	44	-0.009262	23	45	-0.009204
23	46	-0.062675	23	47	-0.052999	23	48	-0.029145	23	49	0.029726
23	51	0.030836	23	52	0.047727	23	53	0.007444	23	57	0.007412
23	58	-0.024866	23	59	0.001261	23	60	-0.040023	23	62	0.041017
23	63	0.008064	23	64	0.018553	24	24	0.169801	24	27	-0.027214
24	28	0.029878	24	29	0.094465	24	30	-0.014662	24	31	0.033959
24	32	0.099997	24	36	0.024351	24	37	-0.116745	24	38	0.038998

TABLE XXVI (Continued)

G MATRIX OF XYLITOL

i^a	j	G_{ij}	i^a	j	G_{ij}	i^a	j	G_{ij}	i^a	j	G_{ij}
24	39	0.028199	24	43	0.030378	24	44	-0.053655	24	45	-0.062189
24	46	-0.012378	24	47	-0.014453	24	48	-0.041213	24	49	-0.061520
24	52	0.009314	24	53	0.048870	24	54	-0.015164	24	56	-0.066820
24	57	-0.035931	24	58	-0.043874	24	59	0.008843	24	60	-0.017086
24	63	0.017736	24	64	0.004457	24	65	-0.025502	25	25	0.173098
25	26	0.040693	25	27	0.027549	25	28	-0.008853	25	33	-0.009379
25	34	-0.012788	25	35	-0.057513	25	40	-0.005755	25	41	-0.009417
25	42	-0.057551	25	43	0.030516	25	44	-0.004065	25	50	0.016638
25	51	0.020419	25	55	-0.140568	25	57	0.013901	25	58	-0.007294
25	59	-0.002507	25	61	-0.010184	25	62	-0.046321	26	26	0.059762
26	27	-0.014674	26	28	0.023279	26	33	-0.027103	26	34	0.012123
26	35	-0.028168	26	40	-0.044934	26	41	0.048929	26	42	0.033262
26	43	0.055887	26	44	-0.029229	26	50	-0.013686	26	51	-0.038501
26	55	-0.032296	26	57	0.010609	26	58	-0.008467	26	59	0.033406
26	61	-0.002542	26	62	-0.046554	27	27	0.168093	27	28	-0.047882
27	29	-0.046859	27	30	-0.001938	27	35	-0.006340	27	36	0.023491
27	40	0.021626	27	41	-0.048246	27	42	-0.117451	27	43	-0.004199
27	44	0.100911	27	45	0.021874	27	46	0.028682	27	51	0.023794
27	52	-0.026609	27	57	0.002773	27	58	0.021170	27	59	-0.045103
27	60	0.018155	27	62	-0.163514	27	63	-0.026132	28	28	0.165389
28	29	-0.024604	28	30	0.016428	28	35	0.023513	28	36	-0.007759
28	40	-0.022849	28	41	0.031057	28	42	0.023954	28	43	0.098085
28	44	-0.005192	28	45	-0.112699	28	46	-0.045319	28	51	-0.033399
28	52	0.071718	28	57	-0.038557	28	58	0.008301	28	59	0.006980
28	60	-0.037390	28	62	-0.016642	28	63	-0.139805	29	29	0.166475
29	30	-0.062120	29	31	0.012778	29	32	0.011871	29	36	-0.003412
29	37	-0.057112	29	43	0.021673	29	44	-0.116385	29	45	-0.001239
29	46	-0.034000	29	47	0.040801	29	48	0.001548	29	49	-0.013511
29	52	0.013671	29	53	0.027352	29	57	-0.042224	29	58	-0.008607
29	59	0.001613	29	60	0.004453	29	63	0.168444	29	64	-0.041662
30	30	0.167680	30	31	-0.017079	30	32	0.030038	30	36	-0.059460
30	37	-0.010566	30	43	-0.012158	30	44	0.038405	30	45	-0.035894
30	46	-0.006845	30	47	-0.117210	30	48	-0.049698	30	49	0.019699
30	52	0.027368	30	53	0.014851	30	57	0.006625	30	58	0.002635
30	59	-0.007156	30	60	-0.003486	30	63	-0.038809	30	64	0.165355
31	31	0.061128	31	32	0.037668	31	37	-0.029973	31	38	0.010660
31	39	-0.030186	31	45	0.019510	31	46	0.055176	31	47	0.033360
31	48	0.054145	31	49	-0.044085	31	53	-0.041127	31	54	-0.020901
31	56	-0.030598	31	58	0.004703	31	59	0.005623	31	60	-0.009232
31	64	0.041680	31	65	-0.034689	32	32	0.173565	32	37	-0.058653
32	38	-0.011748	32	39	-0.010968	32	45	-0.011602	32	46	0.027682
32	47	-0.064627	32	48	-0.009708	32	49	-0.008869	32	53	0.019120
32	54	-0.095196	32	56	-0.140432	32	58	-0.014924	32	59	0.009888
32	60	-0.013915	32	64	0.046275	32	65	-0.117143	33	33	1.004426
33	34	0.008342	33	40	-0.451893	33	41	-0.140044	33	42	-0.057925
33	50	0.080283	33	55	-0.402777	33	57	0.738676	33	58	-0.052805
33	61	-0.050982	34	34	1.007560	34	40	-0.141625	34	41	-0.468479
34	42	0.020298	34	50	-0.097889	34	55	-0.388285	34	57	-0.727071
34	58	0.047060	34	61	0.064703	35	35	0.959234	35	40	0.036100
35	41	0.021240	35	42	-0.402421	35	43	-0.413035	35	44	0.034506
35	51	-0.098102	35	57	-0.725306	35	58	0.708046	35	59	-0.009267
35	62	0.019335	36	36	0.961974	36	43	0.036268	36	44	-0.396026
36	45	-0.390323	36	46	0.033512	36	52	-0.097784	36	57	-0.009057
36	58	0.727433	36	59	-0.709459	36	60	0.058457	36	63	-0.024530

TABLE XXVI (Continued)

G MATRIX OF XYLITOL

i[a]	j	G_{ij}	i[a]	j	G_{ij}	i[a]	j	G_{ij}	i[a]	j	G_{ij}
37	37	0.962094	37	45	0.030601	37	46	-0.421979	37	47	-0.368658
37	48	0.016971	37	49	0.042012	37	53	-0.096038	37	58	0.055435
37	59	-0.713962	37	60	0.744616	37	64	-0.029380	38	38	1.005187
38	39	0.010131	38	47	0.015799	38	48	-0.471960	38	49	-0.141119
38	54	0.019597	38	56	-0.388276	38	59	-0.045541	38	60	0.726009
38	65	0.078647	39	39	1.004484	39	47	-0.057586	39	48	-0.140765
39	49	-0.468196	39	54	0.080108	39	56	-0.391608	39	59	0.053979
39	60	-0.732069	39	65	0.044789	40	40	1.005973	40	41	0.004475
40	42	-0.048354	40	43	-0.055977	40	44	0.029018	40	50	0.054960
40	51	0.008191	40	55	-0.431401	40	57	-0.002681	40	58	-0.035968
40	59	-0.033010	40	61	-0.828183	40	62	0.022783	41	41	1.005973
41	42	0.105273	41	43	0.024752	41	44	-0.024390	41	50	-0.041932
41	51	-0.028091	41	55	-0.431401	41	57	-0.011165	41	58	0.042592
41	59	0.034758	41	61	0.003774	41	62	0.023260	42	42	0.962288
42	43	-0.422945	42	44	-0.056665	42	50	-0.032910	42	51	-0.009809
42	55	0.036364	42	57	-0.006220	42	58	-0.704271	42	59	0.052235
42	61	0.037358	42	62	0.842453	43	43	0.958397	43	44	-0.048009
43	45	-0.053414	43	46	-0.018168	43	51	-0.036903	43	52	0.008152
43	57	0.711845	43	58	0.003554	43	59	0.040275	43	60	-0.002784
43	62	-0.829159	43	63	-0.021822	44	44	0.960903	44	45	-0.450868
44	46	0.015716	44	51	0.003032	44	52	-0.004802	44	57	0.036649
44	58	0.016435	44	59	0.670059	44	60	-0.015752	44	62	-0.024983
44	63	-0.854747	45	45	0.954444	45	46	0.098989	45	47	0.013462
45	48	0.028602	45	49	-0.017064	45	52	-0.039918	45	53	-0.035465
45	57	0.047475	45	58	-0.687207	45	59	-0.002601	45	60	0.035872
45	63	0.847335	45	64	0.023074	46	46	0.960106	46	47	-0.450254
46	48	0.027495	46	49	-0.055513	46	52	-0.035641	46	53	-0.041796
46	57	0.028989	46	58	0.043261	46	59	-0.001771	46	60	-0.698030
46	63	0.020058	46	64	0.829903	47	47	0.963733	47	48	0.105558
47	49	-0.039614	47	53	-0.001603	47	54	-0.001936	47	56	0.041434
47	58	-0.016678	47	59	0.692864	47	60	0.008315	47	64	-0.868603
47	65	-0.001976	48	48	1.006800	48	49	0.005266	48	53	-0.024932
48	54	-0.050290	48	56	-0.425674	48	58	0.017599	48	59	-0.047445
48	60	0.012845	48	64	-0.022792	48	65	-0.819765	49	49	1.006802
49	53	0.005803	49	54	-0.016926	49	56	-0.425674	49	58	-0.002659
49	59	0.037442	49	60	0.001240	49	64	-0.023696	49	65	-0.030791
50	50	1.224163	50	55	-0.010652	50	57	-0.038345	50	58	-0.040850
50	61	-0.053020	51	51	1.221271	51	57	-0.034328	51	58	0.045721
51	59	-0.021797	51	62	0.020150	52	52	1.221737	52	57	-0.021312
52	58	0.029747	52	59	-0.042978	52	60	-0.038813	52	63	-0.026244
53	53	1.222578	53	58	-0.040054	53	59	-0.041794	53	60	0.030049
53	64	-0.031161	54	54	1.223056	54	56	0.068817	54	59	0.012410
54	60	0.013655	54	65	0.083533	55	55	1.847488	55	57	-0.002838
55	58	0.004996	55	61	0.843735	56	56	1.846179	56	59	-0.008240
56	60	0.004000	56	65	0.893212	57	57	2.878352	57	58	-0.489003
57	59	0.015472	57	60	0.012760	57	61	-0.474442	57	62	-0.398404
57	63	-0.001803	58	58	1.924766	58	59	-0.516137	58	60	0.003984
58	61	0.038333	58	62	-0.430866	58	63	-0.390504	58	64	0.040926
59	59	1.906343	59	60	-0.521533	59	62	0.006935	59	63	-0.411857
59	64	-0.451707	59	65	0.019258	60	60	2.882328	60	63	0.037086
60	64	-0.361642	60	65	-0.560925	61	61	2.276561	62	62	2.390083
63	63	2.412371	64	64	2.403720	65	65	2.341802	-1	0	0.0

[a] i = row, j = column.

TABLE XXVII

$\underset{\sim}{G}$ MATRIX OF RIBITOL

i	j	G_{ij}	i	j	G_{ij}	i	j	G_{ij}	i	j	G_{ij}
1	1	0.166512	1	2	-0.031861	1	5	-0.029157	1	6	-0.029021
1	10	-0.027752	1	11	-0.027752	1	12	-0.027752	1	22	-0.050142
1	23	-0.049630	1	25	-0.054649	1	26	-0.019134	1	27	0.060606
1	28	0.020732	1	33	0.062615	1	34	0.064410	1	35	0.062223
1	40	-0.071816	1	41	-0.071816	1	42	-0.070084	1	43	0.060356
1	44	0.034325	1	50	-0.054500	1	51	0.018281	1	55	0.074132
1	58	0.008071	1	59	0.007823	1	61	-0.078581	1	62	-0.060151
2	2	0.166512	2	3	-0.033730	2	6	-0.030452	2	7	-0.024897
2	12	-0.021511	2	13	-0.027752	2	22	-0.050939	2	23	-0.049913
2	24	0.023356	2	25	0.016248	2	26	-0.029363	2	27	-0.054530
2	28	-0.055948	2	29	0.057546	2	30	-0.049871	2	35	0.057488
2	36	0.053654	2	40	0.035000	2	41	-0.049952	2	42	0.059533
2	43	-0.071812	2	44	-0.070085	2	45	0.069832	2	46	0.029338
2	51	0.031093	2	52	-0.039292	2	57	-0.017340	2	59	0.006993
2	60	0.048101	2	62	0.065609	2	63	-0.092800	3	3	0.166512
3	4	-0.033198	3	7	-0.029070	3	8	-0.028202	3	13	-0.029919
3	14	-0.027752	3	22	-0.049113	3	23	-0.049620	3	24	-0.050297
3	27	0.033728	3	28	0.058058	3	29	-0.054941	3	30	-0.054817
3	31	-0.026338	3	32	-0.049731	3	36	0.060288	3	37	0.066406
3	43	0.017591	3	44	0.069849	3	45	-0.069370	3	46	-0.070084
3	47	0.061376	3	48	0.027173	3	49	0.030479	3	52	-0.010153
3	53	0.007560	3	57	0.007660	3	58	-0.017835	3	60	0.013246
3	63	0.094304	3	64	-0.102860	4	4	0.166512	4	8	-0.024936
4	9	-0.026418	4	14	-0.020603	4	15	-0.027752	4	16	-0.027752
4	23	0.023428	4	24	-0.050066	4	29	0.025904	4	30	0.056190
4	31	-0.020106	4	32	-0.055641	4	37	0.054302	4	38	0.074344
4	39	0.061264	4	45	-0.049769	4	46	0.059969	4	47	-0.072024
4	48	-0.071816	4	49	-0.071816	4	53	-0.049988	4	54	-0.054680
4	56	0.061737	4	58	0.048397	4	59	-0.017743	4	64	0.099549
4	65	0.088035	5	5	0.145758	5	10	-0.024798	5	11	-0.026932
5	17	-0.021377	5	22	0.016473	5	25	-0.051645	5	26	-0.007863
5	33	-0.072715	5	34	-0.072077	5	40	0.060561	5	41	0.062750
5	42	-0.051179	5	50	-0.060550	5	55	0.069091	5	57	0.003837
5	58	-0.052980	6	6	0.145758	6	12	-0.025432	6	18	-0.021377
6	22	0.058489	6	23	0.034335	6	25	0.030522	6	26	0.066943
6	27	-0.050513	6	28	-0.049715	6	35	-0.070783	6	40	-0.051150
6	41	0.020937	6	42	0.060170	6	43	0.056689	6	44	0.010656
6	51	-0.060550	6	57	0.017023	6	58	-0.015078	6	59	0.040525
7	7	0.145758	7	13	-0.020218	7	19	-0.021377	7	22	0.021413
7	23	0.054224	7	24	0.026469	7	27	-0.050972	7	28	-0.051790
7	29	-0.051158	7	30	0.024489	7	36	-0.072111	7	43	0.030889
7	44	0.049677	7	45	0.056312	7	46	-0.050959	7	52	-0.060550
7	57	-0.051042	7	58	0.023991	7	59	-0.013953	7	60	-0.047738
8	8	0.145758	8	14	-0.031532	8	20	-0.021377	8	23	-0.051324
8	24	0.053272	8	29	0.024589	8	30	-0.051367	8	31	0.068362
8	32	0.020427	8	37	-0.068798	8	45	0.030547	8	46	0.065130
8	47	0.055803	8	48	0.022712	8	49	-0.052067	8	53	-0.060550
8	58	-0.002296	8	59	0.008985	8	60	-0.005301	9	9	0.145758
9	15	-0.040324	9	16	-0.026941	9	21	-0.021377	9	24	-0.051427
9	31	-0.003300	9	32	-0.052012	9	38	-0.066642	9	39	-0.072074
9	47	0.031800	9	48	0.073008	9	49	0.059327	9	54	-0.060550
9	56	0.074819	9	59	-0.008481	9	60	0.010821	10	10	1.075350
10	11	-0.030076	10	22	0.035717	10	25	0.051665	10	26	0.030946
10	33	-0.055696	10	34	0.061599	10	40	-0.051984	10	41	0.064283

TABLE XXVII (Continued)

G MATRIX OF RIBITOL

i	j	G_{ij}	i	j	G_{ij}	i	j	G_{ij}	i	j	G_{ij}
10	42	0.018035	10	50	0.023608	10	55	-0.071029	10	57	0.009919
10	58	0.040882	10	61	-0.018360	11	11	1.075351	11	22	-0.050976
11	25	0.053732	11	26	-0.003678	11	33	0.062365	11	34	-0.055207
11	40	0.064283	11	41	-0.051984	11	42	0.031717	11	50	0.031256
11	55	-0.071029	11	57	-0.013444	11	58	0.011025	11	61	0.096513
12	12	1.075349	12	22	0.048423	12	23	0.018588	12	25	-0.051514
12	26	-0.024804	12	27	0.046622	12	28	0.031271	12	35	-0.055790
12	40	0.018035	12	41	0.031717	12	42	-0.051983	12	43	-0.052431
12	44	-0.050821	12	51	-0.054928	12	57	0.000245	12	58	0.007455
12	59	-0.053623	12	62	-0.003554	13	13	1.075350	13	22	0.035028
13	23	0.057949	13	24	-0.050645	13	27	0.010794	13	28	0.044424
13	29	0.049248	13	30	0.030298	13	36	-0.056876	13	43	-0.049599
13	44	-0.051170	13	45	-0.050948	13	46	0.017301	13	52	0.053905
13	57	0.040375	13	58	-0.002861	13	59	0.005859	13	60	-0.006046
13	63	-0.006603	14	14	1.075349	14	23	0.030255	14	24	0.048481
14	29	-0.051272	14	30	0.057112	14	31	-0.026032	14	32	0.032490
14	37	-0.053922	14	45	0.017479	14	46	-0.051472	14	47	-0.053140
14	48	-0.053035	14	49	0.021282	14	53	0.041343	14	58	-0.045547
14	59	0.008217	14	60	-0.008799	14	64	0.012599	15	15	1.075350
15	16	-0.016061	15	24	0.027936	15	31	-0.003998	15	32	0.064260
15	38	-0.051332	15	39	0.065696	15	47	-0.051607	15	48	-0.051710
15	49	0.049811	15	54	0.021921	15	56	-0.074741	15	59	0.047449
15	60	-0.037066	15	65	0.016894	16	16	1.075349	16	24	0.031335
16	31	0.031232	16	32	0.051808	16	38	0.059756	16	39	-0.055516
16	47	0.020709	16	48	0.049811	16	49	-0.051710	16	54	0.035489
16	56	-0.074742	16	59	-0.044854	16	60	0.029820	16	65	-0.118069
17	17	1.054594	17	25	-0.041047	17	33	0.017446	17	34	0.023302
17	50	-0.041158	17	57	-0.003237	17	61	-0.011631	18	18	1.054595
18	26	-0.011791	18	27	0.023568	18	35	-0.040694	18	51	-0.041332
18	57	-0.041583	18	58	0.036483	18	62	-0.002321	19	19	1.054594
19	28	-0.029048	19	29	-0.007643	19	36	0.039201	19	52	-0.041361
19	58	0.030857	19	59	-0.043379	19	63	-0.003303	20	20	1.054595
20	30	0.005668	20	31	0.012138	20	37	0.031513	20	53	-0.041101
20	59	0.043266	20	60	-0.018841	20	64	0.010798	21	21	1.054595
21	32	-0.040676	21	38	0.017676	21	39	0.026459	21	54	-0.041390
21	60	0.008077	21	65	0.020720	22	22	0.171299	22	23	0.097923
22	24	-0.011164	22	25	-0.031996	22	26	0.039027	22	27	-0.025678
22	28	-0.039669	22	29	0.028306	22	30	0.014467	22	33	-0.055805
22	34	0.033822	22	35	-0.117704	22	36	-0.056742	22	40	-0.071181
22	41	0.101590	22	42	-0.006251	22	43	-0.005411	22	44	-0.068913
22	45	0.022734	22	46	-0.004282	22	50	-0.007002	22	51	-0.048597
22	52	0.021456	22	55	0.020379	22	57	0.026823	22	58	0.003063
22	59	-0.008477	22	60	-0.011163	22	61	-0.049604	22	62	-0.005802
22	63	-0.040501	23	23	0.171198	23	24	-0.046961	23	25	0.000516
23	26	0.012037	23	27	-0.067395	23	28	-0.021051	23	29	-0.021166
23	30	0.098877	23	31	-0.030592	23	32	-0.001882	23	35	-0.059008
23	36	-0.114488	23	37	0.030281	23	40	-0.013079	23	41	0.012346
23	42	0.039697	23	43	-0.034637	23	44	-0.019881	23	45	-0.020734
23	46	-0.060111	23	47	-0.053000	23	48	-0.023121	23	49	0.029350
23	51	-0.017599	23	52	0.049722	23	53	-0.000237	23	57	-0.002218
23	58	0.010993	23	59	-0.012841	23	60	-0.047994	23	62	0.024953
23	63	-0.001277	23	64	0.022862	24	24	0.172542	24	27	-0.018484
24	28	-0.045932	24	29	-0.051411	24	30	-0.019297	24	31	0.035449
24	32	0.097754	24	36	0.019057	24	37	-0.121019	24	38	0.037192

TABLE XXVII (Continued)

G MATRIX OF RIBITOL

i	j	G_{ij}	i	j	G_{ij}	i	j	G_{ij}	i	j	G_{ij}
24	39	0.028978	24	43	0.031802	24	44	0.023503	24	45	0.102843
24	46	-0.005480	24	47	-0.007024	24	48	-0.055822	24	49	-0.062615
24	52	-0.033618	24	53	0.042477	24	54	0.012986	24	56	-0.065927
24	57	-0.032655	24	58	-0.040831	24	59	0.012713	24	60	-0.016557
24	63	-0.015325	24	64	0.003520	24	65	-0.028167	25	25	0.171671
25	26	0.048239	25	27	-0.046267	25	28	-0.029204	25	33	-0.006909
25	34	-0.009758	25	35	0.017317	25	40	-0.004318	25	41	-0.007498
25	42	0.102041	25	43	0.029214	25	44	0.027836	25	50	0.100281
25	51	0.032184	25	55	-0.140769	25	57	-0.002042	25	58	0.043475
25	59	0.037564	25	61	0.082236	25	62	0.012966	26	26	0.060022
26	27	-0.012121	26	28	-0.030021	26	33	-0.022295	26	34	0.013362
26	35	-0.027405	26	40	-0.044840	26	41	0.041615	26	42	0.033573
26	43	0.054919	26	44	0.015983	26	50	0.015234	26	51	-0.002900
26	55	-0.036419	26	57	0.014860	26	58	-0.006126	26	59	0.030560
26	61	0.005903	26	62	0.007860	27	27	0.170886	27	28	0.094641
27	29	0.015456	27	30	-0.008726	27	35	-0.001968	27	36	0.045652
27	40	0.014542	27	41	0.030112	27	42	-0.119051	27	43	0.001573
27	44	-0.021281	27	45	-0.052083	27	46	0.026879	27	51	-0.057968
27	52	0.003082	27	57	0.005648	27	58	-0.002215	27	59	-0.032110
27	60	0.022764	27	62	-0.026542	27	63	0.025011	28	28	0.165907
28	29	-0.025650	28	30	0.024859	28	35	0.025772	28	36	0.001026
28	40	0.027686	28	41	0.000836	28	42	-0.056324	28	43	-0.056488
28	44	0.007669	28	45	-0.116699	28	46	0.018414	28	51	-0.013396
28	52	0.069692	28	57	0.038863	28	58	-0.011224	28	59	0.000610
28	60	-0.002177	28	62	-0.013276	28	63	0.136826	29	29	0.170735
29	30	-0.046895	29	31	0.022334	29	32	-0.011939	29	36	-0.005800
29	37	0.026738	29	43	-0.047240	29	44	-0.117359	29	45	-0.000178
29	46	0.100878	29	47	0.018322	29	48	0.029907	29	49	-0.019986
29	52	0.018707	29	53	-0.032368	29	57	0.041483	29	58	0.001569
29	59	0.006734	29	60	0.049209	29	63	-0.159230	29	64	0.018483
30	30	0.168861	30	31	-0.015715	30	32	0.029347	30	36	-0.055624
30	37	-0.016012	30	43	-0.006467	30	44	0.028210	30	45	-0.060692
30	46	-0.012971	30	47	-0.113089	30	48	-0.048175	30	49	0.019541
30	52	0.031987	30	53	-0.013755	30	57	-0.000666	30	58	0.006892
30	59	-0.013194	30	60	-0.015035	30	63	0.038985	30	64	0.169967
31	31	0.060269	31	32	0.036547	31	37	-0.030309	31	38	0.009985
31	39	-0.029048	31	45	0.010800	31	46	0.057371	31	47	0.032074
31	48	0.043962	31	49	-0.043682	31	53	-0.045606	31	54	0.018587
31	56	-0.030293	31	58	0.008423	31	59	-0.000590	31	60	0.007174
31	64	0.038366	31	65	-0.051231	32	32	0.169178	32	37	-0.061993
32	38	-0.027847	32	39	-0.007052	32	45	0.013510	32	46	0.025773
32	47	-0.059088	32	48	-0.022579	32	49	-0.003354	32	53	0.011420
32	54	0.098454	32	56	-0.129102	32	58	-0.016459	32	59	0.012939
32	60	-0.019709	32	64	0.045421	32	65	-0.087705	33	33	1.003523
33	34	0.006486	33	40	-0.433035	33	41	-0.139403	33	42	0.041854
33	50	-0.043627	33	55	-0.411079	33	57	-0.749166	33	58	0.020680
33	61	0.072360	34	34	1.006259	34	40	-0.140780	34	41	-0.447323
34	42	0.028336	34	50	-0.059045	34	55	-0.398863	34	57	0.737100
34	58	0.052306	34	61	-0.158739	35	35	0.961409	35	40	0.041015
35	41	-0.056884	35	42	-0.413481	35	43	-0.394520	35	44	0.039719
35	51	0.102073	35	57	-0.716981	35	58	0.696354	35	59	0.007842
35	62	0.014062	36	36	0.954977	36	43	0.013217	36	44	-0.334488
36	45	-0.394676	36	46	0.039460	36	52	-0.095269	36	57	0.017643
36	58	-0.757443	36	59	0.723392	36	60	0.058095	36	63	0.025270
37	37	0.968045	37	45	-0.057820	37	46	-0.445212	37	47	-0.357038

TABLE XXVII (Continued)

G MATRIX OF RIBITOL

i	j	G_{ij}	i	j	G_{ij}	i	j	G_{ij}	i	j	G_{ij}
37	48	0.031064	37	49	0.041273	37	53	-0.081657	37	58	0.053953
37	59	-0.702713	37	60	0.720832	37	64	-0.052088	38	38	1.024533
38	39	0.004186	38	47	0.022046	38	48	-0.518993	38	49	-0.150541
38	54	-0.048648	38	56	-0.412795	38	59	-0.050076	38	60	0.723874
38	65	-0.076077	39	39	1.007272	39	47	-0.060317	39	48	-0.140875
39	49	-0.412766	39	54	-0.067307	39	56	-0.500386	39	59	0.057686
39	60	-0.790356	39	65	0.186305	40	40	1.006802	40	41	0.001154
40	42	-0.036863	40	43	-0.054927	40	44	-0.012568	40	50	0.041429
40	51	0.000762	40	55	-0.445046	40	57	-0.023041	40	58	-0.033849
40	59	-0.026798	40	61	0.867168	40	62	0.018501	41	41	1.006803
41	42	-0.064830	41	43	0.025900	41	44	-0.014367	41	50	0.033583
41	51	-0.031627	41	55	-0.445046	41	57	0.024815	41	58	-0.011710
41	59	-0.009729	41	61	-0.004358	41	62	-0.030605	42	42	0.963112
42	43	-0.425001	42	44	0.011197	42	50	0.013754	42	51	0.034330
42	55	-0.066450	42	57	-0.004188	42	58	-0.683603	42	59	0.045354
42	61	0.025417	42	62	0.793168	43	43	0.953067	43	44	0.096381
43	45	0.030632	43	46	-0.023918	43	51	0.016024	43	52	-0.026628
43	57	0.704531	43	58	-0.000735	43	59	0.041920	43	60	-0.012054
43	62	-0.795923	43	63	0.017487	44	44	0.960333	44	45	-0.502783
44	46	-0.051970	44	51	0.032351	44	52	-0.008023	44	57	-0.039596
44	58	0.000291	44	59	-0.662579	44	60	-0.050549	44	62	-0.014483
44	63	0.857524	45	45	0.963899	45	46	-0.035780	45	47	0.038366
45	48	-0.004408	45	49	-0.011752	45	52	-0.044135	45	53	0.031483
45	57	-0.051516	45	58	0.665367	45	59	0.006464	45	60	0.002742
45	63	-0.821427	45	64	-0.042009	46	46	0.961360	46	47	-0.435271
46	48	0.021595	46	49	-0.057451	46	52	-0.000860	46	53	-0.050717
46	57	0.032155	46	58	0.033799	46	59	0.001417	46	60	-0.665484
46	63	-0.025760	46	64	0.831629	47	47	0.953761	47	48	0.100905
47	49	-0.040492	47	53	0.016939	47	54	-0.001709	47	56	0.034367
47	58	-0.011387	47	59	0.690470	47	60	0.034639	47	64	-0.887930
47	65	-0.035657	48	48	1.005859	48	49	0.023143	48	53	-0.019610
48	54	0.043390	48	56	-0.354840	48	58	0.022979	48	59	-0.051374
48	60	0.044335	48	64	-0.027647	48	65	-0.896177	49	49	1.005857
49	53	0.008612	49	54	0.029521	49	56	-0.354841	49	58	-0.006242
49	59	0.042888	49	60	-0.025950	49	64	-0.024533	49	65	0.014755
50	50	1.223306	50	55	-0.073278	50	57	0.001898	50	58	0.012861
50	61	0.075238	51	51	1.224042	51	57	0.041487	51	58	-0.043718
51	59	0.029718	51	62	0.014539	52	52	1.224161	52	57	0.020088
52	58	-0.034877	52	59	0.049469	52	60	-0.019003	52	63	0.024223
53	53	1.223063	53	58	-0.041434	53	59	-0.036478	53	60	0.018004
53	64	-0.058887	54	54	1.224290	54	56	-0.063857	54	59	-0.005746
54	60	-0.006078	54	65	-0.099492	55	55	1.850639	55	57	0.004707
55	58	-0.069327	55	61	-0.865504	56	56	1.827174	56	59	-0.002887
56	60	0.008056	56	65	0.942228	57	57	2.877733	57	58	-0.483593
57	59	0.014846	57	60	0.021600	57	61	-0.405915	57	62	-0.467737
57	63	0.002630	58	58	1.903956	58	59	-0.580548	58	60	-0.006362
58	61	0.004152	58	62	-0.452473	58	63	-0.325325	58	64	0.038561
59	59	1.960254	59	60	-0.498623	59	62	-0.000228	59	63	-0.411680
59	64	-0.499425	59	65	0.061584	60	60	2.847345	60	63	-0.039466
60	64	-0.337780	60	65	-0.554220	61	61	2.380278	62	62	2.215719
63	63	2.329207	64	64	2.450256	65	65	2.634606	-1	0	0.0

TABLE XXVIII

$\underset{\sim}{G}$ MATRIX OF ERYTHRITOL

i^a	j	G_{ij}	i^a	j	G_{ij}	i^a	j	G_{ij}	i^a	j	G_{ij}
1	1	0.166512	1	2	-0.031592	1	4	-0.030107	1	5	-0.029700
1	8	-0.027752	1	9	-0.027752	1	10	-0.027752	1	18	-0.050445
1	19	-0.050401	1	20	-0.054017	1	21	-0.018771	1	22	0.054969
1	23	-0.006805	1	26	0.056958	1	27	0.067471	1	28	0.065068
1	32	-0.018524	1	33	-0.018524	1	34	-0.070084	1	35	-0.025973
1	36	0.019710	1	40	0.035686	1	41	0.003767	1	44	0.079229
1	47	-0.015319	1	48	0.002293	1	49	0.014759	1	50	0.099524
2	2	0.166512	2	3	-0.032397	2	5	-0.022956	2	6	-0.027791
2	10	-0.026110	2	11	-0.027752	2	18	-0.050511	2	19	-0.050357
2	20	0.025712	2	21	-0.024024	2	22	-0.055691	2	23	-0.019245
2	24	0.058254	2	25	-0.003429	2	28	0.055237	2	29	0.063477
2	32	-0.004828	2	33	0.026107	2	34	0.063645	2	35	-0.019005
2	36	-0.070084	2	37	0.060130	2	38	0.026710	2	39	-0.003567
2	41	-0.049101	2	42	0.042027	2	46	0.008685	2	48	-0.134891
2	49	0.046633	2	50	-0.095285	2	51	0.069363	2	52	-0.049038
3	3	0.166512	3	6	-0.028825	3	7	-0.031726	3	11	-0.020217
3	12	-0.027752	3	13	-0.027752	3	18	-0.050181	3	19	-0.050226
3	22	0.024235	3	23	-0.027538	3	24	-0.053979	3	25	-0.018279
3	29	0.056646	3	30	0.053983	3	31	0.065472	3	35	-0.003229
3	36	0.058606	3	37	-0.072111	3	38	-0.018698	3	39	-0.018698
3	42	0.004148	3	43	0.011435	3	45	0.083138	3	46	0.002273
3	47	0.017661	3	51	-0.066599	3	52	-0.018936	4	4	0.145758
4	8	-0.016190	4	9	-0.029285	4	14	-0.021377	4	18	0.025910
4	20	-0.050900	4	21	-0.005746	4	26	-0.074718	4	27	-0.071304
4	32	-0.018241	4	33	-0.027348	4	34	-0.050899	4	40	-0.060550
4	44	0.064913	4	46	-0.009819	4	47	0.047353	5	5	0.145758
5	10	-0.028196	5	15	-0.021377	5	18	0.051446	5	19	0.025288
5	20	0.026268	5	21	0.065957	5	22	-0.052409	5	23	0.030380
5	28	-0.069943	5	32	0.025589	5	33	-0.001992	5	34	0.063524
5	35	-0.024411	5	36	0.030620	5	41	-0.060550	5	46	-0.007567
5	47	0.017969	5	48	-0.049832	5	49	-0.046891	6	6	0.145758
6	11	-0.029232	6	16	-0.021377	6	18	0.029955	6	19	0.055983
6	22	-0.051244	6	23	0.066642	6	24	-0.051285	6	25	-0.006512
6	29	-0.069603	6	35	-0.001489	6	36	0.062286	6	37	0.057587
6	38	-0.006712	6	39	0.026479	6	42	-0.060550	6	46	0.045140
6	47	-0.016729	6	48	-0.022346	6	52	0.047362	7	7	0.145758
7	12	-0.011126	7	13	-0.026476	7	17	-0.021377	7	19	0.021997
7	24	0.026310	7	25	0.065005	7	30	-0.073017	7	31	-0.069853
7	37	-0.050481	7	38	-0.015114	7	39	-0.025803	7	43	-0.060550
7	45	0.056323	7	47	-0.049396	7	48	0.198014	8	8	1.075350
8	9	-0.034769	8	18	0.031972	8	20	0.043530	8	21	0.030493
8	26	-0.056832	8	27	0.057859	8	32	0.359455	8	33	-0.030617
8	34	0.018697	8	40	0.021710	8	44	-0.069212	8	46	0.000478
8	47	-0.043599	8	49	-0.090438	9	9	1.075350	9	18	-0.051444
9	20	0.056275	9	21	-0.004723	9	26	0.062328	9	27	-0.054236
9	32	-0.030617	9	33	0.359456	9	34	0.027428	9	40	-0.053491
9	44	-0.069213	9	46	0.008118	9	47	-0.001845	9	49	0.067689
10	10	1.075351	10	18	0.052625	10	19	0.028491	10	20	-0.051471
10	21	-0.026741	10	22	0.048646	10	23	-0.003815	10	28	-0.054514
10	32	-0.000891	10	33	-0.004190	10	34	-0.051473	10	35	0.360542
10	36	-0.051270	10	41	0.044600	10	46	-0.001101	10	47	-0.001525
10	48	0.046926	10	49	0.000289	10	50	-0.011409	11	11	1.075350
11	18	0.020085	11	19	0.047438	11	22	0.030033	11	23	-0.026744
11	24	0.047705	11	25	0.029914	11	29	-0.053874	11	35	0.025902

TABLE XXVIII (Continued)

$\underset{\sim}{G}$ MATRIX OF ERYTHRITOL

i^a	j	G_{ij}	i^a	j	G_{ij}	i^a	j	G_{ij}	i^a	j	G_{ij}
11	36	-0.051405	11	37	-0.053030	11	38	-0.002604	11	39	-0.005138
11	42	-0.050593	11	46	-0.051143	11	47	-0.000385	11	48	0.172611
11	51	-0.006739	11	52	0.002806	12	12	1.075350	12	13	-0.040173
12	19	-0.050987	12	24	0.033969	12	25	-0.015412	12	30	-0.057100
12	31	0.054216	12	37	0.017800	12	38	0.351840	12	39	-0.034420
12	43	-0.055768	12	45	-0.064534	12	47	-0.008173	12	48	-0.015296
12	52	-0.070097	13	13	1.075350	13	19	0.028447	13	24	-0.051536
13	25	-0.026313	13	30	0.058960	13	31	-0.054626	13	37	0.024114
13	38	-0.034420	13	39	0.351840	13	43	0.039540	13	45	-0.064534
13	47	0.046655	13	48	-0.143718	13	52	0.080903	14	14	1.054594
14	20	0.027002	14	26	0.015614	14	27	-0.040312	14	40	-0.040872
14	46	-0.032910	14	49	0.011901	15	15	1.054594	15	21	-0.006475
15	22	-0.036035	15	28	0.033439	15	41	-0.040872	15	46	-0.043645
15	47	0.020064	15	50	-0.008459	16	16	1.054595	16	23	-0.020307
16	24	0.003119	16	29	-0.038117	16	42	-0.040590	16	47	0.027219
16	48	0.043137	16	51	-0.005231	17	17	1.054594	17	25	-0.009143
17	30	-0.039698	17	31	0.029420	17	43	-0.040646	17	48	0.042938
17	52	-0.016362	18	18	0.170143	18	19	0.098822	18	20	-0.050346
18	21	0.031620	18	22	-0.017786	18	23	0.046266	18	24	0.020521
18	25	0.013282	18	26	-0.056222	18	27	0.023830	18	28	-0.117539
18	29	-0.057876	18	32	0.045048	18	33	-0.043201	18	34	-0.011808
18	35	0.032435	18	36	-0.039544	18	37	0.036351	18	38	0.005813
18	39	0.014754	18	40	0.029169	18	41	0.044308	18	42	-0.013674
18	44	0.027795	18	46	-0.013979	18	47	0.002182	18	48	0.031674
18	49	-0.097263	18	50	-0.004087	18	51	0.028166	18	52	0.014259
19	19	0.171059	19	20	-0.008189	19	21	0.005130	19	22	-0.046227
19	23	0.036609	19	24	-0.023751	19	25	0.037079	19	28	-0.060560
19	29	-0.118786	19	30	0.019993	19	31	-0.054846	19	32	0.013952
19	33	0.006076	19	34	0.030605	19	35	0.041645	19	36	-0.003892
19	37	-0.005412	19	38	-0.043457	19	39	0.041819	19	41	0.011231
19	42	-0.045681	19	43	0.034613	19	45	0.033762	19	46	-0.004464
19	47	-0.006944	19	48	0.165041	19	49	-0.011696	19	50	-0.045077
19	51	-0.002811	19	52	0.097940	20	20	0.169663	20	21	0.042816
20	22	-0.046585	20	23	0.004124	20	26	0.002360	20	27	-0.014096
20	28	0.023103	20	32	0.022601	20	33	0.033886	20	34	0.101585
20	35	-0.029937	20	36	0.031026	20	40	-0.065841	20	41	-0.032001
20	44	-0.142466	20	46	0.010357	20	47	-0.041513	20	48	-0.033064
20	49	-0.058862	20	50	-0.015339	21	21	0.058713	21	22	-0.015322
21	23	0.019621	21	26	-0.021012	21	27	0.012253	21	28	-0.025325
21	32	0.030179	21	33	-0.013674	21	34	0.035932	21	35	-0.023639
21	36	0.026428	21	40	0.001407	21	41	-0.012027	21	44	-0.036784
21	46	-0.004552	21	47	0.005250	21	48	-0.034404	21	49	-0.062685
21	50	0.057394	22	22	0.162922	22	23	-0.044815	22	24	0.025209
22	25	0.006850	22	28	-0.002373	22	29	0.029922	22	32	-0.018140
22	33	-0.022050	22	34	-0.113991	22	35	0.027897	22	36	-0.057315
22	37	-0.053329	22	38	-0.001062	22	39	-0.017090	22	41	0.084979
22	42	-0.011545	22	46	-0.006814	22	47	-0.004808	22	48	0.096343
22	49	-0.001214	22	50	0.124327	22	51	-0.014264	22	52	-0.021307
23	23	0.058968	23	24	-0.013945	23	25	-0.005319	23	28	-0.032391
23	29	-0.026323	23	32	0.009274	23	33	-0.004154	23	34	0.011880
23	35	-0.012236	23	36	0.035933	23	37	0.053952	23	38	0.001531
23	39	0.017568	23	41	0.007596	23	42	0.011738	23	46	0.027644
23	47	-0.005572	23	48	-0.074898	23	49	-0.021894	23	50	0.011931
23	51	0.003035	23	52	0.021532	24	24	0.167561	24	25	0.042798

TABLE XXVIII (Continued)

G MATRIX OF ERYTHRITOL

i[a]	j	G_{ij}	i[a]	j	G_{ij}	i[a]	j	G_{ij}	i[a]	j	G_{ij}
24	29	-0.001371	24	30	-0.053724	24	31	0.022250	24	35	0.004583
24	36	-0.116851	24	37	-0.001561	24	38	0.048371	24	39	-0.042872
24	42	-0.007526	24	43	-0.029937	24	45	0.026314	24	46	-0.045330
24	47	-0.008051	24	48	0.122640	24	51	0.017302	24	52	-0.096879
25	25	0.058482	25	29	-0.024197	25	30	-0.031208	25	31	-0.024425
25	35	0.008707	25	36	-0.026181	25	37	-0.042955	25	38	-0.008642
25	39	-0.017658	25	42	-0.016631	25	43	-0.006252	25	45	0.062500
25	46	-0.017372	25	47	-0.037523	25	48	0.195675	25	51	0.007804
25	52	-0.032535	26	26	0.991347	26	27	0.008782	26	32	0.118390
26	33	0.056555	26	34	0.037841	26	40	-0.036762	26	44	-0.411260
26	46	0.762550	26	47	-0.011861	26	49	0.145379	27	27	1.008023
27	32	0.055884	27	33	0.148204	27	34	0.033237	27	40	0.103134
27	44	-0.338466	27	46	-0.708976	27	47	-0.056658	27	49	-0.093258
28	28	0.962892	28	32	-0.029747	28	33	0.006835	28	34	-0.440281
28	35	0.104311	28	36	0.017670	28	41	-0.084631	28	46	0.694181
28	47	-0.744783	28	48	0.009982	28	49	0.055935	28	50	0.045877
29	29	0.962954	29	35	-0.025984	29	36	-0.424295	29	37	-0.388641
29	38	0.010934	29	39	-0.026598	29	42	0.096616	29	46	0.000129
29	47	0.714694	29	48	-0.904480	29	51	0.027249	29	52	-0.060447
30	30	0.925598	30	31	0.007840	30	37	0.035235	30	38	0.110832
30	39	0.053593	30	43	0.089729	30	45	-0.345144	30	47	0.055402
30	48	-0.945813	30	52	0.055986	31	31	0.944396	31	37	0.034078
31	38	0.052957	31	39	0.142312	31	43	-0.073304	31	45	-0.267988
31	47	0.009669	31	48	-0.746542	31	52	-0.133877	32	32	0.259240
32	33	-0.020214	32	34	0.035743	32	35	-0.001659	32	36	0.004117
32	40	0.023373	32	41	0.002000	32	44	0.143342	32	46	-0.001915
32	47	-0.023653	32	48	-0.012139	32	49	-0.073026	32	50	-0.010712
33	33	0.259241	33	34	0.045151	33	35	0.002757	33	36	-0.001971
33	40	-0.028931	33	41	-0.013815	33	44	0.143342	33	46	0.007937
33	47	0.000667	33	48	-0.000763	33	49	0.062739	33	50	-0.037462
34	34	0.961361	34	35	0.142618	34	36	0.028607	34	40	-0.008927
34	41	-0.049540	34	44	-0.065841	34	46	0.008007	34	47	0.686895
34	48	-0.050154	34	49	-0.004372	34	50	-0.818905	35	35	0.258270
35	36	-0.039129	35	37	-0.019819	35	38	-0.004194	35	39	0.000097
35	41	0.020140	35	42	-0.019484	35	46	0.259662	35	47	-0.001889
35	48	0.096863	35	49	0.010286	35	50	-0.320561	35	51	-0.010126
35	52	0.008655	36	36	0.961131	36	37	-0.423780	36	38	-0.028848
36	39	0.009395	36	41	-0.019919	36	42	0.001582	36	46	0.050089
36	47	0.003276	36	48	0.648950	36	49	-0.013075	36	50	0.023306
36	51	-0.801152	36	52	0.054959	37	37	0.952756	37	38	0.035024
37	39	0.041703	37	42	0.041052	37	43	-0.004898	37	45	-0.062781
37	46	0.043581	37	47	-0.704197	37	48	-0.294259	37	51	0.821596
37	52	-0.000214	38	38	0.254694	38	39	-0.023420	38	42	0.009861
38	43	-0.036184	38	45	0.155736	38	46	-0.002470	38	47	-0.007444
38	48	-0.043162	38	51	0.026864	38	52	-0.067666	39	39	0.254693
39	42	-0.000712	39	43	0.030191	39	45	0.155736	39	46	0.011930
39	47	0.025623	39	48	-0.105622	39	51	0.008541	39	52	0.064970
40	40	1.222099	40	44	0.045365	40	46	0.033141	40	47	-0.007248
40	49	-0.055609	41	41	1.222096	41	46	0.044190	41	47	-0.022915
41	48	0.018148	41	49	-0.021804	41	50	0.049396	42	42	1.220914
42	46	0.023564	42	47	-0.028471	42	48	-0.179013	42	51	0.029789
42	52	-0.020280	43	43	1.221144	43	45	0.024308	43	47	0.014433
43	48	-0.069483	43	52	0.074206	44	44	1.858497	44	46	-0.012268
44	47	0.064868	44	49	0.032472	45	45	1.747245	45	47	-0.057641
45	48	1.558677	45	52	-0.016186	46	46	2.872236	46	47	-0.507553
46	48	-0.085507	46	49	-0.043782	46	50	-0.477827	46	51	-0.000439
46	52	0.017585	47	47	1.927681	47	48	-0.587418	47	49	0.029718
47	50	-0.331722	47	51	-0.509391	47	52	0.024671	48	48	3.719481
48	49	0.021742	48	50	-0.004772	48	51	-0.498499	48	52	-0.043902
49	49	1.495232	49	50	-0.041070	50	50	2.406438	51	51	2.253054
51	52	-0.029792	52	52	1.461962	-1	0	0.0			

[a] i = row, j = column.

TABLE XXIX

$\underset{\sim}{G}$ MATRIX OF D-ARABINITOL

i	j	G_{ij}	i	j	G_{ij}	i	j	G_{ij}	i	j	G_{ij}
1	1	0.166512	1	2	-0.032931	1	5	-0.027243	1	6	-0.026280
1	10	-0.027752	1	11	-0.027752	1	12	-0.027752	1	22	-0.050142
1	23	-0.050114	1	25	-0.055678	1	26	-0.019728	1	27	0.058591
1	28	0.022429	1	33	0.069324	1	34	0.063472	1	35	0.053467
1	40	-0.071816	1	41	-0.071816	1	42	-0.070085	1	43	0.069100
1	44	0.026719	1	50	-0.052701	1	51	0.031749	1	55	0.065391
1	58	0.010943	1	59	-0.001797	1	61	0.081020	1	62	-0.059845
2	2	0.166512	2	3	-0.031592	2	6	-0.030179	2	7	-0.029700
2	12	-0.030167	2	13	-0.027752	2	22	-0.050307	2	23	-0.050445
2	24	-0.050401	2	25	0.026733	2	26	-0.028131	2	27	-0.053997
2	28	-0.054126	2	29	0.055025	2	30	0.029427	2	35	0.059846
2	36	0.064999	2	40	0.018764	2	41	-0.050279	2	42	0.069420
2	43	-0.069284	2	44	-0.070085	2	45	0.063862	2	46	0.019710
2	51	0.018032	2	52	0.003840	2	57	-0.012547	2	59	-0.015277
2	60	0.002293	2	62	0.054104	2	63	0.099480	3	3	0.166512
3	4	-0.032397	3	7	-0.023035	3	8	-0.027791	3	13	-0.026110
3	14	-0.027752	3	22	-0.050483	3	23	-0.050511	3	24	-0.050457
3	27	0.025658	3	28	0.053733	3	29	-0.055676	3	30	-0.054237
3	31	-0.027370	3	32	0.021960	3	36	0.055272	3	37	0.063442
3	43	0.029501	3	44	0.063645	3	45	-0.070586	3	46	-0.070084
3	47	0.060177	3	48	-0.049916	3	49	0.027849	3	52	-0.049107
3	53	0.041974	3	57	-0.001823	3	58	0.010745	3	60	-0.003472
3	63	-0.095163	3	64	0.069315	4	4	0.166512	4	8	-0.028863
4	9	-0.031726	4	14	-0.020217	4	15	-0.027752	4	16	-0.027752
4	23	-0.050181	4	24	-0.050226	4	29	0.024263	4	30	0.058380
4	31	-0.019058	4	32	-0.053454	4	37	0.056662	4	38	0.055131
4	39	0.066850	4	45	0.027640	4	46	0.058606	4	47	-0.072111
4	48	-0.071816	4	49	-0.071816	4	53	0.004213	4	54	0.011502
4	56	0.085952	4	58	0.002273	4	59	0.017729	4	64	-0.066547
4	65	0.052055	5	5	0.145758	5	10	-0.034517	5	11	-0.028230
5	17	-0.021377	5	22	0.027504	5	25	-0.051758	5	26	0.031217
5	33	-0.069317	5	34	-0.071660	5	40	0.068025	5	41	0.061604
5	42	0.020307	5	50	-0.060550	5	55	0.073924	5	57	0.003750
5	58	0.047739	6	6	0.145758	6	12	-0.018175	6	18	-0.021377
6	22	0.056349	6	23	0.025846	6	25	-0.051945	6	26	0.067640
6	27	-0.050881	6	28	0.026206	6	35	-0.072543	6	40	0.029138
6	41	0.027619	6	42	0.049419	6	43	0.055699	6	44	-0.050881
6	51	-0.060550	6	57	0.022513	6	58	-0.022135	6	59	0.047371
7	7	0.145758	7	13	-0.028119	7	19	-0.021377	7	22	0.022814
7	23	0.051523	7	24	0.025310	7	27	0.026268	7	28	-0.051002
7	29	-0.052394	7	30	-0.052240	7	36	-0.069968	7	43	-0.050593
7	44	0.063446	7	45	0.054326	7	46	0.030584	7	52	-0.060549
7	57	0.049666	7	58	-0.011756	7	59	0.018003	7	60	-0.049800
8	8	0.145758	8	14	-0.029191	8	20	-0.021377	8	23	0.029982
8	24	0.056076	8	29	-0.051244	8	30	-0.051395	8	31	0.066406
8	32	0.026729	8	37	-0.069617	8	45	0.020349	8	46	0.062245
8	47	0.057641	8	48	0.033876	8	49	-0.051374	8	53	-0.060549
8	58	0.045119	8	59	-0.016687	8	60	0.004932	9	9	0.145758
9	15	-0.011127	9	16	-0.026475	9	21	-0.021377	9	24	0.022041
9	31	-0.005429	9	32	-0.050641	9	38	-0.075489	9	39	-0.072218
9	47	-0.050580	9	48	0.049531	9	49	0.065206	9	54	-0.060549
9	56	0.058230	9	59	-0.049494	9	60	-0.006086	10	10	1.075350
10	11	-0.020614	10	22	0.019262	10	25	0.059598	10	26	-0.007282

TABLE XXIX (Continued)

G MATRIX OF D-ARABINITOL

i	j	G_{ij}	i	j	G_{ij}	i	j	G_{ij}	i	j	G_{ij}
10	33	-0.053620	10	34	0.064678	10	40	-0.051641	10	41	0.054439
10	42	-0.050338	10	50	0.013180	10	55	-0.073801	10	57	-0.022038
10	58	-0.052169	10	61	0.018917	11	11	1.075350	11	22	-0.051613
11	25	0.053680	11	26	-0.006560	11	33	0.062108	11	34	-0.055432
11	40	0.054439	11	41	-0.051642	11	42	0.030862	11	50	0.041712
11	55	-0.073801	11	57	0.019311	11	58	0.001864	11	61	-0.105982
12	12	1.075351	12	22	0.057806	12	23	0.029719	12	25	0.020261
12	26	-0.018675	12	27	0.047926	12	28	-0.050476	12	35	-0.056540
12	40	-0.050338	12	41	0.030862	12	42	-0.051642	12	43	-0.050885
12	44	0.020667	12	51	-0.055760	12	57	-0.007672	12	58	0.009741
12	59	-0.044642	12	62	0.003407	13	13	1.075351	13	22	0.027428
13	23	0.052625	13	24	0.028491	13	27	-0.051472	13	28	0.054831
13	29	0.048627	13	30	0.020498	13	36	-0.054534	13	43	0.020906
13	44	-0.051473	13	45	-0.051772	13	46	-0.051270	13	52	0.044594
13	57	-0.047423	13	58	0.001002	13	59	-0.001605	13	60	0.046926
13	63	-0.011424	14	14	1.075349	14	23	0.020085	14	24	0.047488
14	29	0.030006	14	30	0.054206	14	31	-0.025391	14	32	-0.053071
14	37	-0.053885	14	45	-0.050906	14	46	-0.051404	14	47	-0.053134
14	48	0.018351	14	49	0.024860	14	53	-0.050625	14	58	-0.051143
14	59	-0.000509	14	60	-0.001508	14	64	-0.006718	15	15	1.075350
15	16	-0.040173	15	24	-0.051087	15	31	-0.010050	15	32	0.039473
15	38	-0.057299	15	39	0.055082	15	47	0.017835	15	48	-0.051642
15	49	0.074413	15	54	-0.055968	15	56	-0.066719	15	59	-0.008189
15	60	0.011692	15	65	0.004468	16	16	1.075351	16	24	0.028503
16	31	0.031229	16	32	0.054788	16	38	0.060028	16	39	-0.054816
16	47	0.024161	16	48	0.074413	16	49	-0.051642	16	54	0.039657
16	56	-0.066719	16	59	0.046747	16	60	-0.005695	16	65	-0.052791
17	17	1.054594	17	25	-0.039344	17	33	0.010218	17	34	0.031278
17	50	-0.041566	17	57	0.014192	17	61	0.018356	18	18	1.054595
18	26	-0.016657	18	27	0.013649	18	35	-0.040308	18	51	-0.040872
18	57	-0.035165	18	58	0.041337	18	62	0.001514	19	19	1.054594
19	28	0.002900	19	29	-0.036050	19	36	0.033423	19	52	-0.040872
19	58	-0.043640	19	59	0.020042	19	63	-0.008441	20	20	1.054595
20	30	0.031412	20	31	-0.006667	20	37	-0.038134	20	53	-0.040590
20	59	0.027270	20	60	-0.043141	20	64	-0.005205	21	21	1.054595
21	32	0.008776	21	38	-0.039840	21	39	0.029508	21	54	-0.040787
21	60	0.043082	21	65	0.001178	22	22	0.172084	22	23	0.099318
22	24	0.013597	22	25	-0.052588	22	26	0.037741	22	27	-0.023702
22	28	-0.044444	22	29	0.025959	22	30	-0.006947	22	33	-0.059529
22	34	0.022082	22	35	-0.113092	22	36	-0.056404	22	40	-0.038411
22	41	0.102926	22	42	-0.020002	22	43	-0.019651	22	44	-0.054382
22	45	0.031384	22	46	-0.006389	22	50	-0.016974	22	51	-0.049673
22	52	0.034324	22	55	0.038114	22	57	-0.000577	22	58	-0.018350
22	59	0.005640	22	60	0.000669	22	61	0.054724	22	62	0.005649
22	63	0.040462	23	23	0.170143	23	24	0.098849	23	25	-0.006537
23	26	0.006953	23	27	-0.050257	23	28	-0.016714	23	29	-0.017875
23	30	-0.056909	23	31	0.008827	23	32	-0.004717	23	35	-0.054799
23	36	-0.117507	23	37	-0.057877	23	40	-0.006401	23	41	0.014231
23	42	0.028996	23	43	-0.060057	23	44	-0.011808	23	45	-0.011776
23	46	-0.039544	23	47	0.036341	23	48	0.014016	23	49	-0.008950
23	51	-0.028510	23	52	0.044242	23	53	-0.013704	23	57	0.004902
23	58	-0.017863	23	59	0.002095	23	60	-0.001175	23	62	0.027469
23	63	-0.004162	23	64	0.028141	24	24	0.171398	24	27	-0.008175
24	28	0.025672	24	29	-0.046311	24	30	-0.023584	24	31	0.036536

TABLE XXIX (Continued)

$\underset{\sim}{G}$ MATRIX OF D-ARABINITOL

i	j	G_{ij}	i	j	G_{ij}	i	j	G_{ij}	i	j	G_{ij}
24	32	-0.043751	24	36	-0.060522	24	37	-0.118888	24	38	0.019690
24	39	-0.056027	24	43	-0.006701	24	44	0.030605	24	45	-0.055382
24	46	-0.003825	24	47	-0.005572	24	48	0.101631	24	49	-0.056702
24	52	0.011182	24	53	-0.045754	24	54	0.034801	24	56	0.034974
24	57	-0.001140	24	58	-0.004912	24	59	-0.007053	24	60	-0.004921
24	63	-0.045077	24	64	-0.002876	24	65	-0.012204	25	25	0.170444
25	26	-0.046130	25	27	0.023828	25	28	-0.023836	25	33	-0.019539
25	34	-0.010190	25	35	0.037117	25	40	-0.015065	25	41	-0.005967
25	42	-0.039649	25	43	-0.053711	25	44	0.029770	25	50	0.095870
25	51	-0.007976	25	55	-0.133455	25	57	-0.019120	25	58	-0.031825
25	59	-0.033138	25	61	-0.071759	25	62	0.012511	26	26	0.059829
26	27	-0.014101	26	28	0.023078	26	33	-0.032752	26	34	-0.031225
26	35	-0.032302	26	40	0.051374	26	41	0.049582	26	42	0.025164
26	43	0.053741	26	44	-0.029430	26	50	0.006546	26	51	0.004379
26	55	0.016308	26	57	0.016587	26	58	-0.010083	26	59	0.032451
26	61	-0.009527	26	62	0.006936	27	27	0.169728	27	28	-0.050949
27	29	-0.046583	27	30	-0.020993	27	35	-0.003966	27	36	0.023068
27	40	-0.047184	27	41	0.023458	27	42	-0.117686	27	43	0.000730
27	44	0.101618	27	45	0.021001	27	46	0.031041	27	51	-0.033292
27	52	-0.031988	27	57	-0.002526	27	58	0.020905	27	59	-0.041523
27	60	-0.033089	27	62	-0.004753	27	63	-0.015270	28	28	0.169291
28	29	-0.020189	28	30	0.021261	28	35	0.018019	28	36	-0.012611
28	40	0.032176	28	41	-0.007416	28	42	0.024699	28	43	0.101989
28	44	-0.010199	28	45	-0.116132	28	46	-0.049213	28	51	0.033064
28	52	-0.007058	28	57	-0.038264	28	58	0.002807	28	59	0.005140
28	60	0.045907	28	62	-0.013253	28	63	-0.166902	29	29	0.162993
29	30	0.094208	29	31	-0.030042	29	32	-0.025342	29	36	-0.002369
29	37	0.029940	29	43	0.017689	29	44	-0.114038	29	45	-0.000094
29	46	-0.057285	29	47	-0.053384	29	48	-0.011259	29	49	0.029912
29	52	0.085044	29	53	-0.011536	29	57	-0.042133	29	58	-0.004999
29	59	-0.004890	29	60	0.041258	29	63	0.124232	29	64	-0.014255
30	30	0.166181	30	31	-0.013642	30	32	-0.046304	30	36	0.040877
30	37	-0.011052	30	43	0.028194	30	44	-0.055418	30	45	-0.039299
30	46	-0.009398	30	47	-0.112224	30	48	0.016346	30	49	0.021388
30	52	0.007860	30	53	-0.075395	30	57	-0.031886	30	58	-0.036439
30	59	0.003045	30	60	0.004991	30	63	0.021080	30	64	-0.039611
31	31	0.059302	31	32	0.043648	31	37	-0.029086	31	38	0.013804
31	39	-0.025953	31	45	0.020994	31	46	0.057909	31	47	0.031190
31	48	0.056952	31	49	-0.044999	31	53	-0.011840	31	54	0.011868
31	56	-0.032796	31	58	0.032199	31	59	-0.004086	31	60	0.001585
31	64	0.006897	31	65	-0.023838	32	32	0.171354	32	37	0.024504
32	38	0.006323	32	39	-0.011909	32	45	0.030308	32	46	0.027735
32	47	0.098324	32	48	0.013218	32	49	-0.010045	32	53	0.032762
32	54	-0.021537	32	56	-0.145971	32	58	0.035150	32	59	0.046471
32	60	0.007260	32	64	0.014182	32	65	0.000312	33	33	1.017846
33	34	0.003697	33	40	-0.479126	33	41	-0.146827	33	42	0.033166
33	50	-0.027274	33	55	-0.426059	33	57	0.733543	33	58	-0.001071
33	61	-0.080681	34	34	1.009708	34	40	-0.142412	34	41	-0.431944
34	42	-0.058323	34	50	-0.080427	34	55	-0.465123	34	57	-0.761473
34	58	-0.060622	34	61	0.166854	35	35	0.950438	35	40	0.014754
35	41	-0.057740	35	42	-0.339650	35	43	-0.397149	35	44	0.035607
35	51	0.095874	35	57	-0.748823	35	58	0.728262	35	59	-0.009964
35	62	-0.012835	36	36	0.962795	36	43	0.038471	36	44	-0.439754

TABLE XXIX (Continued)

$\underset{\sim}{G}$ MATRIX OF D-ARABINITOL

i	j	G_{ij}	i	j	G_{ij}	i	j	G_{ij}	i	j	G_{ij}
36	45	-0.348798	36	46	0.017682	36	52	-0.084550	36	57	-0.009260
36	58	0.697233	36	59	-0.744488	36	60	0.009948	36	63	0.045913
37	37	0.962902	37	45	0.029916	37	46	-0.424018	37	47	-0.388824
37	48	-0.060737	37	49	0.035616	37	53	0.096635	37	58	0.000147
37	59	0.714899	37	60	-0.692710	37	64	0.027155	38	38	0.984578
38	39	0.011198	38	47	0.036734	38	48	-0.386096	38	49	-0.127629
38	54	0.090515	38	56	-0.370158	38	59	0.057077	38	60	0.751095
38	65	-0.016233	39	39	1.004078	39	47	0.035480	39	48	-0.136675
39	49	-0.476954	39	54	-0.074096	39	56	-0.287508	39	59	0.010704
39	60	-0.697488	39	65	0.017791	40	40	1.005621	40	41	0.016257
40	42	0.102425	40	43	0.030130	40	44	-0.025376	40	50	0.049939
40	51	0.029663	40	55	-0.381374	40	57	0.030999	40	58	0.041880
40	59	0.035810	40	61	-0.883424	40	62	0.007115	41	41	1.005624
41	42	-0.062797	41	43	0.028557	41	44	-0.006559	41	50	0.020801
41	51	-0.022668	41	55	-0.381375	41	57	-0.011163	41	58	-0.004554
41	59	-0.000778	41	61	0.010768	41	62	-0.021751	42	42	0.961941
42	43	-0.494651	42	44	-0.052465	42	50	0.006793	42	51	0.019059
42	55	0.022945	42	57	0.024539	42	58	-0.677193	42	59	0.047364
42	61	-0.041528	42	62	0.801825	43	43	0.964191	43	44	-0.042854
43	45	-0.054704	43	46	-0.023618	43	51	0.036714	43	52	-0.005746
43	57	0.669692	43	58	-0.001519	43	59	0.038176	43	60	0.031837
43	62	-0.777726	43	63	-0.028856	44	44	0.961364	44	45	-0.450510
44	46	0.028607	44	51	-0.004742	44	52	-0.049621	44	57	0.035298
44	58	0.014564	44	59	0.686929	44	60	-0.050154	44	62	-0.013704
44	63	-0.818866	45	45	0.959213	45	46	0.101907	45	47	0.015909
45	48	-0.003224	45	49	-0.020735	45	52	0.012890	45	53	0.025767
45	57	0.048800	45	58	-0.686044	45	59	0.003846	45	60	-0.044638
45	63	0.880701	45	64	-0.014850	46	46	0.961130	46	47	-0.423729
46	48	0.040289	46	49	-0.057937	46	52	-0.019922	46	53	0.001677
46	57	0.035622	46	58	0.047963	46	59	0.003456	46	60	0.669972
46	63	0.023290	46	64	-0.801116	47	47	0.953086	47	48	-0.034761
47	49	-0.047091	47	53	0.041077	47	54	-0.004932	47	56	-0.065035
47	58	0.043649	47	59	-0.704027	47	60	0.006037	47	64	0.821271
47	65	-0.013102	48	48	1.005627	48	49	-0.013667	48	53	-0.027697
48	54	0.043322	48	56	-0.532228	48	58	0.005034	48	59	0.002669
48	60	-0.009120	48	64	-0.030566	48	65	-0.813171	49	49	1.005622
49	53	-0.000597	49	54	-0.054338	49	56	-0.532224	49	58	-0.031953
49	59	-0.040337	49	60	0.002349	49	64	0.016481	49	65	-0.008709
50	50	1.225039	50	55	-0.064670	50	57	-0.010945	50	58	-0.003838
50	61	-0.096548	51	51	1.222098	51	57	0.041976	51	58	-0.048763
51	59	0.023943	51	62	-0.011959	52	52	1.222092	52	57	-0.017520
52	58	0.044037	52	59	-0.022942	52	60	0.018177	52	63	0.049379
53	53	1.220910	53	58	0.023591	53	59	-0.028459	53	60	0.047262
53	64	0.029669	54	54	1.221735	54	56	0.025259	54	59	0.014502
54	60	-0.055793	54	65	-0.013907	55	55	1.834797	55	57	0.003215
55	58	0.059266	55	61	0.892358	56	56	1.867546	56	59	-0.059710
56	60	-0.009290	56	65	0.827069	57	57	2.884469	57	58	-0.547828
57	59	0.022504	57	60	-0.042220	57	61	-0.480652	57	62	-0.401360
57	63	0.008291	58	58	1.963326	58	59	-0.517907	58	60	0.008488
58	61	-0.013653	58	62	-0.445242	58	63	-0.479380	58	64	-0.000455
59	59	1.927879	59	60	-0.472558	59	62	-0.000195	59	63	-0.332034
59	64	-0.509025	59	65	-0.023424	60	60	2.822545	60	63	-0.004752
60	64	-0.415781	60	65	-0.414290	61	61	2.497846	62	62	2.170375
63	63	2.405368	64	64	2.252611	65	65	2.188244	-1	0	0.0

APPENDIX II

DATA NECESSARY FOR THE COMPUTATION OF THE $\underset{\sim}{F}$ MATRIX

The information reported in this appendix is as follows:

TABLE XXX

DESCRIPTION OF THE INDEPENDENT FORCE CONSTANTS (Φ_{ij}) APPEARING IN TABLES XXXI-XXXIV

Φ_{ij}	Coordinate(s) Involved
	(Stretch)
1	CH(methylene)
2	CH(methine)
3	CC(methine)
4	CC(methylene)
5	CO(methine)
6	CO(methylene)
7	OH(methylene)
8	OH(methine)
	(Bend)
9	HCH(methylene)
10	HCC(methylene)
11	HCO(methylene)
12	HCO(methine)
13	HCC(methine)
14	COH(methine)
15	COH(methylene)
16	CCC(methine)
17	CCC(methylene)
18	CCO(methylene)
19	CCO(methine)
	(Torsion)
20	(X)CC(X)
21	($\overline{X}$)CO($\overline{X}$)
	(Stretch-Stretch)
22	Dummy parameter[a]
23	CO,CH
24	CC,CH
25	CC,CC
26	CC,CO
27	Dummy parameter
	(Stretch-Bend)
28	CC,CCH
29	CH,CCH
30	CC,CCO
31	CO,CCO
32	CH,HCO

Φ_{ij}	Coordinate(s) Involved
	(Stretch-Bend)
33	CC,CCC
34	CH,HCH
35	CO,COH
36	OH,COH
37	CO,HCO
38	Dummy parameter
39	Dummy parameter
	(Bend-Bend)
40	($\underline{H}$)CC($\underline{H}$)gauche
41	($\underline{H}$)CC($\underline{H}$)trans
42	($\underline{C}$)CC($\underline{C}$)trans
43	($\underline{C}$)CC($\underline{C}$)gauche
44	($\underline{O}$)CC($\underline{O}$)gauche
45	($\underline{O}$)CC($\underline{O}$)trans
46	CCO,CCO(common CO)
47	CCO,CCC(common CC)
48	($\underline{H}$)CC($\underline{C}$)gauche
49	($\underline{H}$)CC($\underline{C}$)trans
50	($\underline{H}$)CC($\underline{O}$)gauche
51	Dummy parameter
52	HCC,CCO(common CC)
53	HCO,HCO(common CO)
54	HCO,HCH(common CH)
55	HCO,HCC(common CH)
56	CCO,COH(common CO)
57	($\underline{H}$)CO($\underline{H}$)gauche
58	($\underline{H}$)CO($\underline{H}$)trans
59	HCO,CCO(common CO)
60	HCC,CCC(common CC)
61	HCH,HCC(common CH)
62	($\underline{C}$)CC($\underline{O}$)trans
63	($\underline{C}$)CC($\underline{O}$)gauche
64	($\underline{C}$)CO($\underline{H}$)gauche

[a] Variable constant having a value of 0.0 in $\underset{\sim}{Z}$ matrix.

TABLE XXXI

THE $\underset{\sim}{Z}$ MATRIX FOR XYLITOL

i^a	j	Φ_{ij}		i^a	j	Φ_{ij}		i^a	j	Φ_{ij}		i^a	j	Φ_{ij}	
1	1	4	1.000000	1	2	25	1.000000	1	5	26	1.000000	1	6	26	1.000000
1	10	24	1.000000	1	11	24	1.000000	1	12	24	1.000000	1	22	33	1.000000
1	25	30	1.000000	1	26	30	1.000000	1	40	28	1.000000	1	41	28	1.000000
1	42	28	1.000000	2	2	3	1.000000	2	3	25	1.000000	2	6	26	1.000000
2	7	26	1.000000	2	12	24	1.000000	2	13	24	1.000000	2	22	33	1.000000
2	23	33	1.000000	2	27	30	1.000000	2	28	30	1.000000	2	43	28	1.000000
2	44	28	1.000000	3	3	3	1.000000	3	4	25	1.000000	3	7	26	1.000000
3	8	26	1.000000	3	13	24	1.000000	3	14	24	1.000000	3	23	33	1.000000
3	24	33	1.000000	3	29	30	1.000000	3	30	30	1.000000	3	45	28	1.000000
3	46	28	1.000000	4	4	4	1.000000	4	8	26	1.000000	4	9	26	1.000000
4	14	24	1.000000	4	15	24	1.000000	4	16	24	1.000000	4	24	33	1.000000
4	31	30	1.000000	4	32	30	1.000000	4	47	28	1.000000	4	48	28	1.000000
4	49	28	1.000000	5	5	6	1.000000	5	10	23	1.000000	5	11	23	1.000000
5	17	27	1.000000	5	25	31	1.000000	5	33	37	1.000000	5	34	37	1.000000
5	50	35	1.000000	6	6	5	1.000000	6	12	23	1.000000	6	18	27	1.000000
6	26	31	1.000000	6	27	31	1.000000	6	35	37	1.000000	6	51	35	1.000000
7	7	5	1.000000	7	13	23	1.000000	7	19	27	1.000000	7	28	31	1.000000
7	29	31	1.000000	7	36	37	1.000000	7	52	35	1.000000	8	8	5	1.000000
8	14	23	1.000000	8	20	27	1.000000	8	30	31	1.000000	8	31	31	1.000000
8	37	37	1.000000	8	53	35	1.000000	9	9	6	1.000000	9	15	23	1.000000
9	16	23	1.000000	9	21	27	1.000000	9	32	31	1.000000	9	38	37	1.000000
9	39	37	1.000000	9	54	35	1.000000	10	10	1	1.000000	10	11	22	1.000000
10	33	32	1.000000	10	40	29	1.000000	10	55	34	1.000000	11	11	1	1.000000
11	34	32	1.000000	11	41	29	1.000000	11	55	34	1.000000	12	12	2	1.000000
12	35	32	1.000000	12	42	29	1.000000	12	43	29	1.000000	13	13	2	1.000000
13	36	32	1.000000	13	44	29	1.000000	13	45	29	1.000000	14	14	2	1.000000
14	37	32	1.000000	14	46	29	1.000000	14	47	29	1.000000	15	15	1	1.000000
15	16	22	1.000000	15	38	32	1.000000	15	48	29	1.000000	15	56	34	1.000000
16	16	1	1.000000	16	39	32	1.000000	16	49	29	1.000000	16	56	34	1.000000
17	17	7	1.000000	17	50	36	1.000000	18	18	8	1.000000	18	51	36	1.000000
19	19	8	1.000000	19	52	36	1.000000	20	20	8	1.000000	20	53	36	1.000000
21	21	7	1.000000	21	54	36	1.000000	22	22	17	1.000000	22	23	42	1.000000
22	25	62	1.000000	22	26	47	1.000000	22	27	47	1.000000	22	28	63	1.000000
22	40	48	1.000000	22	41	48	1.000000	22	42	60	1.000000	22	43	60	1.000000
22	44	48	1.000000	23	23	16	1.000000	23	24	43	1.000000	23	27	63	1.000000
23	28	47	1.000000	23	29	47	1.000000	23	30	62	1.000000	23	43	48	1.000000
23	44	60	1.000000	23	45	60	1.000000	23	46	48	1.000000	24	24	17	1.000000
24	29	62	1.000000	24	30	47	1.000000	24	31	47	1.000000	24	32	62	1.000000
24	45	48	1.000000	24	46	60	1.000000	24	47	60	1.000000	24	48	48	1.000000
24	49	48	1.000000	25	25	18	1.000000	25	26	44	1.000000	25	33	59	1.0 0 0
25	34	59	1.000000	25	40	52	1.000000	25	41	52	1.000000	25	42	50	1.000000
25	50	56	1.000000	26	26	19	1.000000	26	27	46	1.000000	26	35	59	1.000000
26	40	51	1.000000	26	41	51	1.000000	26	42	52	1.000000	26	51	56	1.000000
27	27	19	1.000000	27	28	44	1.000000	27	35	59	1.000000	27	43	52	1.000000

TABLE XXXI (Continued)

THE Z MATRIX FOR XYLITOL

i^a	j	Φ_{ij}	i^a	j	Φ_{ij}	i^a	j	Φ_{ij}	i^a	j	Φ_{ij}
27	44	51 1.000000	27	51	64 1.000000	28	28	19 1.000000	28	29	46 1.000000
28	36	59 1.000000	28	43	51 1.000000	28	44	52 1.000000	28	52	56 1.000000
29	29	19 1.000000	29	30	44 1.000000	29	36	59 1.000000	29	45	52 1.000000
29	46	50 1.000000	29	52	64 1.000000	30	30	19 1.000000	30	31	46 1.000000
30	37	59 1.000000	30	45	50 1.000000	30	46	52 1.000000	30	53	64 1.000000
31	31	19 1.000000	31	32	44 1.000000	31	37	59 1.000000	31	47	52 1.000000
31	48	5 1.000000	31	49	51 1.000000	31	53	56 1.000000	32	32	18 1.000000
32	38	59 1.000000	32	39	59 1.000000	32	47	50 1.000000	32	48	52 1.000000
32	49	52 1.000000	32	54	64 1.000000	33	33	11 1.000000	33	34	53 1.000000
33	40	55 1.000000	33	50	57 1.000000	33	55	54 1.000000	34	34	11 1.000000
34	41	55 1.000000	34	50	57 1.000000	34	55	54 1.000000	35	35	12 1.000000
35	42	55 1.000000	35	43	55 1.000000	35	51	57 1.000000	36	36	12 1.000000
36	44	55 1.000000	36	45	55 1.000000	36	52	57 1.000000	37	37	12 1.000000
37	46	55 1.000000	37	47	55 1.000000	37	53	57 1.000000	38	38	11 1.000000
38	39	53 1.000000	38	48	55 1.000000	38	54	57 1.000000	38	56	54 1.000000
39	39	11 1.000000	39	49	55 1.000000	39	54	58 1.000000	39	56	54 1.000000
40	40	10 1.000000	40	41	38 1.000000	40	42	40 1.000000	40	55	61 1.000000
41	41	10 1.000000	41	42	41 1.000000	41	55	61 1.000000	42	42	13 1.000000
42	43	39 1.000000	43	43	13 1.000000	43	44	40 1.000000	44	44	13 1.000000
44	45	39 1.000000	45	45	13 1.000000	45	46	41 1.000000	46	46	13 1.000000
46	47	39 1.000000	47	47	13 1.000000	47	48	41 1.000000	47	49	40 1.000000
48	48	10 1.000000	48	49	38 1.000000	48	56	61 1.000000	49	49	10 1.000000
49	56	61 1.000000	50	50	15 1.000000	51	51	14 1.000000	52	52	14 1.000000
53	53	14 1.000000	54	54	15 1.000000	55	55	9 1.000000	56	56	9 1.000000
57	57	20 1.000000	58	58	20 1.000000	59	59	20 1.000000	60	60	20 1.000000
61	61	21 1.000000	62	62	21 1.000000	63	63	21 1.000000	64	64	21 1.000000
65	65	21 1.000000	-2								

[a] i and j denote row and column, respectively; Φ_{ij} = force constant associated with the Z_{ij} element.

TABLE XXXII

THE $\underset{\sim}{Z}$ MATRIX FOR RIBITOL

i^a	j	Φ_{ij}	i^a	j	Φ_{ij}	i^a	j	Φ_{ij}	i^a	j	Φ_{ij}
1	1	4 1.000000	1	2	25 1.000000	1	5	26 1.000000	1	6	26 1.00000
1	10	24 1.000000	1	11	24 1.000000	1	12	24 1.000000	1	22	33 1.000000
1	25	30 1.000000	1	26	30 1.000000	1	40	28 1.000000	1	41	28 1.000000
1	42	28 1.000000	2	2	3 1.000000	2	3	25 1.000000	2	6	26 1.000000
2	7	26 1.000000	2	12	24 1.000000	2	13	24 1.000000	2	22	33 1.000000
2	23	33 1.000000	2	27	30 1.000000	2	28	30 1.000000	2	43	28 1.000000
2	44	28 1.000000	3	3	3 1.000000	3	4	25 1.000000	3	7	26 1.000000
3	8	26 1.000000	3	13	24 1.000000	3	14	24 1.000000	3	23	33 1.000000
3	24	33 1.000000	3	29	30 1.000000	3	30	30 1.000000	3	45	28 1.000000
3	46	28 1.000000	4	4	4 1.000000	4	8	26 1.000000	4	9	26 1.000000
4	14	24 1.000000	4	15	24 1.000000	4	16	24 1.000000	4	24	33 1.000000
4	31	30 1.000000	4	32	30 1.000000	4	47	28 1.000000	4	48	28 1.000000
4	49	28 1.000000	5	5	6 1.000000	5	10	23 1.000000	5	11	23 1.000000
5	17	27 1.000000	5	25	31 1.000000	5	33	37 1.000000	5	34	37 1.000000
5	50	35 1.000000	6	6	5 1.000000	6	12	23 1.000000	6	18	27 1.000000
6	26	31 1.000000	6	27	31 1.000000	6	35	37 1.000000	6	51	35 1.000000
7	7	5 1.000000	7	13	23 1.000000	7	19	27 1.000000	7	28	31 1.000000
7	29	31 1.000000	7	36	37 1.000000	7	52	35 1.000000	8	8	5 1.000000
8	14	23 1.000000	8	20	27 1.000000	8	30	31 1.000000	8	31	31 1.000000
8	37	37 1.000000	8	53	35 1.000000	9	9	6 1.000000	9	15	23 1.000000
9	16	23 1.000000	9	21	27 1.000000	9	32	31 1.000000	9	38	37 1.000000
9	39	37 1.000000	9	54	35 1.000000	10	10	1 1.000000	10	11	22 1.000000
10	33	32 1.000000	10	40	29 1.000000	10	55	34 1.000000	11	11	1 1.000000
11	34	32 1.000000	11	41	29 1.000000	11	55	34 1.000000	12	12	2 1.000000
12	35	32 1.000000	12	42	29 1.000000	12	43	29 1.000000	13	13	2 1.000000
13	36	32 1.000000	13	44	29 1.000000	13	45	29 1.000000	14	14	2 1.000000
14	37	32 1.000000	14	46	29 1.000000	14	47	29 1.000000	15	15	1 1.000000
15	16	22 1.000000	15	38	32 1.000000	15	48	29 1.000000	15	56	34 1.000000
16	16	1 1.000000	16	39	32 1.000000	16	49	29 1.000000	16	56	34 1.000000
17	17	7 1.000000	17	50	36 1.000000	18	18	8 1.000000	18	51	36 1.000000
19	19	8 1.000000	19	52	36 1.000000	20	20	8 1.000000	20	53	36 1.000000
21	21	7 1.000000	21	54	36 1.000000	22	22	17 1.000000	22	23	42 1.000000
22	25	63 1.000000	22	26	47 1.000000	22	27	47 1.000000	22	28	63 1.000000
22	40	48 1.000000	22	41	49 1.000000	22	42	60 1.000000	22	43	60 1.000000
22	44	48 1.000000	23	23	16 1.000000	23	24	43 1.000000	23	27	63 1.000000
23	28	47 1.000000	23	29	47 1.000000	23	30	62 1.000000	23	43	48 1.000000
23	44	60 1.000000	23	45	60 1.000000	23	46	48 1.000000	24	24	17 1.000000
24	29	63 1.000000	24	30	47 1.000000	24	31	47 1.000000	24	32	62 1.000000
24	45	49 1.000000	24	46	60 1.000000	24	47	60 1.000000	24	48	48 1.000000
24	49	48 1.000000	25	25	18 1.000000	25	26	44 1.000000	25	33	59 1.000000
25	34	59 1.000000	25	40	52 1.000000	25	41	52 1.000000	25	42	51 1.000000
25	50	56 1.000000	26	26	19 1.000000	26	27	46 1.000000	26	35	59 1.000000
26	40	51 1.000000	26	41	50 1.000000	26	42	52 1.000000	26	51	64 1.000000
27	27	19 1.000000	27	28	45 1.000000	27	35	59 1.000000	27	43	52 1.000000
27	44	50 1.000000	27	51	64 1.000000	28	28	19 1.000000	28	29	46 1.000000
28	36	59 1.000000	28	43	50 1.000000	28	44	52 1.000000	28	52	56 1.000000
29	29	19 1.000000	29	30	44 1.000000	29	36	59 1.000000	29	45	52 1.000000
29	46	51 1.000000	29	52	64 1.000000	30	30	19 1.000000	30	31	46 1.000000
30	37	59 1.000000	30	45	50 1.000000	30	46	52 1.000000	30	53	64 1.000000
31	31	19 1.000000	31	32	44 1.000000	31	37	59 1.000000	31	47	52 1.000000
31	48	50 1.000000	31	49	51 1.000000	31	53	56 1.000000	32	32	18 1.000000

TABLE XXXII (Continued)

THE $\underset{\sim}{Z}$ MATRIX FOR RIBITOL

i^a	j	Φ_{ij}		i^a	j	Φ_{ij}		i^a	j	Φ_{ij}		i^a	j	Φ_{ij}	
32	38	59	1.000000	32	39	59	1.000000	32	47	50	1.000000	32	48	52	1.000000
32	49	52	1.000000	32	54	56	1.000000	33	33	11	1.000000	33	34	53	1.000000
33	40	55	1.000000	33	50	57	1.000000	33	55	54	1.000000	34	34	11	1.000000
34	41	55	1.000000	34	50	57	1.000000	34	55	54	1.000000	35	35	12	1.000000
35	42	55	1.000000	35	43	55	1.000000	35	51	58	1.000000	36	36	12	1.000000
36	44	55	1.000000	36	45	55	1.000000	36	52	57	1.000000	37	37	12	1.000000
37	46	55	1.000000	37	47	55	1.000000	37	53	57	1.000000	38	38	11	1.000000
38	39	53	1.000000	38	48	55	1.000000	38	54	57	1.000000	38	56	54	1.000000
39	39	11	1.000000	39	49	55	1.000000	39	54	57	1.000000	39	56	54	1.000000
40	40	10	1.000000	40	41	38	1.000000	40	42	40	1.000000	40	55	61	1.000000
41	41	10	1.000000	41	42	40	1.000000	41	55	61	1.000000	42	42	13	1.000000
42	43	39	1.000000	43	43	13	1.000000	43	44	41	1.000000	44	44	13	1.000000
44	45	39	1.000000	45	45	13	1.000000	45	46	40	1.000000	46	46	13	1.000000
46	47	39	1.000000	47	47	13	1.000000	47	48	41	1.000000	47	49	40	1.000000
48	48	10	1.000000	48	49	38	1.000000	48	56	61	1.000000	49	49	10	1.000000
49	56	61	1.000000	50	50	15	1.000000	51	51	14	1.000000	52	52	14	1.000000
53	53	14	1.000000	54	54	15	1.000000	55	55	9	1.000000	56	56	9	1.000000
57	57	20	1.000000	58	58	20	1.000000	59	59	20	1.000000	60	60	20	1.000000
61	61	21	1.000000	62	62	21	1.000000	63	63	21	1.000000	64	64	21	1.000000
65	65	21	1.000000	-2											

[a] i and j denote row and column, respectively; Φ_{ij} = force constant associated with the Z_{ij} element.

TABLE XXXIII

THE Z MATRIX FOR ERYTHRITOL

i^a	j	Φ_{ij}		i^a	j	Φ_{ij}		i^a	j	Φ_{ij}		i^a	j	Φ_{ij}	
1	1	4	1.000000	1	2	25	1.000000	1	4	26	1.000000	1	5	26	1.000000
1	8	24	1.000000	1	9	24	1.000000	1	10	24	1.000000	1	18	33	1.000000
1	20	30	1.000000	1	21	30	1.000000	1	32	28	1.000000	1	33	28	1.000000
1	34	28	1.000000	2	2	3	1.000000	2	3	25	1.000000	2	5	26	1.000000
2	6	26	1.000000	2	10	24	1.000000	2	11	24	1.000000	2	18	33	1.000000
2	19	33	1.000000	2	22	30	1.000000	2	23	30	1.000000	2	35	28	1.000000
2	36	28	1.000000	3	3	4	1.000000	3	6	26	1.000000	3	7	26	1.000000
3	11	24	1.000000	3	12	24	1.000000	3	13	24	1.000000	3	19	33	1.000000
3	24	30	1.000000	3	25	30	1.000000	3	37	28	1.000000	3	38	28	1.000000
3	39	28	1.000000	4	4	6	1.000000	4	8	23	1.000000	4	9	23	1.000000
4	14	27	1.000000	4	20	31	1.000000	4	26	37	1.000000	4	27	37	1.000000
4	40	35	1.000000	5	5	5	1.000000	5	10	23	1.000000	5	15	27	1.000000
5	21	31	1.000000	5	22	31	1.000000	5	28	37	1.000000	5	41	35	1.000000
6	6	5	1.000000	6	11	23	1.000000	6	16	27	1.000000	6	23	31	1.000000
6	24	31	1.000000	6	29	37	1.000000	6	42	35	1.000000	7	7	6	1.000000
7	12	23	1.000000	7	13	23	1.000000	7	17	27	1.000000	7	25	31	1.000000
7	30	37	1.000000	7	31	37	1.000000	7	43	35	1.000000	8	8	1	1.000000
8	9	22	1.000000	8	26	32	1.000000	8	32	29	1.000000	8	44	34	1.000000
9	9	1	1.000000	9	27	32	1.000000	9	33	29	1.000000	9	44	34	1.000000
10	10	2	1.000000	10	28	32	1.000000	10	34	29	1.000000	10	35	29	1.000000
11	11	2	1.000000	11	29	32	1.000000	11	36	29	1.000000	11	37	29	1.000000
12	12	1	1.000000	12	13	22	1.000000	12	30	32	1.000000	12	38	29	1.000000
12	45	34	1.000000	13	13	1	1.000000	13	31	32	1.000000	13	39	29	1.000000
13	45	34	1.000000	14	14	7	1.000000	14	40	36	1.000000	15	15	8	1.000000
15	41	36	1.000000	16	16	8	1.000000	16	42	36	1.000000	17	17	7	1.000000
17	43	36	1.000000	18	18	17	1.000000	18	19	42	1.000000	18	20	63	1.000000
18	21	47	1.000000	18	22	47	1.000000	18	23	63	1.000000	18	32	49	1.000000
18	33	48	1.000000	18	34	60	1.000000	18	35	60	1.000000	18	36	48	1.000000
19	19	17	1.000000	19	22	63	1.000000	19	23	47	1.000000	19	24	47	1.000000
19	25	63	1.000000	19	35	48	1.000000	19	36	60	1.000000	19	37	60	1.000000
19	38	48	1.000000	19	39	49	1.000000	20	20	18	1.000000	20	21	44	1.000000
20	26	59	1.000000	20	27	59	1.000000	20	32	52	1.000000	20	33	52	1.000000
20	34	51	1.000000	20	40	56	1.000000	21	21	19	1.000000	21	22	46	1.000000
21	28	59	1.000000	21	32	50	1.000000	21	33	51	1.000000	21	34	52	1.000000
21	41	64	1.000000	22	22	19	1.000000	22	23	45	1.000000	22	28	59	1.000000
22	35	52	1.000000	22	36	50	1.000000	22	41	64	1.000000	23	23	19	1.000000
23	24	46	1.000000	23	29	59	1.000000	23	35	50	1.000000	23	36	52	1.000000
23	42	64	1.000000	24	24	19	1.000000	24	25	44	1.000000	24	29	59	1.000000
24	37	52	1.000000	24	38	51	1.000000	24	39	50	1.000000	24	42	64	1.000000
25	25	18	1.000000	25	30	59	1.000000	25	31	59	1.000000	25	37	51	1.000000
25	38	52	1.000000	25	39	52	1.000000	25	43	56	1.000000	26	26	11	1.000000
26	27	53	1.000000	26	32	55	1.000000	26	40	57	1.000000	26	44	54	1.000000
27	27	11	1.000000	27	33	55	1.000000	27	40	57	1.000000	27	44	54	1.000000

TABLE XXXIII (Continued)

THE $\underset{\sim}{Z}$ MATRIX FOR ERYTHRITOL

i^a	j	Φ_{ij}		i^a	j	Φ_{ij}		i^a	j	Φ_{ij}		i^a	j	Φ_{ij}	
28	28	12	1.000000	28	34	55	1.000000	28	35	55	1.000000	28	41	58	1.000000
29	29	12	1.000000	29	36	55	1.000000	29	37	55	1.000000	29	42	58	1.000000
30	30	11	1.000000	30	31	53	1.000000	30	38	55	1.000000	30	43	57	1.000000
30	45	54	1.000000	31	31	11	1.000000	31	39	55	1.000000	31	43	57	1.000000
31	45	54	1.000000	32	32	10	1.000000	32	33	38	1.000000	32	34	40	1.000000
32	44	61	1.000000	33	33	10	1.000000	33	34	40	1.000000	33	44	61	1.000000
34	34	13	1.000000	34	35	39	1.000000	35	35	13	1.000000	35	36	41	1.000000
36	36	13	1.000000	36	37	39	1.000000	37	37	13	1.000000	37	38	40	1.000000
37	39	40	1.000000	38	38	10	1.000000	38	39	38	1.000000	38	45	61	1.000000
39	39	10	1.000000	39	45	61	1.000000	40	40	15	1.000000	41	41	14	1.000000
42	42	14	1.000000	43	43	15	1.000000	44	44	9	1.000000	45	45	9	1.000000
46	46	20	1.000000	47	47	20	1.000000	48	48	20	1.000000	49	49	21	1.000000
50	50	21	1.000000	51	51	21	1.000000	52	52	21	1.000000	-2			

[a] i and j denote row and column, respectively; Φ_{ij} = force constant associated with the Z_{ij} element.

TABLE XXXIV

THE $\underset{\sim}{Z}$ MATRIX FOR D-ARABINITOL

i^a	j	Φ_{ij}		i^a	j	Φ_{ij}		i^a	j	Φ_{ij}		i^a	j	Φ_{ij}	
1	1	4	1.000000	1	2	25	1.000000	1	5	26	1.000000	1	6	26	1.000000
1	10	24	1.000000	1	11	24	1.000000	1	12	24	1.000000	1	22	33	1.000000
1	25	30	1.000000	1	26	30	1.000000	1	40	28	1.000000	1	41	28	1.000000
1	42	28	1.000000	2	2	3	1.000000	2	3	25	1.000000	2	6	26	1.000000
2	7	26	1.000000	2	12	24	1.000000	2	13	24	1.000000	2	22	33	1.000000
2	23	33	1.000000	2	27	30	1.000000	2	28	30	1.000000	2	43	28	1.000000
2	44	28	1.000000	3	3	3	1.000000	3	4	25	1.000000	3	7	26	1.000000
3	8	26	1.000000	3	13	24	1.000000	3	14	24	1.000000	3	23	33	1.000000
3	24	33	1.000000	3	29	30	1.000000	3	30	30	1.000000	3	45	28	1.000000
3	46	28	1.000000	4	4	4	1.000000	4	8	26	1.000000	4	9	26	1.000000
4	14	24	1.000000	4	15	24	1.000000	4	16	24	1.000000	4	24	33	1.000000
4	31	30	1.000000	4	32	30	1.000000	4	47	28	1.000000	4	48	28	1.000000
4	49	28	1.000000	5	5	6	1.000000	5	10	23	1.000000	5	11	23	1.000000
5	17	27	1.000000	5	25	31	1.000000	5	33	37	1.000000	5	34	37	1.000000
5	50	35	1.000000	6	6	5	1.000000	6	12	23	1.000000	6	18	27	1.000000
6	26	31	1.000000	6	27	31	1.000000	6	35	37	1.000000	6	51	35	1.000000
7	7	5	1.000000	7	13	23	1.000000	7	19	27	1.000000	7	28	31	1.000000
7	29	31	1.000000	7	36	37	1.000000	7	52	35	1.000000	8	8	5	1.000000
8	14	23	1.000000	8	20	27	1.000000	8	30	31	1.000000	8	31	31	1.000000
8	37	37	1.000000	8	53	35	1.000000	9	9	6	1.000000	9	15	23	1.000000
9	16	23	1.000000	9	21	27	1.000000	9	32	31	1.000000	9	38	37	1.000000
9	39	37	1.000000	9	54	35	1.000000	10	10	1	1.000000	10	11	22	1.000000
10	33	32	1.000000	10	40	29	1.000000	10	55	34	1.000000	11	11	1	1.000000
11	34	32	1.000000	11	41	29	1.000000	11	55	34	1.000000	12	12	2	1.000000
12	35	32	1.000000	12	42	29	1.000000	12	43	29	1.000000	13	13	2	1.000000
13	36	32	1.000000	13	44	29	1.000000	13	45	29	1.000000	14	14	2	1.000000
14	37	32	1.000000	14	46	29	1.000000	14	47	29	1.000000	15	15	1	1.000000
15	16	22	1.000000	15	38	32	1.000000	15	48	29	1.000000	15	56	34	1.000000
16	16	1	1.000000	16	39	32	1.000000	16	49	29	1.000000	16	56	34	1.000000
17	17	7	1.000000	17	50	36	1.000000	18	18	8	1.000000	18	51	36	1.000000
19	19	8	1.000000	19	52	36	1.000000	20	20	8	1.000000	20	53	36	1.000000
21	21	7	1.000000	21	54	36	1.000000	22	22	17	1.000000	22	23	42	1.000000
22	25	63	1.000000	22	26	47	1.000000	22	27	47	1.000000	22	28	63	1.000000
22	40	49	1.000000	22	41	48	1.000000	22	42	60	1.000000	22	43	60	1.000000
22	44	48	1.000000	23	23	16	1.000000	23	24	42	1.000000	23	27	63	1.000000
23	28	47	1.000000	23	29	47	1.000000	23	30	63	1.000000	23	43	48	1.000000
23	44	60	1.000000	23	45	60	1.000000	23	46	48	1.000000	24	24	17	1.000000
24	29	63	1.000000	24	30	47	1.000000	24	31	47	1.000000	24	32	63	1.000000
24	45	48	1.000000	24	46	60	1.000000	24	47	60	1.000000	24	48	49	1.000000
24	49	48	1.000000	25	25	18	1.000000	25	26	45	1.000000	25	33	59	1.000000
25	34	59	1.000000	25	40	52	1.000000	25	41	52	1.000000	25	42	50	1.000000
25	50	56	1.000000	26	26	19	1.000000	26	27	46	1.000000	26	35	59	1.000000
26	40	50	1.000000	26	41	50	1.000000	26	42	52	1.000000	26	51	64	1.000000
27	27	19	1.000000	27	28	44	1.000000	27	35	59	1.000000	27	43	52	1.000000
27	44	51	1.000000	27	51	64	1.000000	28	28	19	1.000000	28	29	46	1.000000
28	36	59	1.000000	28	43	51	1.000000	28	44	52	1.000000	28	52	64	1.000000
29	29	19	1.000000	29	30	45	1.000000	29	36	59	1.000000	29	45	52	1.000000
29	46	50	1.000000	29	52	56	1.000000	30	30	19	1.000000	30	31	46	1.000000
30	37	59	1.000000	30	45	50	1.000000	30	46	52	1.000000	30	53	64	1.000000

TABLE XXXIV (Continued)

THE $\underset{\sim}{Z}$ MATRIX FOR D-ARABINITOL

i[a]	j	Φ_{ij}	i[a]	j	Φ_{ij}	i[a]	j	Φ_{ij}	i[a]	j	Φ_{ij}
31	31	19 1.000000	31	32	44 1.000000	31	37	59 1.000000	31	47	52 1.000000
31	48	50 1.000000	31	49	51 1.000000	31	53	64 1.000000	32	32	18 1.000000
32	38	59 1.000000	32	39	59 1.000000	32	47	51 1.000000	32	48	52 1.000000
32	49	52 1.000000	32	54	64 1.000000	33	33	11 1.000000	33	34	53 1.000000
33	40	55 1.000000	33	50	57 1.000000	33	55	54 1.000000	34	34	11 1.000000
34	41	55 1.000000	34	50	57 1.000000	34	55	54 1.000000	35	35	12 1.000000
35	42	55 1.000000	35	43	55 1.000000	35	51	58 1.000000	36	36	12 1.000000
36	44	55 1.000000	36	45	55 1.000000	36	52	57 1.000000	37	37	12 1.000000
37	46	55 1.000000	37	47	55 1.000000	37	53	58 1.000000	38	38	11 1.000000
38	39	53 1.000000	38	48	55 1.000000	38	54	58 1.000000	38	56	54 1.000000
39	39	11 1.000000	39	49	55 1.000000	39	54	57 1.000000	39	56	54 1.000000
40	40	10 1.000000	40	41	38 1.000000	40	42	40 1.000000	40	55	61 1.000000
41	41	10 1.000000	41	42	41 1.000000	41	55	61 1.000000	42	42	13 1.000000
42	43	39 1.000000	43	43	13 1.000000	43	44	40 1.000000	44	44	13 1.000000
44	45	39 1.000000	45	45	13 1.000000	45	46	41 1.000000	46	46	13 1.000000
46	47	39 1.000000	47	47	13 1.000000	47	48	40 1.000000	47	49	40 1.000000
48	48	10 1.000000	48	49	38 1.000000	48	56	61 1.000000	49	49	10 1.000000
49	56	61 1.000000	50	50	15 1.000000	51	51	14 1.000000	52	52	14 1.000000
53	53	14 1.000000	54	54	15 1.000000	55	55	9 1.000000	56	56	9 1.000000
57	57	20 1.000000	58	58	20 1.000000	59	59	20 1.000000	60	60	20 1.000000
61	61	21 1.000000	62	62	21 1.000000	63	63	21 1.000000	64	64	21 1.000000
65	65	21 1.000000	-2								

[a] i and j denote row and column, respectively; Φ_{ij} = force constant associated with the Z_{ij} element.

APPENDIX III

RESULTS OF THE ANALYSES

The information reported in this appendix is as follows:

TABLE XXXV

RIBITOL

DOMINANT INTERNAL COORDINATES AND POTENTIAL CONSTANTS

No.	Calc. Freq., cm^{-1}	Relative Contribution, %[a] Diagonal Force Constants[b]	Internal Coordinates[c]
1	3351.8	O'H(99)	O1H(99)
2	3351.8	O'H(99)	O5H(99)
3	3330.8	OH(99)	O2H(72) O3H(27)
4	3330.8	OH(99)	O4H(99)
5	3330.1	OH(99)	O3H(72) O2H(27)
6	2968.4	C'H(97)	C1H(50) C1H'(46)
7	2949.1	C'H(89) CH(8)	C5H'(50) C5H(38)
8	2934.0	CH(96)	C3H(50) C2H(45)
9	2922.8	CH(83) C'H(15)	C4H(81) C5H(14)
10	2914.7	CH(98)	C2H(50) C3H(47)
11	2901.7	C'H(91) CH(7)	C5H'(46) C5H(44)
12	2880.8	C'H(97)	C1H'(51) C1H(47)
13	1482.6	H'CH(47) HC'O(46)	HC5H(46) HC5O(25) HC'O(21)
14	1471.5	HC'H(55) HC'O(21) HC'C(6)	HC1H(54) H'CO(11) HC1O(10)
15	1452.0	HCC(30) HCO(18) HC'C(11) CO(13)	6CCH(22) HC4O(16) 8CCH(7) C4O(13)
16	1426.6	HCO(46) HCC(13) COH(12) CO(17)	HC2O(37) COH2(11) 1CCH(10) C2O(16)
17	1381.1	HCC(53) HC'C(13) HCO(12) CO(10)	5CCH(32) HC3O(11) 4CCH(8) 8CCH(8)
18	1368.1	HCC(63) HCO(17)	3CCH(25) 4CCH(16) HC4O(14) 2CCH(7) 6CCH(7) 5CCH(7)
19	1353.7	HCC(28) HC'C(26) HCO(15) HC'O(11) C'O(10)	CCH'(14) HC4O(13) 2CCH(11) 3CCH(9) 'CCH(8)
20	1331.4	HCO(20) COH(19) HC'C(19) HCC(10) CO(12)	COH4(18) HC3O(18) CCH'(14) C4O(11)
21	1312.5	HCC(30) HCO(26) HC'C(13) COH(10) C'OH(7)	HC4O(25) 7CCH(23) 8CCH(7)
22	1295.3	HCO(39) HC'C(16) HCC(13) CO(13)	HC2O(30) 1CCH(14) C2O(12) H'CO(10)
23	1292.3	HCO(47) HCC(17) COH(10) C'OH(7)	HC3O(37) COH4(8)

TABLE XXXV (Continued)

RIBITOL

DOMINANT INTERNAL COORDINATES AND POTENTIAL CONSTANTS

No.	Calc. Freq., cm^{-1}	Relative Contribution, %[a] Diagonal Force Constants[b]	Internal Coordinates[c]
24	1268.9	C'OH(54) HC'O(11) HCO(11) C'O(9)	COH1(45) COH5(9)
25	1265.0	C'OH(47) HC'O(25) HC'C(17) C'O(8)	COH5(34) HC'O(18) COH1(13) CCH'(13)
26	1252.5	HCC(29) HC'O(24) HC'C(19) COH(12) C'OH(5)	HC10(22) 'CCH(13) 7CCH(10) COH3(10)
27	1231.8	HC'O(51) HCC(12) COH(12) HC'C(11)	HC10(24) H'CO(15) COH3(10)
28	1213.8	HC'O(52) HC'C(26) COH(10)	HC50(32) 8CCH(18)
29	1202.1	COH(29) HC'C(22) HCO(16) HC'O(15) CO(15)	1CCH(16) COH2(15) COH3(13) HC'O(13) C30(12)
30	1154.0	CC(28) C'C(25) COH(16)	C3C4(22) C1C2(13) C4C5(12) COH3(13)
31	1138.5	C'C(27) CC(24) CO(11) HC'C(12)	C1C2(25) C2C3(22) C10(6) C30(5)
32	1084.8	HC'C(33) COH(31) CC(11)	COH4(30) CCH'(13) C3C4(10) 8CCH(11)
33	1073.2	C'C(34) CO(14) C'O(10) COH(25)	C1C2(17) C4C5(16) C20(12) COH2(24) 'CCH(17)
34	1057.8	C'C(27) CO(22) C'O(15)	C4C5(26) C50(15) C30(11) C3C4(10) COH3(12)
35	1046.8	CO(15) C'O(14) CC(13) C'OH(9)	C20(16) C10(13) C3C4(9) COH1(9)
36	1004.3	C'O(24) CC(22) CO(13) C'OH(12)	C2C3(19) C50(10) C30(11) C10(6) COH5(10)
37	969.2	CO(22) C'O(18) HC'C(25) HCC(10) C'OH(8) COH(8)	C50(17) C40(15) 8CCH(21) COH5(7)
38	935.7	CO(18) C'O(16) COH(22) HC'C(11) CC(10)	C10(14) C30(8) C2C3(8)
39	870.0	C'C(26) C'O(22) CO(12) C'OH(9)	C1C2(20) C10(21) C40(11) COH4(9) COH1(9)
40	852.3	CO(18) C'C(15) C'O(10) COH(13)	C30(17) C4C5(11) C10(9)
41	758.6	CCO(22) C'C(13) HCC(12)	C4C5(12) 5CCO(11) 6CCO(10)

TABLE XXXV (Continued)

RIBITOL

DOMINANT INTERNAL COORDINATES AND POTENTIAL CONSTANTS

No.	Calc. Freq., cm^{-1}	Relative Contribution, %[a] Diagonal Force Constants[b]	Internal Coordinates[c]
42	609.7	CC'O(34) CCO(12)	1CCO(33) 5CCO(9) C3CC(4)
43	524.0	CCO(37) CCC(10)	3CCO(27) C2CC(10)
44	490.6	CCO(28) C'CC(11) CC(27)	4CCO(20) C1CC(9) C2C3(21)
45	426.3	CC'O(39) CCO(21)	8CCO(37) 3CCO(6)
46	380.7	-CO-(53) CCO(30)	TC30(27) TC40(21) 6CCO(9) 4CCO(8) 3CCO(7)
47	347.0	-CO-(76)	TC10(44) TC30(17)
48	339.3	-CO-(80)	TC50(36) TC10(20) TC40(18)
49	333.4	-CO-(88)	TC20(79)
50	326.7	-CO-(83)	TC50(44) TC10(13) TC40(12)
51	305.5	-CO-(27) -CC-(15) CCO(12)	TCC1(13) TC40(10) 1CCO(9)
52	266.7	CCO(38) -CO-(23) -CC-(18) C'CC(7)	TC30(18) 5CCO(17) 4CCO(13) TCC4(10) TCC1(7) C1CC(7)
53	252.9	CCO(47) -CC-(13) C'CC(10)	6CCO(19) 7CCO(11) C3CC(8) 5CCO(7)
54	218.6	-CC-(48) CCO(24) CCC(11) C'CC(9)	TCC4(29) TCC1(17) C2CC(11) 3CCO(11)
55	192.3	-CC-(47) CCO(32) C'CC(19)	TCC4(24) C3CC(16) TCC2(13)
56	174.9	CCO(62) -CC-(21) HCC(15)	2CCO(26) 7CCO(14) C3CC(11) 3CCO(11) C2CC(9)
57	124.8	CCO(61) C'CC(52) -CC-(30)	C1CC(52) 2CCO(49) TCC1(22)
58	116.0	-CC-(58) CCO(35) C'CC(15)	TCC3(53) 7CCO(24) C3CC(15)
59	85.1	CCO(37) C'CC(36) -CC-(32)	C3CC(36) 7CCO(27) TCC2(23) C2CC(11)
60	71.4	-CC-(66) CCO(22) C'CC(10)	TCC2(39) TCC3(18) 7CCO(12)

[a] The contributions are relative and may total more than 100% due to the presence of negative off-diagonal interaction constants.

[b] The force constants given are described in Table V.

[c] Only the dominant coordinates are given. The individual coordinates for each molecule are coded in the manner described in Tables XIX-XXI.

TABLE XXXVI

XYLITOL

DOMINANT INTERNAL COORDINATES AND POTENTIAL CONSTANTS

No.	Calc. Freq., cm^{-1}	Relative Contribution, %[a] Diagonal Force Constants[b]	Internal Coordinates[c]
1	3351.6	O'H(99)	O1H(99)
2	3351.6	O'H(99)	O5H(99)
3	3330.4	OH(99)	O3H(98)
4	3330.4	OH(99)	O4H(99)
5	3330.4	OH(99)	O2H(98)
6	2966.9	C'H(94)	C1H(50) C1H'(44)
7	2963.9	C'H(93)	C5H'(49) C5H(44)
8	2934.2	CH(93)	C3H(46) C4H(46)
9	2922.9	CH(93)	C2H(90)
10	2914.1	CH(96)	C3H(51) C4H(43)
11	2884.3	C'H(95)	C5H'(48) C5H(47)
12	2882.7	C'H(96)	C1H'(48) C1H(47)
13	1463.3	HC'H(51) HC'O(33)	HC1H(47) H'CO(14) HC1O(12)
14	1462.5	HC'H(43) HC'O(43)	HC5H(37) HC5O(20) HC'O(18)
15	1439.6	HCC(36) HC'C(14) HCO(14) CO(16)	4CCH(17) 1CCH(12) 3CCH(11) HC2O(11) C2O(16)
16	1435.2	HCC(24) HC'C(20) HCO(15) CO(16)	6CCH(19) HC4O(15) 8CCH(15) HC5H(8) C4O(16)
17	1396.8	HCC(33) HC'C(17) HCO(15) HC'H(9) CO(8) COH(6)	5CCH(15) CCH'(15) 6CCH(12) HC3O(10)
18	1362.1	HCO(26) HCC(25) HC'C(22) HC'O(10) C'OH(8)	HC3O(20) 3CCH(10) 1CCH(9) 7CCH(7)
19	1355.7	HCC(27) HC'C(20) HCO(20) C'OH(12)	2CCH(23) HC2O(18) 'CCH(18) COH1(9)
20	1347.8	HCC(53) HCO(20)	7CCH(24) 3CCH(15) HC4O(14)
21	1323.8	HCO(39) COH(18) HCC(10) CO(14)	HC2O(24) COH2(15) HC4O(12) C2O(11)
22	1320.8	HCO(46) HCC(18) COH(13)	HC4O(23) HC2O(21) COH4(9)
23	1297.0	C'OH(23) HCC(19) HC'O(10)	COH5(22)
24	1295.5	HCO(40) HCC(24) HC'C(11)	HC3O(37) 7CCH(9)
25	1274.3	HC'O(39) C'OH(26) HC'C(20)	HC'O(34) COH1(23) 'CCH(17)

TABLE XXXVI (Continued)

XYLITOL

DOMINANT INTERNAL COORDINATES AND POTENTIAL CONSTANTS

No.	Calc. Freq., cm^{-1}	Relative Contribution, %[a] Diagonal Force Constants[b]	Internal Coordinates[c]
26	1245.2	HCC(31) HC'O(23) HC'C(20) C'OH(14)	HC'O(16) 4CCH(16) COH5(12)
27	1233.9	HC'O(34) COH(27) HCC(11) HC'C(11) CO(13)	COH3(26) HC'O(19) HC50(16)
28	1213.5	COH(31) HC'O(27) HCO(15) HC'C(12)	COH3(22) HC50(20) 8CCH(11) HC40(11)
29	1199.2	HC'O(36) HC'C(18) C'OH(17) HCC(11) COH(10)	H'CO(25) COH1(17) 1CCH(15) HC10(10) 2CCH(10)
30	1114.0	CC(67) C'C(11) COH(13)	C2C3(44) C3C4(24) C1C2(10) COH2(11)
31	1109.5	CC(23) CO(18) C'C(17) HC'C(21) HCO(12) HC'O(11) COH(9)	C1C2(16) C2C3(12) C30(12) C3C4(10) 1CCH(17)
32	1087.3	CC(26) C'C(14) C'O(12) COH(22)	C3C4(23) C1C2(13) C10(8) COH4(17)
33	1070.0	HC'C(29) COH(26) HC'O(12) C'O(10)	COH4(13) 'CCH(12) C10(9)
34	1059.6	C'C(29) CO(16) C'O(8) COH(23) HC'C(11)	C1C2(24) C20(12) COH2(16)
35	1028.9	C'C(53) CO(16) C'O(13) C'OH(24)	C4C5(53) C40(15) C50(13) COH5(24)
36	1009.8	C'O(35) C'C(13) HC'C(12) HCC(10)	C50(34) C4C5(9) 8CCH(8)
37	974.8	C'O(42) C'OH(19) C'C(9)	C10(40) COH1(18) C1C2(7)
38	928.8	CO(41) C'O(10) COH(21) HC'C(11)	C30(30) C50(10) C20(9) COH3(14)
39	893.3	CO(19) C'C(14) COH(16) HC'C(16)	C40(18) COH4(14) CCH'(9)
40	842.8	CO(31) CC(14) C'C(8) COH(19)	C20(23) C2C3(14) COH2(13)
41	773.1	CCO(36)	3CCO(16) 4CCO(15) 1CCO(6)
42	614.8	CCO(31) CC'O(25) HCC(17) C'CC(6)	8CCO(26) 5CCO(18) 6CCO(8) 5CCH(9)
43	511.0	CC'O(30) CCO(19) CCC(13)	1CCO(30) C2CC(12) 4CCO(8)

TABLE XXXVI (Continued)

XYLITOL

DOMINANT INTERNAL COORDINATES AND POTENTIAL CONSTANTS

No.	Calc. Freq., cm^{-1}	Relative Contribution, %[a] Diagonal Force Constants[b]	Internal Coordinates[c]
44	437.0	CCO(29) -CO-(18) HCC(12) C'CC(7)	3CCO(12) TC30(10) 5CCO(7)
45	398.9	CC'O(23) CCO(23) -CO-(17)	6CCO(19) TC40(16) 1CCO(12) 8CCO(12) C3CC(5)
46	371.3	-CO-(51) CCO(14) CC'O(6)	TC20(28) TC50(13) 3CCO(8)
47	360.7	-CO-(67) CCO(9)	TC30(33) TC50(21)
48	349.8	-CO-(74)	TC10(41) TC50(32)
49	335.4	-CO-(59) HCC(12) CC'O(11)	TC40(40) TC20(12) 8CCO(10) 7CCH(9)
50	334.1	-CO-(74) HCC(11)	TC20(33) TC30(18) TC10(14)
51	321.0	-CO-(46) CC'O(6) CCO(5)	TC10(18) TC40(16) TC50(11)
52	275.9	CCO(38) -CO-(21) -CC-(15) HCC(12)	4CCO(24) TCC1(11) TC30(10) 3CCO(8)
53	241.2	CCO(55) -CO-(17) -CC-(9) C'CC(9)	5CCO(25) 6CCO(12) 3CCO(11) TC30(10)
54	215.5	-CC-(55) CCO(27)	TCC1(38) TCC4(13) 3CCO(8) 6CCO(8)
55	197.9	-CC-(64) CCO(19) C'CC(12)	TCC4(47) TCC2(11) C3CC(8) TCC1(7)
56	172.2	CCO(47) -CC-(20) C'CC(20) CCC(14)	7CCO(27) TCC1(14) C3CC(14) C2CC(13) 6CCO(10)
57	144.0	CCO(61) C'CC(40) -CC-(33)	2CCO(45) C1CC(37) TCC3(27)
58	102.3	-CC-(47) C'CC(42) CCO(39)	TCC3(40) C1CC(33) 2CCO(28)
59	87.9	-CC-(69) HCC(19) CCO(15)	TCC2(54) 7CCO(10)
60	74.5	CCO(54) C'CC(39) -CC-(27)	C3CC(38) 7CCO(36) C2CC(16) TCC2(9)

[a] The contributions are relative and may total more than 100% due to the presence of negative off-diagonal interaction constants.

[b] The force constants given are described in Table V.

[c] Only the dominant coordinates are given. The individual coordinates for each molecule are coded in the manner described in Tables XIX-XXI.

TABLE XXXVII

ERYTHRITOL

DOMINANT INTERNAL COORDINATES AND POTENTIAL CONSTANTS

No.	Calc. Freq., cm^{-1}	Relative Contribution, %[a] Diagonal Force Constants[b]	Internal Coordinates[c]
1	3351.7	O'H(99)	O4H(99)
2	3351.6	O'H(99)	O1H(99)
3	3331.0	OH(99)	O2H(99)
4	3330.9	OH(99)	O3H(99)
5	2974.1	C'H(98)	C4H(50) C4H'(48)
6	2964.5	C'H(98)	C1H(52) C1H'(46)
7	2921.7	CH(97)	C3H(87) C2H(10)
8	2909.9	CH(98)	C2H(88) C3H(10)
9	2872.3	C'H(97)	C1H'(52) C1H(45)
10	2867.5	C'H(97)	C4H'(49) C4H(48)
11	1498.0	HC'O(33) HC'H(22) C'O(15)	HC4H(22) HC'O(21) HC4O(11) C4O(15)
12	1457.8	HC'O(50) HC'H(28) C'O(8)	HC1H(28) HC1O(28) H'CO(21)
13	1418.2	HCO(77) HCC(11)	HC2O(60) HC3O(16)
14	1369.8	HCO(48) COH(16) HCC(14) CO(16)	HC3O(37) COH3(16) 5CCH(13) C3O(16) HC2O(11)
15	1353.6	C'OH(23) HC'H(20) C'C(13) HCO(13) HC'O(12)	COH1(24) HC1H(21) C1C2(13)
16	1331.4	HCC(41) C'C(12) C'OH(11) HCO(8) C'O(8)	4CCH(25) COH4(11) C3C4(12)
17	1320.2	HC'H(23) C'OH(18) HCC(15) C'O(12)	HC4H(21) COH4(16) 5CCH(8) C4O(10)
18	1276.4	COH(26) CO(25) HC'O(12) HCO(8)	COH2(27) C2O(23) HC3O(7)
19	1250.0	HC'O(24) HCO(12) COH(12) C'OH(10) HCC(11) CO(15)	HC4O(12) C3O(12) 5CCH(11) HC3O(11) COH4(11) COH3(8)
20	1245.2	HC'O(50) C'OH(7) C'C(7)	H'CO(23) HC1O(21) HC4O(7)
21	1230.7	HCC(27) HC'O(24) CC(17) C'C(11) HCO(10) COH(8)	HC4O(15) 5CCH(13) 2CCH(12) C2C3(16) COH3(7)
22	1205.3	HC'O(28) HCC(17) CC(13) CO(13)	HC4O(16) 2CCH(15) HC'O(11) C2C3(15) C3O(6)
23	1148.8	C'OH(28) C'C(21) HC'O(18) HC'H(13)	COH1(28) C1C2(17) HC'H(12) HC1O(8)

TABLE XXXVII (Continued)

ERYTHRITOL

DOMINANT INTERNAL COORDINATES AND POTENTIAL CONSTANTS

No.	Calc. Freq., cm^{-1}	Relative Contribution, %[a] Diagonal Force Constants[b]	Internal Coordinates[c]
24	1128.4	HC'O(32) C'OH(14) C'C(12) COH(10)	HC'O(29) C3C4(11) COH4(10) COH3(9)
25	1065.5	CO(22) C'O(6) COH(36) C'OH(12) HCC(11)	COH3(34) C3O(21) COH4(16)
26	1060.5	C'O(28) CC(7) C'OH(17) HC'O(10)	C1O(20) C4O(8) C2C3(7) COH1(7)
27	1030.2	C'O(37) CO(8) C'OH(25) COH(17)	C4O(24) C1O(13) C3O(6) COH4(18) COH3(13) COH1(7)
28	973.0	CO(38) C'C(6) CC(5) COH(42)	C2O(36) C1C2(6) C2C3(5) COH2(39) 2CCH(9)
29	891.2	C'O(23) C'C(17) CC(16) HCC(14)	C1O(18) C3C4(16) C2C3(16) 2CCH(11)
30	837.8	C'C(38) C'O(27) HC'O(14) HC'C(12) HC'H(10)	C1C2(27) C1O(27) C3C4(10) HC1H(7) H'CO(7)
31	699.2	C1CC(33) CC(29) HCC(26) C'C(22)	C2C3(29) C2CC(23) C3C4(18) 3CCH(10)
32	611.5	CCO(22) CC'O(12) C'C(18)	5CCO(20) 1CCO(11) C3C4(15)
33	545.0	CC'O(23) CCO(20) C'C(17) HC'C(15)	1CCO(22) 5CCO(15) C1C2(15)
34	485.4	CC'O(30) C'CC(10) -CO-(10) HCC(9) CCO(8)	1CCO(27) C2CC(8) TC2O(8)
35	431.4	HC'C(53) -CO-(20) C'CC(9) CCO(9)	1CCH(33) 'CCH(15) TC1O(15) C1CC(9)
36	378.3	CCO(36) -CO-(36) HC'C(20)	3CCO(35) TC1O(26)
37	370.2	-CO-(39) HC'C(29) -CC-(20)	TC1O(34) TCC1(20) 1CCH(15) 'CCH(13)
38	348.2	-CO-(82) HC'C(8) CCO(6)	TC4O(75) TC3O(7) CCH'(4) 3CCO(4)
39	335.4	-CO-(83) HC'C(7) HCC(6)	TC3O(75) TC4O(7) 5CCH(5) 6CCH(4)
40	327.3	-CO-(73) HCC(14) CC'O(7)	TC2O(66) 2CCH(12) 1CCO(7) TC1O(6)
41	273.4	CCO(40) HC'C(37) C'CC(12) -CO-(9)	5CCO(27) CCH'(20) 6CCH(17) 4CCO(7)

TABLE XXXVII (Continued)

ERYTHRITOL

DOMINANT INTERNAL COORDINATES AND POTENTIAL CONSTANTS

No.	Calc. Freq., cm^{-1}	Relative Contribution, %[a] Diagonal Force Constants[b]	Internal Coordinates[c]
42	242.0	C'CC(52) -CC-(42) CCO(26) HCC(19) -CO-(15)	C1CC(49) TCC1(41) 2CCO(17) TC1O(15)
43	158.2	CCO(55) -CC-(28) CO(12) HCO(11)	2CCO(48) TCC2(23) C2O(12)
44	149.3	CC'O(69) HC'O(12) CCO(11) -CC-(10) C'O(17)	6CCO(63) C4O(17) TCC2(9) 2CCO(6)
45	125.8	CCO(67) C'CC(52) -CC-(19) HCC(13)	4CCO(49) C2CC(48) C2C3(13)
46	91.6	-CC-(57) CC'O(17) CCO(16)	TCC2(50) 6CCO(16) 2CCO(15)
47	75.5	C'CC(405) HCC(274) CCO(204)	C1CC(311) C2C3(167) 4CCO(135) 3CCH(132) C2CC(93)
48	48.9	-CC-(74) CCO(22) C'CC(12)	TCC3(71) 4CCO(21) C2CC(10)

[a] The contributions are relative and may total more than 100% due to the presence of negative off-diagonal interaction constants.

[b] The force constants given are described in Table V.

[c] Only the dominant coordinates are given. The individual coordinates for each molecule are coded in the manner described in Tables XIX-XXI.

TABLE XXXVIII

D-ARABINITOL

DOMINANT INTERNAL COORDINATES AND POTENTIAL CONSTANTS

No.	Calc. Freq., cm^{-1}	Relative Contribution, %[a] Diagonal Force Constants[b]	Internal Coordinates[c]
1	3351.7	O'H(99)	O1H(99)
2	3351.5	O'H(99)	O5H(99)
3	3330.8	OH(99)	O4H(61) O2H(37)
4	3330.8	OH(99)	O3H(45) O2H(28) O4H(27)
5	3330.8	OH(99)	O3H(53) O2H(36) O4H(11)
6	2982.8	C'H(97)	C5H'(49) C5H(48)
7	2956.0	C'H(92) CH(5)	C1H'(47) C1H(45)
8	2933.9	CH(96)	C3H(48) C4H(48)
9	2921.3	CH(91) C'H(7)	C2H(88)
10	2913.6	CH(98)	C3H(49) C4H(47)
11	2896.2	C'H(95)	C1H'(50) C1H(45)
12	2864.8	C'H(98)	C5H(49) C5H'(48)
13	1476.0	HC'H(56) HC'O(36)	HC1H(56) HC1O(19) H'CO(18)
14	1461.4	HC'H(62) HC'O(13) HC'C(13)	HC5H(62) HC'O(10)
15	1441.7	HCO(41) HCC(38)	HC2O(24) 4CCH(21) HC3O(13) C2O(14)
16	1432.4	HCO(41) HCC(14) COH(14) CO(18)	HC4O(36) C4O(17) COH4(13) 6CCH(11)
17	1382.7	HCC(47) HC'O(14) HC'C(10)	6CCH(17) 7CCH(15) 2CCH(8)
18	1369.9	HCC(61) HCO(11) CO(13)	2CCH(18) 3CCH(17) 6CCH(11) C3O(9)
19	1333.6	HCO(45) HCC(33) HC'O(9) C'OH(6)	HC2O(27) 4CCH(19) HC3O(17) 3CCH(12)
20	1324.5	HCC(32) C'OH(15) HCO(12) HC'C(11)	5CCH(22) COH5(14) C5O(9) CCH'(7)
21	1299.0	HCO(30) HC'C(14) HCC(13) HC'O(13)	HC4O(21) HC3O(9)
22	1293.2	HCC(17) HCO(15) COH(15) C'OH(14)	COH(13) 5CCH(12) HC3O(12) COH1(9)
23	1285.1	C'OH(37) HCO(25) C'O(12)	COH1(35) HC4O(15) C1O(12) HC3O(9)

TABLE XXXVIII (Continued)

D-ARABINITOL

DOMINANT INTERNAL COORDINATES AND POTENTIAL CONSTANTS

No.	Calc. Freq., cm^{-1}	Relative Contribution, %[a] Diagonal Force Constants[b]	Internal Coordinates[c]
24	1270.6	HC'O(29) HC'C(17) HCC(10) C'OH(22)	HC5O(22) COH5(18)
25	1261.1	HC'O(25) HCO(17) COH(14) C'OH(11)	COH2(13) COH1(11) HC5O(12)
26	1246.3	HC'C(54) HC'O(30) HCC(16) C'OH(8)	1CCH(37) HC1O(17) 'CCH(15) 2CCH(10)
27	1219.1	HC'O(45) HCO(25) HC'C(21)	HC1O(23) HC2O(23) H'CO(21)
28	1208.0	HC'O(41) HC'C(23)	HC'O(33) CCH'(20) C4O(9)
29	1190.7	COH(34) HCC(25) HC'O(16) HC'C(15)	COH3(20) COH4(11) HC5O(10)
30	1141.0	C'C(29) CC(18) C'O(8) COH(29)	C1C2(29) C2C3(16) C1O(8) COH2(26)
31	1115.9	C'C(40) CC(12) HC'C(26) COH(15)	C4C5(37) C3C4(11) CCH'(25) COH4(15)
32	1108.0	HC'C(39) CO(11) COH(10) HC'O(10)	'CCH(30) C2O(10) 1CCH(9)
33	1082.3	CC(28) CO(11) C'O(8) HC'O(14) HC'C(12)	C3C4(28) C3O(9) C5O(8) HC'O(10)
34	1070.2	C'C(15) C'O(12) CO(10) COH(15) C'OH(15)	C5O(11) C4C5(9) C4O(9) COH5(14) COH4(13)
35	1019.3	CO(31) C'C(10) COH(26) HC'C(19)	C3O(25) C1C2(8) COH3(19) 'CCH(13)
36	1010.3	C'O(26) CO(20) C'C(13) COH(17)	C1O(15) C3O(14) C1C2(12) C5O(11) COH2(16)
37	969.7	C'O(24) CO(13) CC(22) C'C(9)	C1O(24) C3C4(12) C2C3(11) C4C5(8)
38	937.7	C'O(43) C'C(12) C'OH(22)	C1O(25) C5O(18) C1C2(11) COH1(13)
39	896.2	C'C(33) C'O(19)	C4C5(20) C5O(15) C1C2(13) C2C3(8)
40	858.7	CC(18) CO(17) C'O(13) COH(13)	C5O(11) C2O(9) C2C3(9) C3C4(8)
41	718.1	CCO(23) CC(14) CO(14) HCC(10)	C3O(12) C2C3(12) 4CCO(11) 3CCO(11)

TABLE XXXVIII (Continued)

D-ARABINITOL

DOMINANT INTERNAL COORDINATES AND POTENTIAL CONSTANTS

No.	Calc. Freq., cm^{-1}	Relative Contribution, %[a] Diagonal Force Constants[b]	Internal Coordinates[c]
42	626.3	CC'O(29) CCO(17) HCC(11) C'CC(9)	8CCO(26) 3CCO(10)
43	590.6	CC'O(32) CCO(15)	1CCO(21) 8CCO(10)
44	480.5	CCO(38) C'CC(8)	5CCO(23) 6CCO(14)
45	430.1	CCO(29) CC'O(27)	1CCO(25) 6CCO(17) 5CCO(8)
46	372.3	-CO-(68) CCO(14)	TC30(45) TC50(15)
47	359.2	-CO-(63)	TC50(39) TC20(14)
48	341.0	-CO-(76)	TC20(39) TC40(25)
49	331.8	-CO-(90)	TC40(52) TC20(20) TC10(16)
50	328.6	-CO-(86)	TC10(61) TC30(12)
51	302.3	CCO(28) -CO-(26) -CC-(16)	TC50(19) 6CCO(11)
52	268.0	CCO(35) -CO-(17) -CC-(12)	3CCO(25) 4CCO(10)
53	249.7	CCO(32) -CC-(25) -CO-(19) C'CC(18)	4CCO(20) TCC4(15) C3CC(13) 5CCO(11)
54	211.2	-CC-(42) CCO(39) C'CC(12)	TCC1(30) 2CCO(13) TCC4(11) 5CCO(11)
55	195.9	-CC-(40) CCO(32)	TCC4(22) 7CCO(22)
56	149.1	CCO(48) -CC-(47) C'CC(38)	TCC3(31) C1CC(24) 7CCO(19) 2CCO(16) C3CC(14)
57	135.3	CCO(84) CCC(29) HCC(21)	2CCO(39) C2CC(29) 7CCO(22) 6CCO(11)
58	111.7	C'CC(49) -CC-(34) CCO(32)	C3CC(41) 7CCO(28) TCC4(16)
59	80.5	-CC-(86)	TCC2(38) TCC3(37)
60	74.7	CCO(45) -CC-(40) HCC(31) C'CC(28)	2CCO(35) C1CC(28) TCC2(23) TCC3(16) 2CCH(24)

[a] The contributions are relative and may total more than 100% due to the presence of negative off-diagonal interaction constants.

[b] The force constants given are described in Table V.

[c] Only the dominant coordinates are given. The individual coordinates for each molecule are coded in the manner described in Tables XIX-XXI.

APPENDIX IV

CALCULATED FREQUENCIES FOR DEUTERIUM-SUBSTITUTED RIBITOL AND XYLITOL

Ribitol (COD), ν, cm^{-1}		Xylitol (COD), ν, cm^{-1}	
2968	1094	2966	1062
2949	1036	2963	1035
2933	1016	2934	1011
2922	988	2922	997
2914	976	2914	982
2901	880	2884	858
2880	837	2882	832
2440	785	2440	794
2440	751	2439	763
2425	733	2425	737
2425	715	2423	717
2423	589	2423	591
1480	493	1460	500
1468	480	1453	424
1444	412	1432	382
1406	350	1425	342
1376	304	1383	321
1362	277	1352	297
1346	257	1343	275
1311	249	1342	261
1297	243	1306	256
1291	225	1289	227
1263	216	1276	201
1244	209	1253	193
1224	181	1229	178
1186	164	1225	159
1182	116	1165	134
1145	111	1146	98
1132	82	1127	84
1125	68	1103	72